Journal ALCONPAT

Message from the Editor-in-chief and the Guest editor

LATIN AMERICAN JOURNAL ON QUALITY CONTROL, PATHOLOGY, AND THE RECUPERATION OF CONSTRUCTIONS

It is gratifying for the team of the ALCONPAT Journal to see the first issue of our sixth year published.

The purpose of the ALCONPAT (RA) Journal is to publish case studies related to the topics of our association, such as quality control, pathology, and the recuperation of constructions, all the while motivating the presentation of basic or applied researches, revisions, or documental researches.

This issue presents our fourth special edition, this time dedicated to the **Applications of Special Concretes**.

This edition V6N1 begins with a work from **Spain and Mexico**, in which José Bernal et al. obtain auto-compacting concretes with nano-silica, silica fume, and binary mixtures of both additives that satisfy the demand for high mechanical resistances and durability, determining that the dosage with the best performance is the one that contains 2.5% nano and 2.5% silica fume.

The second work, from **Mexico**, by Marisol Gallardo et al., deals with the synthetization of a calcined calcium sulphoaluminate clinker comprised of a mixture of fly ash, fluorgypsum, aluminum slag, and calcium carbonate at 1250 ºC. The clinker was mixed with 15, 20, or 25% e.p. of $CaSO_4 \cdot \frac{1}{2}H_2O$. They evaluated the resistance to compression of the cements obtained, having been cured in potable water and in corrosive mediums at 40 ºC. The cements cured in potable water developed resistances to compression of 38-39 MPa, whereas those immersed in corrosive mediums showed a decrease in the same. The degradation of the cements due to a chemical attack was due to a decalcification and dealumination of the pastes.

The third article comes from **Brazil**, by Carlos Britez et al., and deals with the Brookfield Century Plaza Commercial Building, located in Alphaville, São Paulo, Brazil, which is supported by two large concrete footings. A high resistance (70 MPa) and auto-compacting (SCC) concrete was developed for these large footings (each one measures 28.4m x 18.6m x 4.5m). A numerical model was developed using an FEM software to predict the hydration thermal gain of different layers of concrete, with the purpose of establishing the most adequate procedure to address the time and construction requirements, without the appearance of cracks. Procedures were established and monitored to control the production of the concrete in the manufacturing company of the same and during the concreting. Finally, the internal temperature of the concrete was registered to provide a better calibration of the model.

The fourth article, by José Manuel Mendoza Rangel et al., comes from **Mexico and Spain**. They evaluate the durability of two mortars elaborated with fly ash (FA) substitutions in weight with regard to the total cement, comparing its performance with three commercial repair mortars when exposed to a CO_2 attack in an industrial environment.

The fifth work in this issue is by Vladimir Ferrari et al., from **Brazil**, who developed and analyzed the behavior of high performance cementitious compounds reinforced with fibers. It is particularly interesting to read how they develop their hybrid compounds and their experimental development. It is certainly an article that merits reading.

The closing article for the special edition is by Alejandro Cabrera Madrid et al., from **Mexico**, who present a revision work on the state-of-the-art cementing system PC-BFS emphasizing its effect on the mechanical resistance of the concrete. The utilization of the cementitious characteristics of the BFS with high replacement levels turns out to be viable, being able to improve the resistance to compression and, in some cases, the resistance to the corrosion of steel. Said improvement shall depend on the quantity of the BFS and the exposure environment of the concrete. In this revision, it was confirmed that BFS replacements of up to 70% were beneficious in humid microclimates or marine environments, and up to 50% in environments prone to carbonation. In these ranges, it is possible to achieve a greater replacement efficiency with respect to the resistance to compression.

This special first issue of the year opens with good news, as all RA articles since the first issue now have a DOI number. Likewise, we are launching an OJS platform where our readers will be able to enjoy the content of the magazine on a brand new and more efficient platform.

We are certain that the articles in this issue will comprise an important reference for those readers involved in matters related to the application of special concretes. We thank the authors participating in this issue for their willingness and effort in presenting quality articles and for their compliance regarding the established deadlines.

By the Editorial Board

Pedro Castro Borges   Bernardo Tutikian
Editor-in-chief   Guest Editor

Journal ALC☉NPAT

CONTENT

ALCONPAT Journal

http://www.revistaalconpat.org

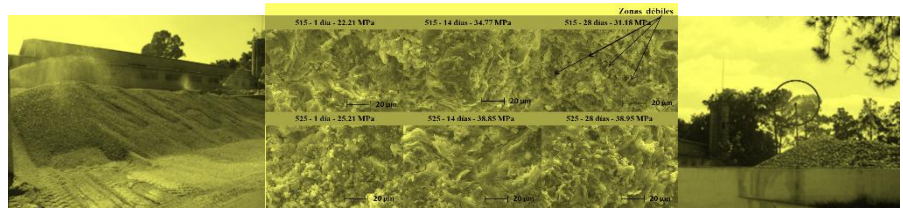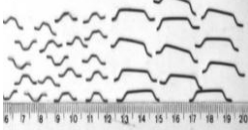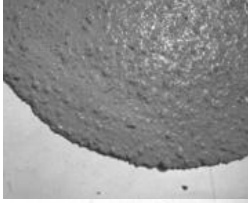Journal of the Latin-American Association of Quality Control, Pathology and Recovery of Construction
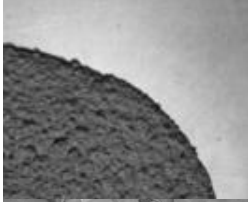
Rheological and mechanical properties of self-compacting concrete with the addition of nano-silica and microsilica

E. Sánchez[1], J. Bernal[2], N. León[3], A. Moragues[3]

[1] Department of Agroforestry Engineering, Universidad Politécnica de Madrid, Spain.
[2] Engineering School Mazatlán. Universidad Autónoma de Sinaloa, Mexico.
[3] Civil Engineering Department: Construction, Universidad Politécnica de Madrid, Spain.

ABSTRACT

Self-compacting concrete is the result of the redesign of quality mixtures with the ability to ensure its correct placement in strongly assembled structures, where the vibration process is too complicated and where there is the risk of altering the position of the reinforcement bars. Along with the advantages of this concrete and due to the greater demand for high performance concrete, silica fume is used, and more recently, nanomaterials with nano-silica as well; mainly, nano-silica. The objective of this work is to obtain self-compacting concretes with nano-silica, silica fume and binary mixtures of both, which satisfy the demands for high mechanical resistance and durability, determining that the dosage with the best features contains: 2.5% of nano and 2.5% of silica fume.
Keywords: Self-compacting; nano-silica; silica fume; rheology; mechanical properties.

RESUMEN

El hormigón autocompactante es el resultado de diseñar mezclas de calidad con capacidad para asegurar su correcta colocación en estructuras fuertemente armadas en las cuales el proceso del vibrado resulta muy complicado y con riesgo de alterar la posición de las armaduras. Unido a las ventajas de este hormigón y debido a la mayor demanda de hormigones de altas prestaciones, se utiliza humo de síl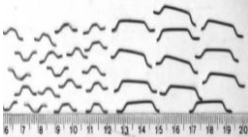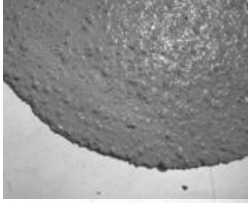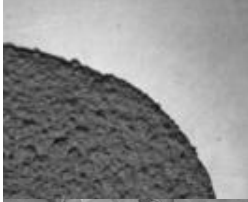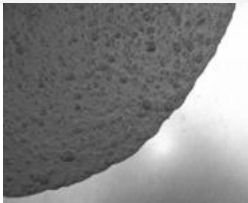ice y, más recientemente, nanomateriales como adiciones. Principalmente nano-sílice. El objetivo de este trabajo es obtener hormigones autocompactantes con nano-sílice, humo de sílice y mezclas binarias de ambas adiciones que satisfagan la demanda de altas resistencias mecánicas y durables, determinando que la dosificación con mejores prestaciones es la que contiene 2.5% de nano y 2.5%.de humo de sílice.
Palabras clave: Autocompactante; nanosílice; humo de sílice; reología; propiedades mecánicas.

RESUMO

O Concreto Auto-adensável é o resultado da concepção de um concreto de qualidade com a capacidade para assegurar a colocação de reforço em estruturas fortemente armados em que o processo de vibração é muito complicado e arriscado por alterar a posição da armadura . Juntamente com as vantagens deste concreto e devido ao aumento da procura de concretos de alto desempenho , o fumo de sílica e mais recentemente , os nano-materiais são usados como adições . Principalmente a nano- sílica. O objetivo deste trabalho é a obtenção de concreto auto- adensável com nano- sílica , sílica ativa e misturas binárias das duas adições para atender a demanda de alta resistência mecânica e durável. A mistura com melhores desempenhos é aquela que contém 2,5 % de nano - sílica e 2,5% de pó de sílica.
Palavras-chave: Auto-compactável; nano-sílica; sílica activa; reologia; propriedades mecánicas.

_____
Corresponding author: Elvira Sánchez (elvira.sanchez.espinosa@upm.es)

1. INTRODUCTION

Self-compacting concrete is the result of the design of quality concrete with the ability to ensure its correct placement in the strongly assembled structures, where the vibration process is too complicated and where there is the risk of altering the position of the reinforcement bars. Professor Okamura and Ozawa (1996) began the development of said concrete at the University of Tokyo during the mid-1990s, improving it in the following years (Okamura, 1997; Okamura and Ouchi, 1999; Okamura, Ozawa, and Ouchi, 2000; Okamura, Maekawa, and Mishima, 2005). This concrete is characterized by a diminished water/cement ratio and a high content of fines, for which chalky filler is added to the mixture, as well as having a reduced content in coarse aggregate and the inclusion of superplasticizers. All of this allows obtaining a concrete with very high fluidity, that due to its own weight is able to achieve a good consolidation without exudation or segregation (De la Peña, 2001, EHE-08, 2010). In the industry of prefabs, the advantages of using this cement are even greater, as they increase the useful life of the molds due to the fact that the absence of vibration allows these to be lighter and, therefore, the maintenance costs are reduced.

Combined with the advantages of the self-compacting cement and as consequence of the increase in the demand for high resistance cement, nano-materials are starting to be used as additives. The aim of this is to provide the material with special characteristics, be it in terms of resistance or in their durability. Therefore, the cement that is sought is considered a high-performance cement, as it should not only satisfy the demand for high mechanical resistance, but also comply with the high demands regarding its durability.

There are several nano-particles that are being researched, the most commonly used are silica, titanium, alumina, and iron (Sanchez and Sobolev, 2010). The nature of the type of the additive to be selected depends on the properties that are required to be improved or conferred to the material, according to the functionality intended. The highest concentration of studies regarding the incorporation of nano-particles in the field of civil engineering are the ones related to nano-SiO_2 (Kawashima, Hou, Corr, Shah, 2013). The majority of studies coincide in stating that the incorporation of said nano-particles produces microstructural changes as it is a catalyst for the pozzolanic additives (Bjornstrom, Martinelli, Matic, Borjesson, Panas, 2004). Similar to the already known fumed silica or micro-silica, the nano-SiO_2 reacts with the calcium hydroxide ($Ca(OH)_2$), producing a larger amount of CSH gel that densifies the material with the consequent reduction of its permeability (Said, Zreidan, Bassuoni, Tian, 2012) and control of the leaching Ca^{2+} (Nazari and Riahi, 2010). The size of the silica that is added produces changes in the mean number and size of the portlandite crystals. These microstructural changes are associated to the changes in the macrostructural properties of mortars and concrete such as resistance to compression, elastic module (Yu, Spiesz, Brouwers, 2014; Zyganitidis, Stefanidou, Kalfagiannis, Logothetidis, 2011), and durability (León, Massana, Alonso, Moragues, Sánchez-Espinosa, 2014), among others.

There are several studies on the influence of nano and micro silica on concrete in which they compare different parameters (Mondal, Shah, Marks, Gaitero, 2010; Borralleras, 2012; Craeye, Van Itterbeeck, Desnerck, Boel, De Schutter, 2014; Rong, Sun, Xiao, Jiang, 2015), but there are few works where binary mixtures of both additives are included in self-compacting concrete with high performance. Thus, this work intends to study the influence of nano-silica, micro-silica or fumed silica, as well as that of the additives of ternary mixtures on the rheological and mechanical properties of self-compacting concrete, in order to establish the differences between the different dosages and to be able to determine the mixture with the best behavior in light of these properties, both in fresh and hardened concrete.

2. PROCEDURE

For the manufacture of the mixtures, Portland cement CEM I 52,5 R (PC) was used according to EN 197-1, the properties of which can be seen in table 1.

Table 1. Physical-chemical properties of Portland cement (PC), nanoSi (nSi), and microSi (mSi).

	SiO_2	Al_2O_3	Fe_2O_3	CaO	MgO	SO_3	K_2O	Na_2O	Lost fire (%)	Density (g/cm^3)	Specific surface (m^2/g)
CP	19.20	6.07	1.70	63.41	2.56	3.38	0.2	0,33	2,09	3,5	0,42
nSi	99.90	-	-	-	-	-	-	-	0,10	1,29	200
mSi	94	-	-	-	-	-	-	-			

The nanosilica (nSi) used is Levasil 200/40% in aqueous dispersion form with 40% richness, a specific surface of 200 m^2/g and a particle size of 15 nm (approx.) (see Table 1). The micro silica or silica fume (mSi) used is Elkem Microsilica MS 940 U, composed of non-porous, submicron size, amorphous spheres of SiO_2 and small agglomerates of these, with a specific surface of 15-30 m^2/g and a mean sphere particle size of approximately 0.15 microns. Even though some of the spheres may be found individually, the majority of them form agglomerates of primary particles with a typical range of 0.1-1 micron (see Table 1). The additives used were: SIKA Viscocrete 5720 (SP) (polycarboxylate polymer) superplasticizer and a viscosity modifier (VM) additive SIKA Stabilizer 4R. The coarse aggregates used in the mixtures were: river sand smaller than 4 mm, 6 to 12 mm gravel, and limestone filler whose granulometry complies with the UNE standards 12620:2003+A1:2009, with a maximum diameter of 63 μm.

Ten dosages were designed (see Table 2). All samples maintained a water/cementing material relation of 0.36. The dosages were: three with 2.5%, 5%, and 7.5% of nano-SiO_2 ([nSi]-2.5; [nSi]-5; [nSi]-7.5), three with 2.5%, 5%, and 7.5% of micro-SiO_2 ([mSi]-2.5; [mSi]-5; [mSi]-7.5), and three with mixtures of both with the percentages of each additive being of 2.5%/2.5%, 5%/2.5%, and 2.5%/5% of nano-SiO_2 and micro-SiO_2, respectively ([nmSi]-2.5/2.5; [nmSi]-5/2.5; [nmSi]-2.5/5), with regard to the weight of the cement. A tenth mixture without any type of additives was designed, which will be considered the reference concrete.

In order to evaluate the self-compacting characteristics of the designed concretes, the standardized tests were done in fresh material with the EHE-08 (2010) instruction. The aforementioned tests are: slump-flow or the extension of flow tests (UNE-EN 12350-8), the V funnel test (UNE-EN 12350-9), the L Shape Box Test (UNE-EN 12350-10), and the slump flow combined with Japanese ring test (UNE-EN 12350-12).

Once the self-compactness of the mixture was confirmed, the manufacture of 12 test tubes of 100 mm in diameter and 200 mm tall, and of 2 standardized test tubes of 150 mm of diameter and 300 mm tall, was carried out. These test tubes were kept in the laboratory for 24 hours. Once this time had elapsed, they were demolded and cured for 28 days inside a chamber at a temperature of 20±2 °C and a humidity greater than 95%, according to the UNE-EN 12390-2 standard.

Table 2. Dosage of the concretes studied

Component (kg/m³)	HAC	[nSi]-2,5	[nSi]-5	[nSi]-7,5	[mSi]-2,5	[mSi]-5	[mSi]-7,5	[nmSi]-2,5/2,5	[nmSi]-5/2,5	[nmSi]-2,5/5
Cement	450	450	450	450	450	450	450	450	450	450
Nano-silica	-	11,25	22,5	33,75	-	-	-	11,25	22,5	11,25
		2,5%	5%	7,50%				2,5%	5%	2,5%
Micro silica	-	-	-	-	11,25	22,5	33,75	11,25	11,25	22,5
					2,5%	5%	7,50%	2,5%	2,5%	5%
Water	162	166,0	170,1	174,1	166,0	170,1	174,1	170,1	174,1	174,1
Filler calizo	100	100	100	100	100	100	100	100	100	100
Sand	1160	1160	1160	1160	1160	1160	1160	1160	1160	1160
Gravel 6/12	585	585	585	585	585	585	585	585	585	585
SP (%)*	2	3,30	4	6	2,30	2,50	2,70	3,60	4,80	3,90
MV (%)*	0,15	0,15	0,15	0,15	0,15	0,15	0,15	0,15	0,15	0,15

(*) Percentage in cement weight.

In order to characterize the concretes according to their mechanical properties, 3 test tubes were evaluated in terms of resistance to compression at 7, 28, and 90 days since their manufacture, according to the UNE-EN 12390-3 standard. The maximum size of the coarse aggregates, inferior to 12 mm, is what enabled their use for said test (Fernandez, 2013). After 28 days of being cured, the resistance to indirect traction was also determined through the testing of two 100x200 mm test tubes in accordance with the UNE-EN 12390-6:2001 standard. The two 150x300 mm test tubes were tested at the same age to determine the elasticity module according to the UNE-EN 83316:1996 standard. The aforementioned tests were carried out in an IBERTEST press with a maximum capacity of 1,500 kN. In order to determine the elasticity module, the deformities in the standardized test tubes were measured through a differential transformer of lineal variation from the IBERTEST house with a computer controlled data acquisition system. The loads were increased evenly to the velocity of 0.2 MPa/s during 3 successive load and unload cycles, up to a 40% of the compression resistance. The resistance values to compression, indirect traction, and the elasticity module are the mean value of the results obtained in their corresponding test.

The remaining test tube is used for the microstructural characterization of the mixtures. For this, a thermogravimetric analysis (TGA) at 7, 28, and 90 days was done for all ages and mixtures designed, in accordance with the ASTM E1131:(2008) standard.

For this test, a powder sample was used with a particle size inferior to 0.5 mm. In order to obtain these characteristics, a sample of 20 mm obtained from the test tube after having eliminated the outermost 20 mm was used. The sample obtained went through a grinder in order to obtain particles smaller to 8 mm. These particles were placed in a desiccator connected to a vacuum pump that guaranteed a vacuum pressure between 1 and 5 kPa. The desiccator was left running for 45 minutes. Subsequently, it was submerged for 24 hours in 95% isopropanol in order to stop the hydration processes in concrete. Afterward, it was dried on a stove at 40°C during a minimum period of 72 hours to guarantee the complete drying of the sample.

Prior to the completion of the test, the particles were grinded in a manual steel mortar, finishing the refining of the grain in a Retsch RM 200 agate mortar. The process finalizes through the sieving of the powder through a 0.5 mm sieve. The grinded mass, of a weight of approximately 300 g, was

stirred in an air-tight seal bag in order to homogenize it. The total sample was then divided into 8 parts and a portion of each part was then taken in order to complete two samples of 2 g each, which were placed on a stove at 40°C during 7 days in order to stabilize the mass. The equipment used for the thermogravimetric analysis was a simultaneous thermal analyzer of the SETARAM brand, model LABSYS EVO, with a precision balance of 0.1 µg. For the test, a sample of approximately 55 mg was used, having been subjected to a dynamic heating ramp rate that varied between 40°C and 1,100°C with a heating rate of 10°C/minute. Alumina crucibles were used as reference material, α-alumina (α–Al_2O_3), previously burnt out at 1,200°C, and a nitrogen test atmosphere (N_2). This analysis allowed determining the quantity of CSH gel and portlandite (Ca $(OH)_2$ that is present in each concrete. For this, the gel water loss values were determined, which were obtained subjecting the sample to temperatures between 105ºC and 400ºC approximately. The water losses of free portlandite were obtained within a temperature range of approximately 400°C and 600°C.

3. RESULTS AND DISCUSSION

3.1 Rheological properties

In the 0 we can observe the visual inspection of the 10 mixtures, where in no case did segregation or exudation of the grout present itself. This result is contrary to the one obtained by Dubey and Kumar (2012) who state that with amounts larger than 2% of a SP of carboxylate type, similar to the one used in this study, a segregation of the mixture can be observed.

Nevertheless, the visual evaluation of the mixtures showed a great amount of bubbling in those that contained nSi. This phenomenon is attributed to the amount of SP that is used to obtain the necessary workability, as indicated by Borrelleras Mas (2012).

In the case of this study, no air occlusion test was carried out on the mixtures. However, Yu *et al.* (2014) carried out tests in high performance concrete with nano-silica contents between 1% and up to 5% of additive with a steady amount of SP, and they obtain an exponential increase of the content of occluded air as the amount of nSi rose, which leads us to conclude that both the amount of SP as well as that that of nSi result in an increase in the amount of occluded air.

On the other hand, in order to evaluate whether this amount of air could be eliminated from the mixtures, those created with the nSi additive were repeated and a table-top vibration was carried out; there, it was observed that the air bubbles did not reached the surface and that the mixture moved from a homogenous form within the molds, forming one mass that moved uniformly. Furthermore, the superficial layer had a plastic appearance that did not allow the expulsion of said bubbles. Subsequently, resistance to compression and PIM tests were done on these vibrated mixtures, and in no case, were there significant differences, therefore the values of the same are not shown in this study.

The proposal of the authors in this study to mitigate the amount of bubbles is to increase the mixing energy for the concrete and to increase the mixing time in the mixer, thereby making it possible for this amount of bubbles to escape due to the mechanical movements of the mixer—thus obtaining a greater workability in the mixtures. The use of condensed polyethylene, along with polycarboxylate, acting as a defoamer, is also recommended.
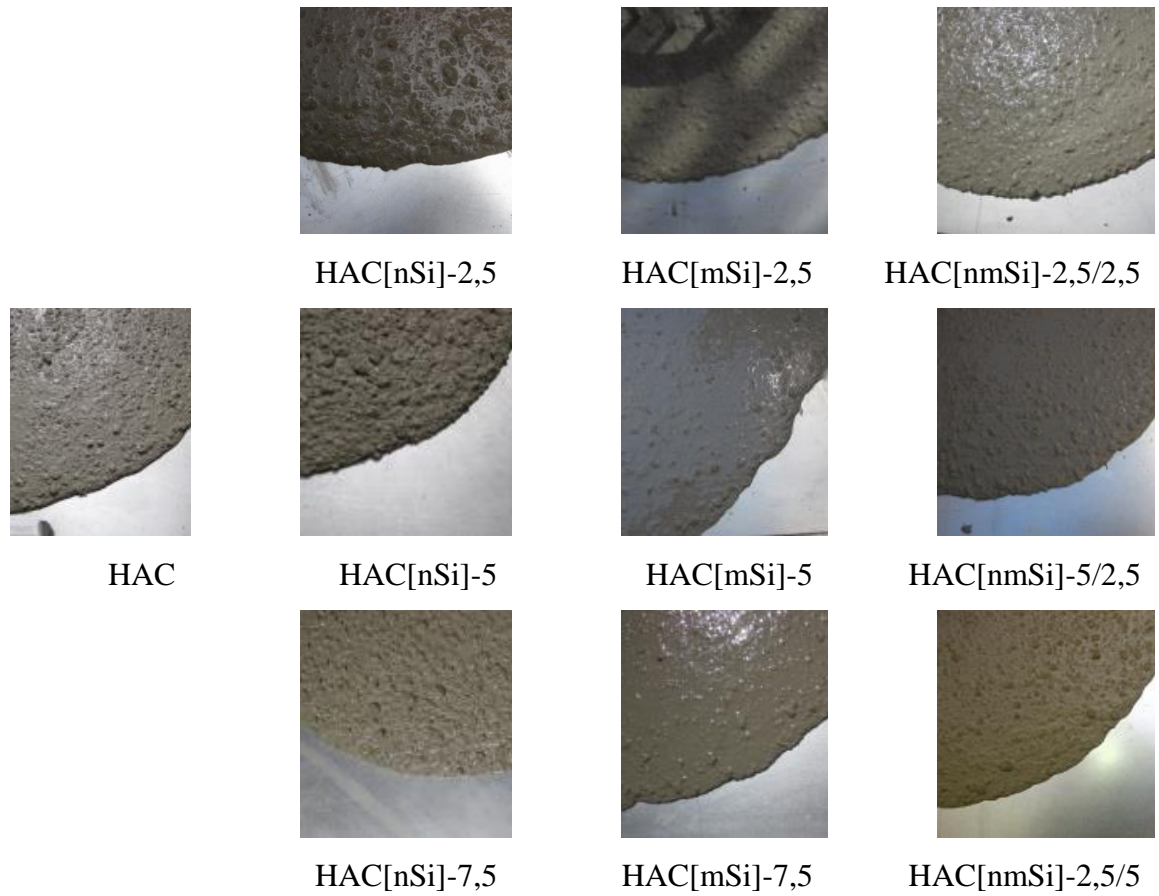
Figure 1. Border aspect of the different mixtures designed, fresh, after the slump-flow test

The values obtained in the different tests for the verification of the self-compacting characteristic of the mixtures, according to the EHE-08 (2010), are collected in Figures 2, 3, 4, and 5. These show the slump-flow diameter of the mixtures (d_f) and the SP used for their manufacture (Figure 2), the Tb time of passage through the V funnel (Figure 3), the capacity of passage through the L shaped box (C_{bl}) (Figure 4), and the slump-flow diameter combined with Japanese ring (d_{jf}) (Figure 5).

In figure 2 and in a general manner, it can be observed that the slump-flow diameter can be found between 550 mm and 850 mm, thus all mixtures comply with said parameter. Furthermore, they do not present segregation or exudation despite the fact that they possess high amounts of SP and even, for the mixture [nSi]-7.5, superior to the 5% that is allowed by the *Instrucción Española del Hormigón Estructural* (EHE-08). These results contradict Dubey and Kumar (2012) who state that with amounts greater than 2% of a SP of the carboxylate type, similar to the one used in this study, segregation of the mixture can be observed. Furthermore, there are authors (Borralleras, 2012) that defend that the maximum amount of SP is determined when the additive stops producing rheological improvements in the fresh material.
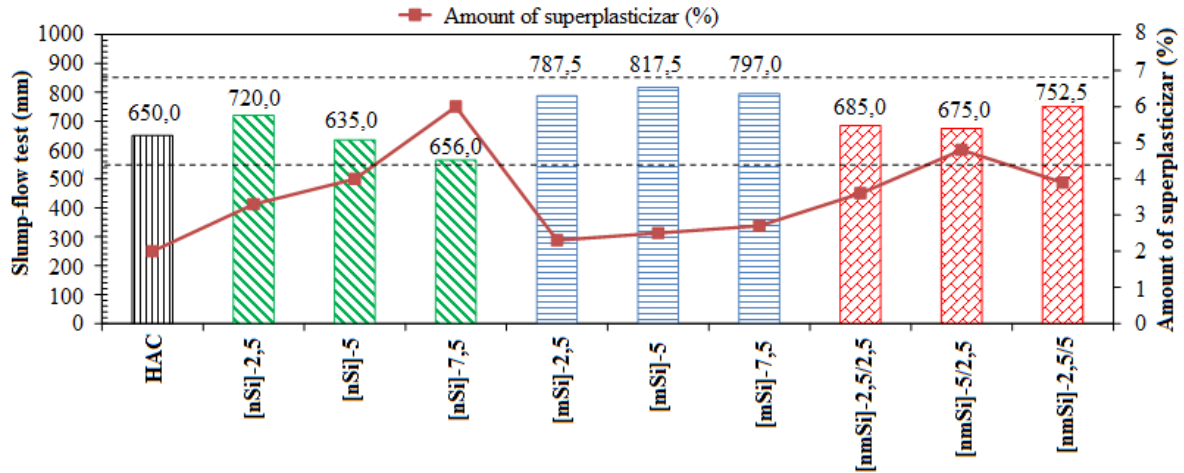
Figure 2. Slump-flow test (d_f) (mm) and amount of superplasticizer.

The existence of a clear influence of the type of additive can also be observed. Therefore, the mixtures with addition of nSi show a decrease in the slump-flow diameter as said addition increases. This can be translated into a lesser workability of the mixture, even when there is an increase of up to 6% in the amount of SP, superior to the recommended amount by the EHE. This phenomenon does not appear when mSi is used as the additive. In this case, there is very little variability in the diameter, which is around 800 mm. Lastly, regarding the binary mixtures, it can be observed how the nSi compromises the workability of the material, making it necessary to increase the amount of SP when increasing the amount of nSi incorporated. Jalal *et al.* (2012) state that both the nSi and the mSi improve the consistence of the self-compacting concrete, but they do not have part in the valuation of the increase of said consistency regarding the content or the type of these. Nevertheless, they determine what quantities of the nSi of the 2% regarding the weight of the cement do not significantly cause a variation in the slump-flow diameter, and if they do, then they are mixed with a 10% of mSi and 2% of nSi. On the other hand, this quantity of additive produces an important amount of bubbling that is directly proportional to the amount added (Nazari and Riahi, 2010). These bubbles may cause the formation of pores that are not interconnected in the hardened material and which could compromise the resistance characteristics of this concrete so that the use of a condensed polyethylene, along with polycarboxylate, acting as defoamer, is recommended (Jalal *et al.*, 2012).
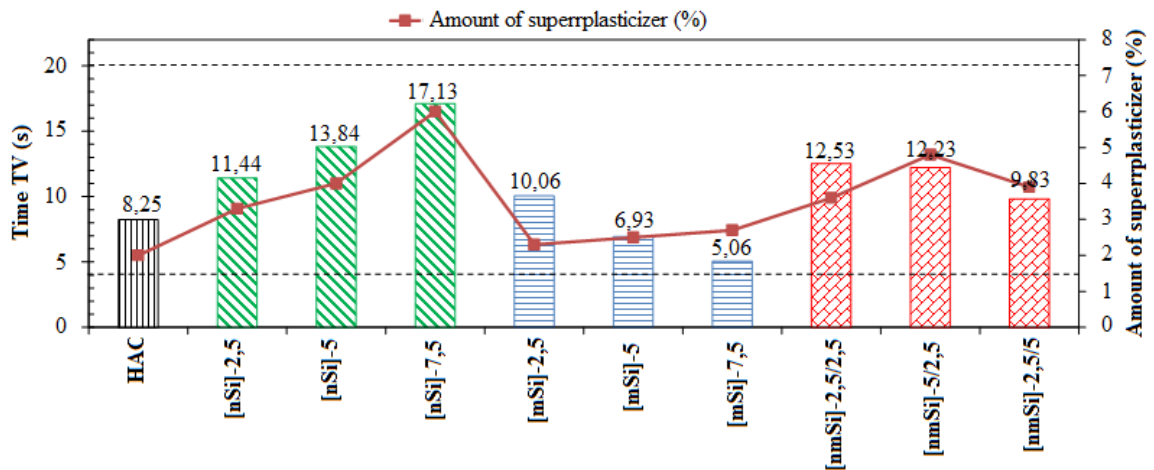
Figure 3. Time (TV) of passage (s) through the V funnel and amount of superplasticizer.

In figure 3, the passage time TV through the V funnel is shown. Also, for this parameter, the requirements of the EHE-08 are fulfilled with regard to the self-compacting characteristic, as the values vary between 4 s and 20 s.

In it, it can be observed that the behavior of the mixtures is clearly different. Those that contain only nSi increase TV as the content in nSi is increased, meaning, they densify, whereas in the mSi mixtures the effect is the opposite, reducing the TV down to 5.06 seconds when the content of mSi is of 7.5% with regard to the amount of cement. In both cases, an increase in SP is necessary—the quantity of it being rather superior in the dosages with nSi. Therefore, it can be confirmed that in the mixtures with nSi, with a similar amount of SP, similar d_f are achieved, though the mixture becomes more liquid due to the action of the higher amount of SP in them. The binary mixtures present a behavior that is somewhat inconclusive, as with a higher content of nSi there is a greater demand for SP even though its TV is similar, making the mixture more viscous when increasing the amount of mSi even though the demand of SP is lower. These results are inconsistent with the ones obtained by Jalal *et al*. (2012), who obtained a minimum passage time through the V funnel of 4 s for the mixture with 500 kg/m³ and a 2% of nSi, and maximum (12 s) for the binary mixture of 10%mSi+2%nSi and 400 kg/m³. The differences in the contents of the cement could be the reason for these significant differences in the results, as an increase in the amount of cement improves all rheological properties due to an increase in the volume of the paste (Jalal *et al*., 2012). In figure 4, the measure of the capacity of passage C_{bl} can be observed, with all the concretes having values that remain within the limit values of 0.75 and 1. Despite this fact, a different behavior can be observed according to the type of addition. Thus, the capacity of passage for mixtures with nSi experiences a decrease when increasing the amount of nSi.
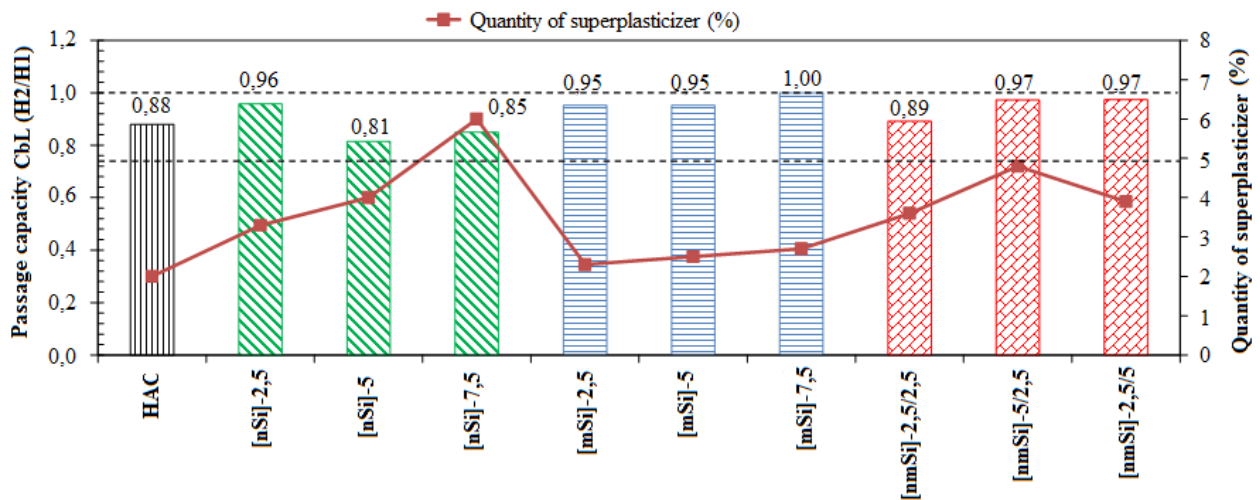
Figure 4. Passage capacity through the L shaped box and quantity of superplasticizer.

Furthermore, this parameter provides information on the capacity of self-leveling of the concrete (EHE-08, 2010), being less self-leveling when the content of nSi is higher. However, the values remain practically constant for both the dosages with nSi as well as for the mixtures with binary additions. It is worth noting the great self-leveling capacity of the concrete that contains a total of 7.5% of mSi with a value of the unit. This good behavior can be due to the fact that this mixture is the one that presents the minimum velocity of PV passage, i.e., it is the most liquid mixture of all the ones that were studied.

In figure 5, the value of the slump-flow diameter combined with Japanese ring (d_{jf}) is shown. The EHE-08 limits the value of this parameter regarding the slump-flow diameter (d_f) obtained in the

same mixture, having to comply in that its difference be inferior to 50 mm, which is fulfilled for the entirety of the designed mixtures.
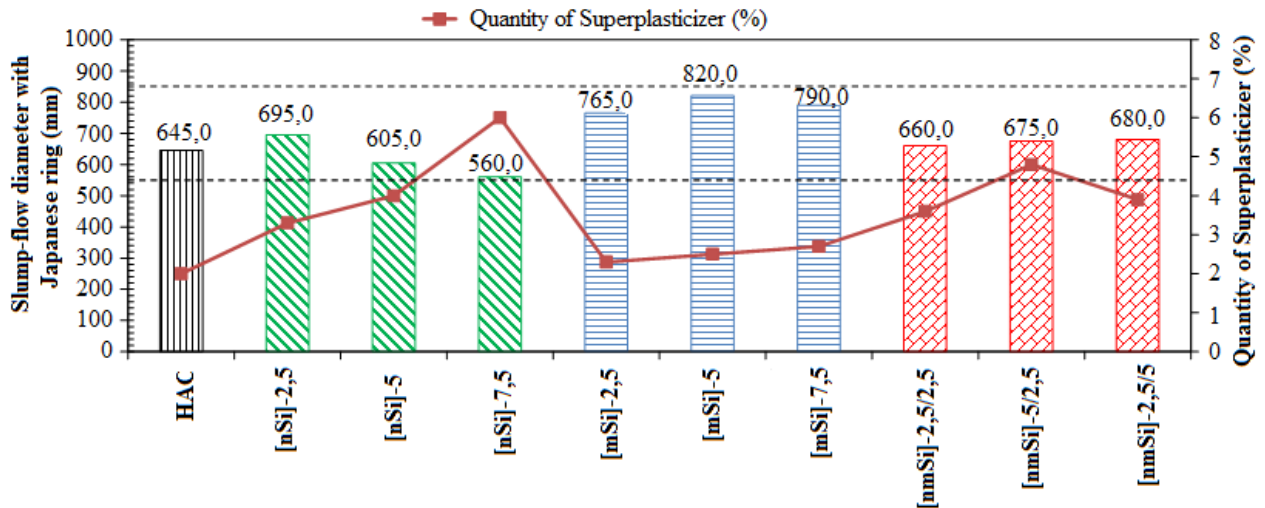
Figure 5. Slump-flow diameter with Japanese ring (cm) and quantity of superplasticizer.

When observing figure 5, it stands out that the concretes with the addition of nSi have a similar behavior to that of the slump-flow test (d_f), though with inferior values, given that with this it is possible to determine the difficulty that the concrete could have when passing through obstacles. Therefore, the greater quantity of nSi the lower the value of this parameter. The highest values are seen in concrete with mSi. In the mixtures with binary additions, the values do not show significant differences among them, not even with the one obtained in [nSi]-2.5. This indicates that it is the content of nSi that governs these mixtures, having to increase the content of SP when the content of nSi increases. An important observation in the manufacture of the mixtures was that the concretes with additions of nSi obtained a significant increase in setting speed where, no matter the amount of SP added, the start of the setting was produced a few minutes after the manufacture. This would make it difficult to manipulate the mixture and, therefore, its implementation. However, this phenomenon could be an advantage in the industry of prefabs, wherein a quick setting could be beneficial due to the possibility of demolding in shorter periods of time. This fact coincides with the studies by Bjornstrom *et al*. (2004), who state that the nSi is a catalyst for the pozzolanic reactions.

3.2 Mechanical properties
3.2.1. Resistance to compression
The resistance to compression of the different dosages is presented in Figure 6. There, it can be observed that the concretes with nSi have higher resistance to that obtained in the reference concrete. Furthermore, said resistance increases as the amount of additive increases.
In the case of concretes with mSi, the resistance to compression is slightly higher for the reference concrete, with notable increases in 7 days and moderate for the rest of the ages. Lastly, and in the case of the mixtures with binary additives, there is no consistent behavior that suggests the preponderance of one of the types of additives. However, the highest resistances were obtained with the [mmSi]-2.5/2.5 mixture, and so the authors consider that the resistance to compression not only depends on the size of the particle and on the amount of additive, but also on the granulometric distribution of all the components of the mixture. Therefore, when there is a higher continuity in

the granulometry of the components of the mixture, the higher their compression will be and thus the greater their resistance.

In these mixtures, the resistance values for compression are of 82.17 MPa at 28 days of being cured and of 86.87 MPa at 90 days. This implies an 36% increase with regard to the values obtained for the reference concrete at the curing times of 28 and 90 days, respectively.
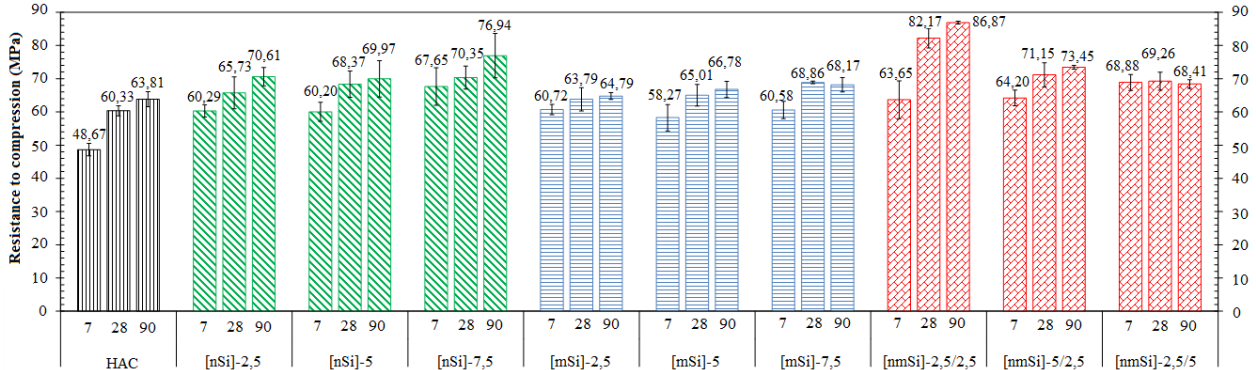
Figure 6. Resistance to compression (MPa)

3.2.2. Resistance to indirect traction and modulus of elasticity

In figures 7 and 8, we present the results to indirect traction resistance as well as the results of the modulus of elasticity.

The value of indirect traction in concretes with additives is significantly higher to the value of the reference concrete, even if these are small differences. However, there are no significant differences between the mixtures with additives. This means that the size and the content of the different additives contained in the different mixtures does not change this property significantly.

Regarding the modulus of elasticity, it can be observed that there are significantly lower values for the mixtures that contain nSi. In the rest of the concretes, the values obtained are similar without them being significant among them or with regard to the reference concrete.
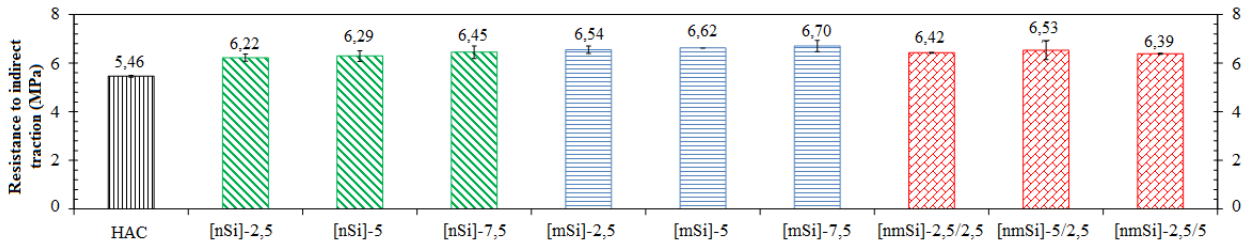
Figure 7. Resistance to indirect traction (MPa)
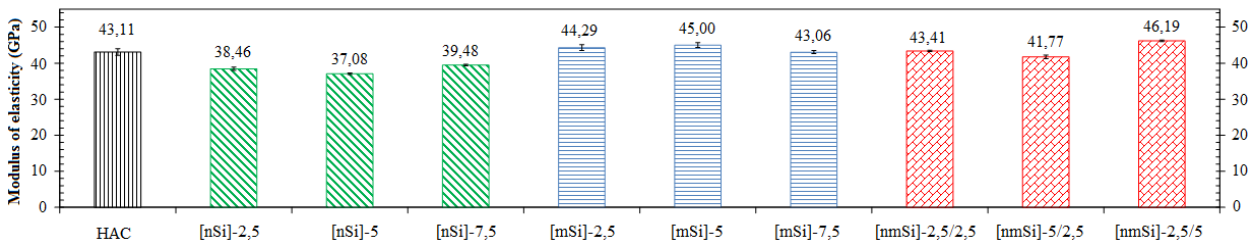
Figure 8. Modulus of elasticity (GPa)

3.3 Microstructural characterization. Thermogravimetric analysis

The results of the thermogravimetric analysis of the ten dosages are shown in Figures 9, 10, and 11 in which the relation between the losses of gel water and of free portlandite water are shown at 7, 28, and 90 days after curing, respectively.

In general, the values obtained allow us to state that, at all ages, the highest values of said relation are the ones obtained in concretes with nSi. This brings to light the fact that the formation of secondary gel or tobermorite gel is higher, which implies a lesser presence of portlandite.
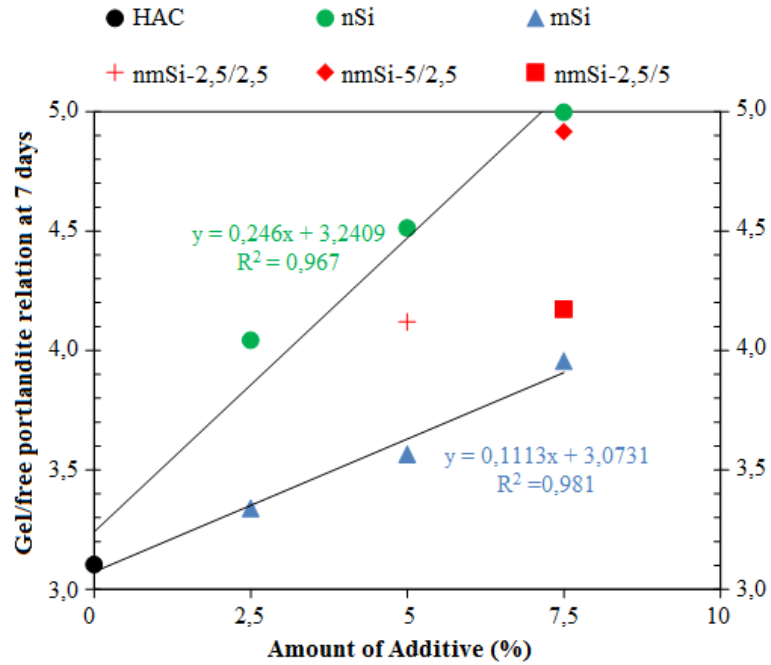
Figure 9. Gel/free portlandite relation at 7 days after curing
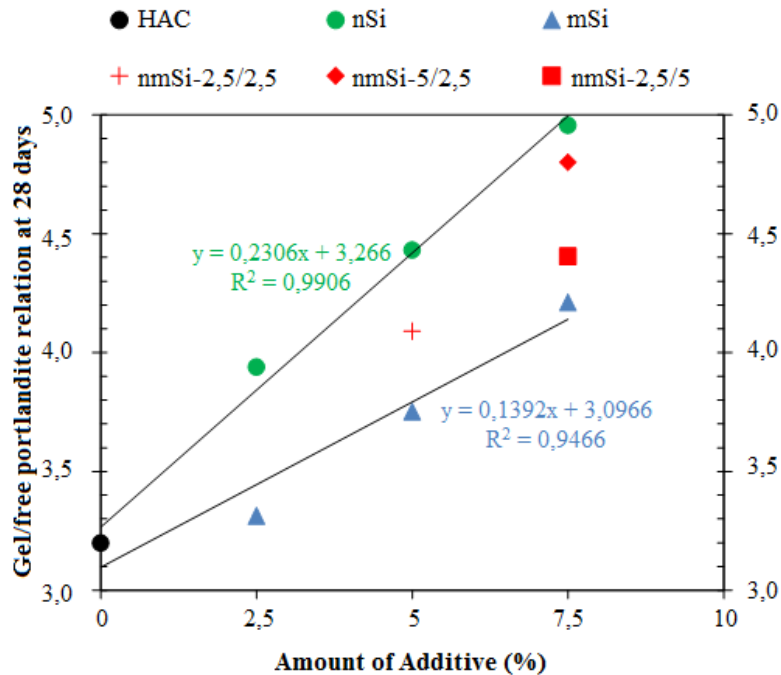
Figure 10. Gel/free portlandite relation at 28 days after curing
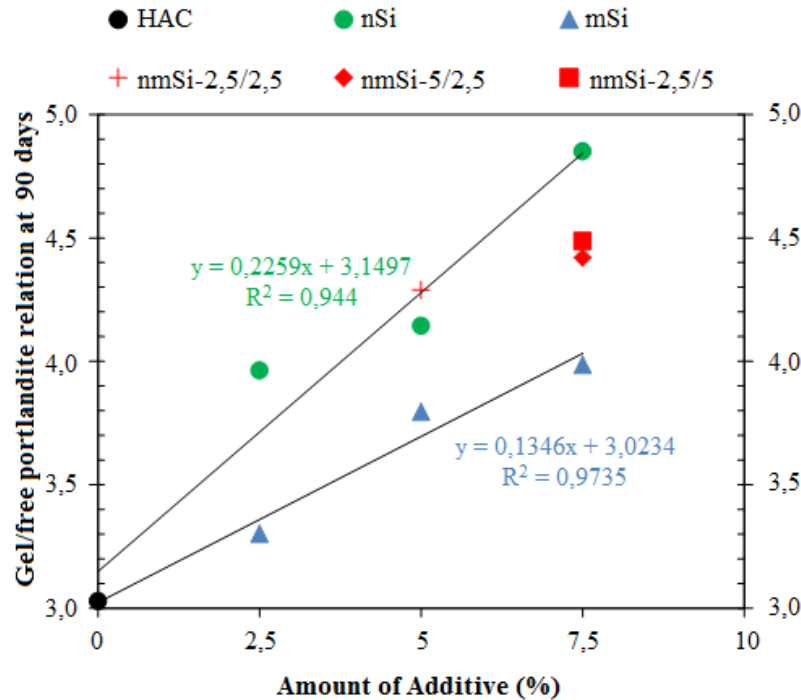
Figure 11. Gel/free portlandite relation at 90 days after curing

Similarly, in the case of concretes with mSi, the relations show lower values, which are consistent with the results obtained by Mondal *et. al.* (2010), Zyganitidis *et al.* (2011), Jalal *et al.* (2012), and León *et al.* (2014). In both cases, the relation increases with the content of the additive. As previously stated, the concretes with a combination of additives do not present a conclusive behavior. The behavior seems to be defined by the higher content of each one of the additives.

On the other hand, it is important to highlight that as curing time passes, the mixtures with nSi show a decrease in the values of the gel/free portlandite relation, a phenomenon that is evidenced by the reduction in the slopes of the lines. This phenomenon can be observed in a progressive manner in Figures 9, 10, and 11. This suggests that the formation of gels is slowed down with the age of curing, being during the early ages when a greater pozzolanic activity can be observed (Jalal *et al.*, 2012). This is consistent with the resistance values to compression at 7 days after curing. However, in concretes with mSi, the values of the gel/free portlandite relation increase as the curing time increases. A smaller particle size accelerates the activation of the pozzolanic reaction.

When analyzing the concretes that comprise binary mixtures, it stands out that in the first ages, the composite mixtures behave in a similar manner to the mixtures that contain a similar additive percentage to the combination of the two, but in each case, they are close to the additive with the higher percentage. When the percentage of both additives is the same, the behavior is practically intermediate. Given that the evolution in time of the micro and nano additive is different, the mixtures that contain both begin matching their behavior, resulting in an intermediate behavior at 90 days to the one that is obtained for the same percentage of each additive. The mixture with 2.5 of nano and micro silica has a differential behavior at longer ages. In this case, their gel/portlandite relation is superior to the one obtained using 5% of nano silica. This result is consistent with the mechanical and durability behavior of the mixture. This behavior could indicate that in this dosage, the relation between the surface of the additive and the free water has been optimal.

4. CONCLUSIONS

The incorporation of nSi generates a loss of workability of the material associated to an increase in the setting speed; a phenomenon that complicates its placement. The viscosity and adaptation to the mold is significantly hindered when nSi is incorporated to the mass. The concretes with a content of 7.5% of mSi or with binary mixtures [nmSi]-5/2.5; [nmSi]-2.5/5 may be considered concretes with a self-leveling capacity. However, the addition of nSi as the only additive implies the loss of this property. The difficulty that the concrete may have due to obstacles increases with a higher amount of nSi. Nevertheless, in concretes with mSi or with binary additives, this property can be considered independent from the content of said additives, even though it is important to note that it is the mixtures with mSi that present a better behavior.

The incorporation of nSi generates a significant increase in the resistance to compression when compared to the concretes with mSi and to the one used as reference. It is the [nmSi]-2.5/2.5 mixture that represents the highest values. Considering all the components of the concrete, this could be due to a more continuous granulometric distribution, being that there is less formation of holes, therefore obtaining a more compact concrete. The incorporation of nSi, mSi, or binary mixtures of both additives cause a slight increase in the value of indirect traction in the designed concretes. The concretes with only nSi show a decrease in their modulus of elasticity, which entails having mixtures with less ductility.

The concretes with mSi show the highest values in the relations between the loss of gel water and that of portlandite during the first stages, which confirms that the formation of secondary gel or tobermorite is higher when nano additives are used. Similarly, in the case of the concretes with mSi, the relations show lower values, which is consistent with the lower resistance that they present. In binary mixtures with the same total amount of additives and with longer ages, the values of the relation come close to the intermediate values of the two additives in the same ratio. The uniquely good behavior of the [nmSi]-2.5/2.5 mixture could suggest that there is an optimal surface / free water relation that could improve the behavior of any of the two individually studied additives.

5. ACKNOWLEDGEMENTS

6. REFERENCES

Bjornstrom, J., Martinelli, A., Matic, A., Borjesson, L., Panas, I. (2004), "*Accelerating effects of colloidal nano-silica for beneficial calcium-silica-hydrate formation in cement*", Chem Phys Lett 392 (1-3), 242-248.

Borralleras, P. (2012), "*Criterios de selección del aditivo superplastificante en HAC*", 3° Congreso Iberoamericano sobre hormigón autocompactante: Avances y oportunidades., 3-4 diciembre. Madrid. España.

Craeye, B., Van Itterbeeck, P., Desnerck, P., Boel, V., De Schutter, G. (2014), "*Modulus of elasticity and tensile strength of self-compacting concrete: Survey of experimental data and structural design codes*", Cement and Concrete Composites 54, 53–61.

De la Peña R. Bernardo (2001), "*Hormigón Autocompactante*", Revista BIT, pp. 7-12.

Dubey, R., Kumar, P. (2012), *"Effect of superplastizer dosages on compressive strength of self compacting concrete"*, International Journal of civil, structural, environmental and infrastructure engineering research and development vol. 2, (3), pp 98-105.

EHE-08. (2010), *"Instrucción de Hormigón Estructural"*, Serie Normativa, Ministerio de Fomento. Secretaría General Técnica. 4ª Edición. Madrid. España.

Jalal, M., Mansouri, E., Sharifipour, M., Pouladkhan, A. R. (2012), *"Mechanical, rheological, durability and microstructural properties of high performance self-compacting concrete containing SiO$_2$ micro and nanoparticles"*, Materials and Design 34, 389–400

Kawashima, S., Hou, P., Corr, D. J., Shah, S. P. (2013), *"Modification of cement-based materials with nanoparticles"*, Cement and Concrete Composites. 36, 8-15.

León, N., Massana, J., Alonso, F., Moragues, A., Sánchez-Espinosa; E. (2014), *"Effect of nano-Si$_2$O and nano-Al$_2$O$_3$ on cement mortars for use in agriculture and livestock production"*, Biosystems engineering 123, 1-11.

Mondal, P., Shah, S. P.; Marks, L. D.; Gaitero, J. J. (2010), *"Comparative Study of the Effects of Microsilica and Nanosilica in Concrete"*, Transportation Research Record: Journal of the Transportation Research Board, nº 2141, Transportation Research Board of the National Academies, Washington, D.C., pp. 6–9.

Nazari, A., Riahi, S. (2010), *"Microstructural, thermal, physical and mechanical behavior of the self-compacting concrete containing SiO$_2$ nanoparticles",* Materials Science and Engineering A 527.7663–7672.

Okamura, H., Ozawa, K. (1996), *"Self-compactable high-performance concrete in Japan"*, ACI publicación especial SP159-02, pp. 31-44.

Okamura, H. (1997), *"Self-compacting high-performance concrete"*, Concrete International, 19 (7), pp. 50-54.

Okamura, H., Ouchi, M. (1999), *"Self-compacting concrete development, present and future"*, Proceedings of the First International RILEM Symposium, pp. 3-14.

Okamura, H., Ozawa, K., Ouchi, M. (2000), *"Self compacting concrete"*, Structural Concrete, 1, pp. 3-17.

Okamura, H., Maekawa, K., Mishima, T. (2005), *"Performance based design for self-compacting structural high-strength concrete"*, ACI publicación especial SP228-02, pp. 13- 33.

Rong, Z., Sun, W., Xiao, H., Jiang, G. (2015), "*Effects of nano-SiO$_2$ particles on the mechanical and microstructural properties of ultra-high performance cementitious composites"*, Cement and Concrete Composites 56, 25–31.

Said, A. M.; Zeidan, M. S.; Bassuoni, M. T., Tian, Y. (2012), *"Properties of concrete incorporating nano-silica"*, Construction and Building Materials 36. 838–844.

Sánchez, F., Sobolev, K. (2010), "*Nanotechnology in concrete – A Review"*, Construction and Building Materials. 24 2060–2071.

Yu, R., Spiesz, P., Brouwers, H. J. H. (2014), "*Effect of nano-silica on the hydration and microstructure development of Ultra-High Performance Concrete (UHPC) with a low binder amount"*, Construction and Building Materials 65,140–150.

Zyganitidis; I.; Stefanidou, M.; Kalfagiannis; N.; Logothetidis S.; (2011), "*Nanomechanical characterization of cement-based pastes enriched with SiO$_2$ nanoparticles"*, Materials Science and Engineering B, 176, 1580-1584.

ALCONPAT Journal

http://www.revistaalconpat.org

Journal of the Latin-American Association of Quality Control, Pathology and Recovery of Construction

Mechanical and chemical behavior of calcium sulfoaluminate cements obtained from industrial waste

M. Gallardo H.[1], J. M. Almanza R[1]., D. A. Cortés H.[1], J. C. Escobedo B.[1]

[1]Centro de Investigación y de Estudios Avanzados del Instituto Politécnico Nacional, Av. Industria Metalúrgica 1062, Parque Industrial Saltillo-Ramos Arizpe, Ramos Arizpe, Coah., Mexico, Zip Code 25900.

© 2016 ALCONPAT International

ABSTRACT

A calcium sulfoaluminate clinker was synthesized calcining a mixture of fly ash, fluorogypsum, aluminum slag, and calcium carbonate at 1250 ℃. The clinker was mixed with 15, 20, or 25% e.p. of $CaSO4 \cdot \frac{1}{2}H_2O$. The pastes were prepared with a water/cement ratio of 0.5. Compression resistance of cements cured in potable water and corrosive mediums at 40 ℃ was evaluated. The cements cured in potable water developed compressive strengths of 38-39 MPa; those immersed in corrosive mediums showed a decrease in this property after the chemical attack. Ettringite was the main product of hydration. The degradation of the cements by chemical attack was due to a decalcification and dealumination of the pastes.
Keywords: calcium sulfoaluminate; ettringite; compressive strength; chemical attack.

RESUMEN

Se sintetizó un clínker de sulfoaluminato de calcio calcinando una mezcla de ceniza volante, fluoryeso, escoria de aluminio y carbonato de calcio a 1250 °C. El clinker fue mezclado con 15, 20 o 25 % e.p. de $CaSO_4 \cdot \frac{1}{2}H_2O$. Las pastas se prepararon con relaciones agua/cemento de 0.5. Se evaluó la resistencia a la compresión de cementos curados en agua potable y en medios corrosivos a 40 °C. Los cementos curados en agua potable desarrollaron resistencias a la compresión de 38-39 MPa, los inmersos en medios corrosivos presentaron una disminución en esta propiedad después del ataque químico. La etringita fue el principal producto de hidratación. La degradación de los cementos por ataque químico es debida a una descalcificación y dealuminación de las pastas.
Palabras clave: sulfoaluminato de calcio; etringita; resistencia a la compresión; ataque químico

RESUMO

Foi produzido um clínquer de sulfoaluminato de cálcio a partir da calcinação a 1250°C de uma mistura de cinza volante, escória de alumínio, carbonato de cálcio e gesso de flúor. Esse clínquer foi misturado com 15%, 20% e 25% e.p. de $CaSO_4 \cdot \frac{1}{2}H_2O$. As pastas foram preparadas com relação água/cimento igual a 0,5. Foi avaliada a resistência à compressão das pastas curadas em água potável e em meios corrosivos a 40°C. As pastas curadas em água alcançaram resistências à compressão de 38-39 MPa, enquanto as pastas imersas em meios corrosivos apresentaram uma redução da resistência frente ao ataque químico. A etringita foi o principal produto da hidratação desses cimentos. A degradação dessas pastas de cimento por ataque químico ocorreu devido a uma descalcificação e dealuminização dos produtos hidratados.
Palabras-clave: sulfoaluminato de cálcio; etringita; resistência à compressão; ataque químico.

_____
Corresponding author: Marisol Gallardo Heredia (marisol.gallardo@uadec.edu.mx)

1. INTRODUCTION

Cement is a material utilized in the construction of cities and houses, with a growing demand dependent upon demographic growth. The use of concretes constituted with appropriate materials, conveniently provided and well-consolidated, ensures the durability of the constructions. The most frequently used binding material in construction is Portland cement; however, in its production processes large quantities of fossil fuels and, in a parallel manner in its decarbonation process of raw materials large quantities of CO_2, are emitted into the atmosphere, contributing around 7% of the global CO_2 emissions (Roy et al., 1999; Gartner et al., 2004). There are a variety of alternative and viable materials (industrial wastes) that can be used for the substitution of Portland cement. Their use is based on the importance of minimizing CO_2 emissions, as well as increasing interest in the production of cementive materials that develop good mechanical properties and good stability in corrosive environments.

An alternative to partially or completely substitute the use of Portland cement is the manufacture of calcium sulfoaluminate (CSA) cement which presents a crystalline structure that consists of a tridimentional arrangement of AlO_4 tetrahedrons interlinked with Ca^{+2} and SO_4^{-2} ions located in the existent intervals (Sharp J.H. et al., 1999). This type of cement has low CO_2 emissions, forming at a temperature of approximately 1250 ºC, in addition to developing good mechanical properties (compression resistance) (Older, 2005; Zhou et al., 2006; Garcia-Maté et al., 2015; Hargis et al., 2014). On the other hand, there is a large quantity of wastes such as slag, gypsum, and fly ash among others, that show considerable quantities of Al_2O_3, CaO, and $CaSO_4$ in their chemical composition, these being the main components for the production of CSA clinkers. An important advantage derived from the manufacture of this clinker from industrial waste is the decrease in air, soil, and visual contaminations that these create (stored outdoors) and the decrease in CO_2 emissions to the environment. Li et al. reported the synthesis of CSA utilizing high alumina fly ash, bauxite, and limestone as the starting materials (Li et al., 2007), where the main stages of synthesis were CSA and tricalcium silicate (C_3S). A sulfoaluminate-belita was synthesized at 1150 ºC from fly ash, powders, and muds collected from industrial processes. As a product of synthesis, the clinker obtained showed stages such as gehlenite (formed by the decomposition of belita at temperatures higher than 1100 ºC), CSA, and belita (Li et al., 2001). During the synthesis of CSA utilizing industrial wastes, the formation of gehlenite is obtained as a secundary product of synthesis, this stage being responsible for the decreased formation of CSA (Arjunan et al., 1999). The synthesis of a sulfoaluminate-ferrite through the use of lime, gypsum, red mud, and bauxite at 1250 ºC showed stages such as $C_4(A_3F)_3\bar{S}$, C_4AF, and C_2F. The density of this increased with the rise in the quanity of red mud; finally, the hydration products formed were ettringite and $C_3(AF)H_6$ (Singh et al., 1997). The use of waste from fertilizer, bauxite, and mineral iron processing facilities as raw material for the synthesis of CSA at 1230 ºC generated stages such as CSA, C_4AF, C_2AF, $2C_2S\cdot C\bar{S}$ and a small quantity of free lime. A larger quantity of mineral iron increased the quantity of C_4AF and decreased the quantity of CSA (Singh et al., 2008). CSA has been synthesized from a mixture of jarosite-alunite and waste from a hydrometallurgic process (developed to economically treat ores from low-grade nickel oxides) at 1300 ºC (Katsioti et al., 2005). In general, the pastes prepared with the clinkers obtained from the mentioned industrial wastes or byproducts showed good mechanical properties. Ettringite is the main product of hydration in a CSA cement, occuring as a natural process of the combination of this cement, water, and calcium sulfate (Mehta, 1967). The characteristic morphology of ettringite is comprised of crystals that exhibit hexagonal prisms or plaques (Moore et al., 1968). The formation of ettringite in the first stages of hydration contributes to the development of the mechanical properties. However, the development or

formation of this phase in later stages (delayed ettringite formation, DEF) can be detrimental. The DEF in hardened cementive materials generates micro-cracks deteriorating the mechanical properties, this is due to it being considered expansive. In many cases, DEF is attributed to an excessive quantity of sulfates present in the cement (Taylor, 2001; Gallardo M. et al., 2014). The development of the physical and chemical properties of new construction materials in environments similar to those in which Portland cement is exposed to on a daily basis has given rise to interest in this area of research. Studies have been performed on the durability or chemical stability of various types of cements, whose purpose is the study of the behavior of the reactions that occur on these construction materials varying the conditions to which they are exposed on a daily basis. For example, research on the chemical attack on Portland, pozzolanic, and slag concretes was carried out simulating acid rain with a H_2SO_4 and HNO_3 solution with a pH of 3.5. The results indicated that calcium hydroxide is the compound in which the attack of the solutions begins; therefore, it could act as a barrier against the attack of hydrated silicates. The pozzolanic concretes showed a greater attack than those prepared with slag. The diffusion increased at high water/cement ratios due to the high permeability (R. Sersele et al., 1997). Studies were performed on the chemical durability of an API cement class B (utilized in oil wells) in order to determine the effects resulting from SO_4^{-2}, Mg^{+2}, and Cl^- ion attacks that were carried out using Na_2SO_4, NaCl, and $MgCl_2$ aqueous solutions as the curing medium. The formation of tobermorite, portlandite ettringite, and monocloroaluminate was detected as the result of the transformation of the anhydrous stages of the cement. Portlandite increased in quantity with the passage of time. The interaction between the SO_4^{-2} ions and the cement generated partially soluble gypsum, which subsequently reacted with C_3A facilitating the formation of ettringite. The Cl^- ions were chemically bound to the hydrated calcium aluminates resulting in the formation of Friedel salt. The Mg^{2+} ions contributed to the decalcification of the cement and in turn reacted with hydroxyl, giving rise to the formation of brucite (Martin J.J. et al., 2008). The study of the chemical durability of a geopolymer prepared with metakaolin exposed to an HCl solution for 10 days with a concentration of 0.5 N at 60 ℃ resulted in a degradation of the pastes due to the destruction of the geopolymeric structure and the release of Na, Al, and Si towards the acidic solution. An exchange of ionic species was evidenced between H_3O^+ and Na^+. The chemical attack was more intense on pastes with a higher $SiO_2/Al_2O_3=3$ and $Na_2O/Al_2O_3=0.55$ ratio, with a 33.1% loss of their initial resistance. Pastes with a lesser $SiO_2/Al_2O_3=2.6$ and $Na_2O/Al_2O_3=0.55$ ratio only lost 2% of their initial resistance. The mechanism involved in the deterioration was the ionic exchange of the HCl dissociation on Cl^- and H_3O^+ ions, where Cl^- ions neutralized charges with Na^+ ions giving rise to a NaCl precipitation (Burciaga-Diaz O. et al., 2007). The objective of this paper is the development assessment of the compressive strength and chemical stability of calcium sulfoaluminate cements synthesized from a mixture of fly ash, aluminum slag, and fluorogypsum at 1250 ℃.

2. EXPERIMENTAL PROCEDURE

The materials utilized were fly ash (fa), aluminum slag (as), and fluorogypsum (fg). The latter two were subject to a grinding process until a particle size less than 106 µm (#140 ASTM mesh) was obtained. Subsequently, the chemical composition of each material was analyzed through X-ray fluorescence (XRF), the results of which are shown in Table 1.

Table 1. Chemical composition in oxides of the raw material.

Oxides	Aluminum Slag as (e.p. %)	Fly Ash fa (e.p.%)	Fluorogypsum fg (e.p.%)
Na_2O	2.496	-	-
MgO	5.000	1.377	-
Al_2O_3	63.19	24.81	-
SiO_2	11.69	59.49	0.103
SO_3	0.833	-	56.33
Cl_2	4.636	-	-
K_2O	2.203	1.716	-
CaO	7.263	4.806	43.24
TiO_2	0.983	1.663	-
MnO	0.503	-	-
Fe_2O_3	1.203	6.126	-

Based on the chemical composition, the wastes were mixed in the required proportions in order to obtain CSA in accordance with the following reaction: as + fa + fg + $CaCO_3$ = CSA (80% e.p.) + Ca_2SiO_4 (20% e.p.). The proportions of each starting material were adjusted with $CaCO_3$ (97% purity). The starting materials were homogenized in plastic containers with acetone and alumina balls for 4 hours; they were subsequently dried at 80 ºC for 12 hours. Pills 2 cm in diameter were made through uniaxial pressing at 45 MPa, which were then subject to thermal treatment at 1250 ºC for 4 hours. The formation of the CSA was corraborated through X-ray diffraction. The clinker obtained was grounded until obtaining a specific superficial area of approximately 3800 cm^2/g (ASTM C-204), and was subsequently mixed with 15, 20, or 25% e.p. calcium sulfate ($CaSO_4 \cdot \frac{1}{2}H2O$) in order to prepare the CSA cement. The pastes were prepared with a water/cement ration of 0.5 in accordance with the procedure indicated in the Mexican standard NMX-C-085-ONNCC-2002 (NMX-C-085). The nomenclature of the systems was the following: 515, 520, and 525, where the first number indicates the water/cement ration and the latter two indicate the calcium sulfate content. The mixtures were emptied into Nyalcero molds and vibrated for 60 seconds in order to eliminate porosity. The already filled molds were covered with plastic and placed in isothermic chambers at 40 ºC for 24 hours. Subsequently, the cubes were removed from the molds and placed in containers with water (potable water) in order to begin humid curing at the aforementioned temperature for 1, 3, 7, 14, or 28 days; after each curing period, the compressive strength was evaluated. For the effect of comparison, Ordinary Portland cement (OPC commercial) samples were elaborated as control references. These samples were elaborated and cured under the same conditions as the CSA-based cements.

For chemical durability tests, samples were cured for 7 days in potable water which were subsequently submerged in corrosive mediums for 14, 28, or 42 days for the chemical resistance evaluating by means of measuring their compressive strength. The samples were submerged in 2 liters of H_2SO_4 0.5 N, $MgCl_2$ 06 N, and Na_2SO_4 0.04 N solution (elaborated with deionized water) at 40 ºC in order to simulate aggressive conditions. The compressive strength measurements were done in an automated hydraulic press (Controls model 50-C7024) with a 250 kN capacity, using a loading speed of 350 N/s. The tests were done in accordance with the procedure described in the standard ASTM C109/C109-M95 (ASTM-C109). In order to identify the stages present resulting from the hydration reactions and the chemical attack, samples with 28 (potable water) and 42 (corrosive medium) days of immersion were analyized through X-ray diffraction (XRD).

Fragments were selected, preferably from the surface of each one of the cubes tested in a chemical attack, and were submerged in methanol and dried for 48 hours in an oven at 40 ºC. Samples were analyzed before and after the chemical attack through Scanning Electron Microscopy (SEM).

3. RESULTS

Figure 1 shows the diffraction pattern of the synthesized clinker at a temperature of 1250 ºC. The reflections corresponding to the CSA were primarily observed. Secondary stages such as gehlenite ($Ca_4Al_2SiO_7$), calcium aluminate ($CaAl_2O_4$), mayenite ($Ca_{12}Al_{14}O_{33}$), and pleochroite ($Ca_{20}Al_{26}Mg_3Si_3O_{68}$) were formed. Belite ($Ca_2SiO_4$) was obtained in a lesser percentage than what was intended due to the thermodynamic stability of secondary stages formed at 1250 ºC. On the other hand, gehlenite and spinel are considered non-cementing stages due to their small or lack of reactivity in the presence of water, but these could act as reinforcement stages.
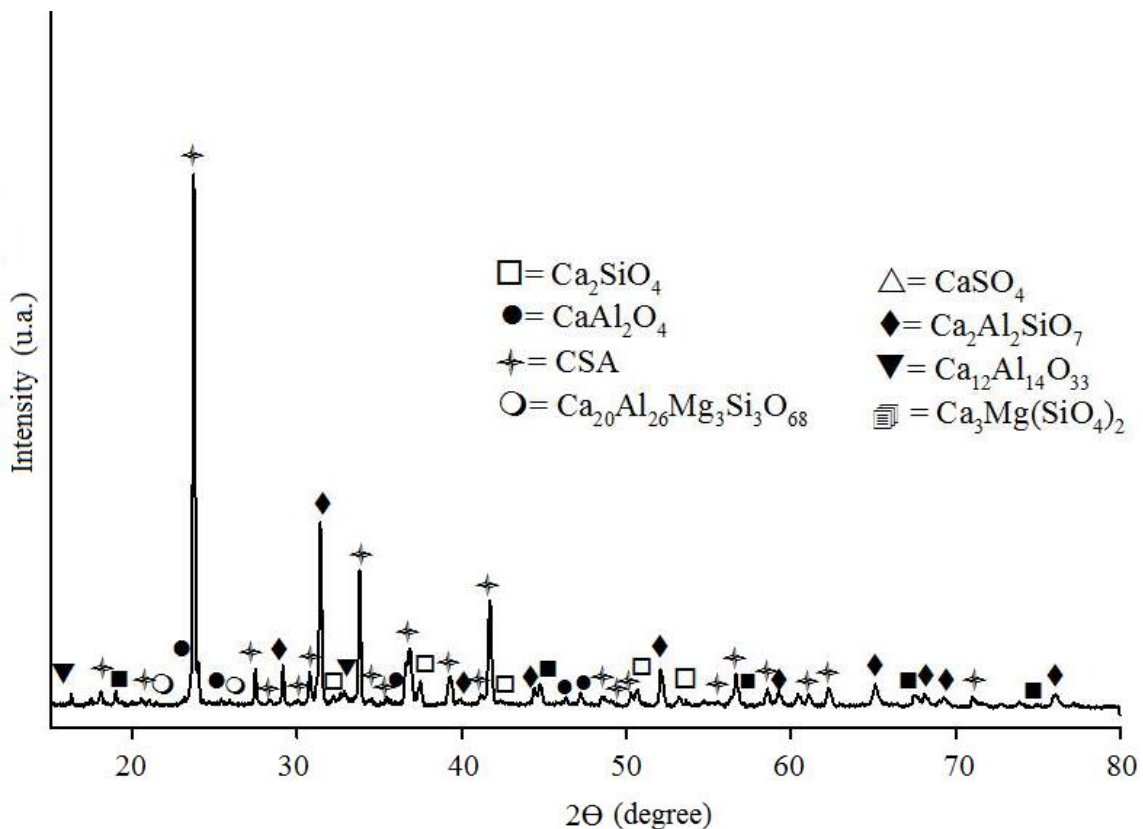
Figue 1. XRD pattern of the synthesized at 1250 ºC.

Figure 2 shows the compressive strength results of systems 515, 520, and 525 cured from 1 to 28 days at 40 ºC. In system 515, a gradual development of the compressive strength was observed from day one and up to 14 days; at 28 days the compressive strength decreased, favored by the delayed ettringite formation. System 520 showed a decrease in compressive strength at 7 days with a slight increase at 14 and 28 days; however, a low strength developed ending with 24.25 MPa. In system 525, an increase in the compressive strength was observed in function with time (from 1 to 14 days); at subsequent times it remained at the same strength of 38.9 MPa at 28 days. It is possible that ettringite formed almost in full during the first days of curing, and the subsequent increase is

due to the growth of this stage within the pores weak zones (micro-cracks). The presence of gypsum and CSA residue in the days following the start of the curing process indicates that the hydration reactions shall continue with the passage of time. This system showed the best compressive strength values. Based on the aforementioned, a greater quantity of gypsum increases the mechanical resistance due to the formation of the largest quantity of ettringite from the first days of curing. The compressive strength results obtained were found within the value established in the standard NMX-C061-ONNCCE-2001 (20-40 MPa at 28 days of curing). The experimentally obtained value for the OPC cement was 38 MPa.
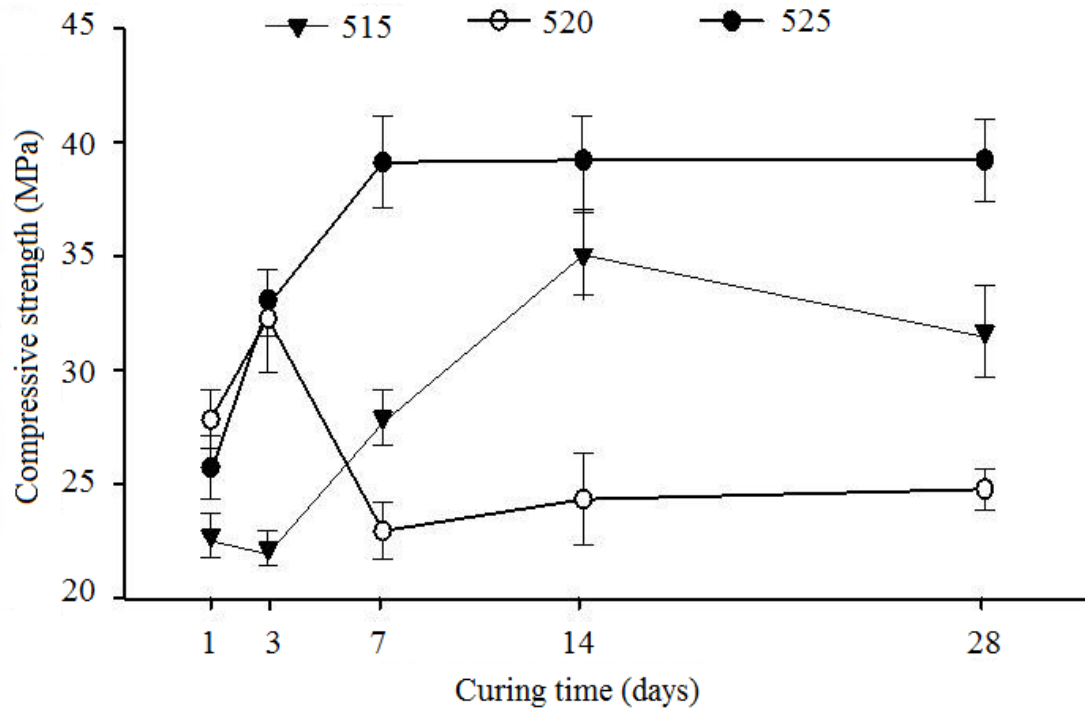
Figure 2. Compressive strength of systems 515, 520, and 525 cured at 40 °C.

Figures 3 and 4 show the XRD patterns of systems 515 and 525 at 1, 14, and 28 days of curing at 40 °C. In system 515 (Figure 3), during the first day reflections were observed corresponding to ettringite and these reflections increased in intensity at 14 and 28 days of curing. In system 525 (Figure 4), during the first day reflections were observed corresponding to the CSA and gypsum, these latter reflections were observed up to 14 days later. The reflections corresponding to ettringite were visible from day one and increased in intensity at 14 and 28 days. The gradual increase in intensity of the reflections of the hydration products indicated the delayed ettringite formation. This was not enough to affect the mechanical properties given that the increase of this stage possibly took place within the present pores. For both systems, reflections corresponding to the spinel and gehlenite were observed without apparent changes in the intensity of the reflections in function to the time of curing, due to these two stages being inert in the presence of water.
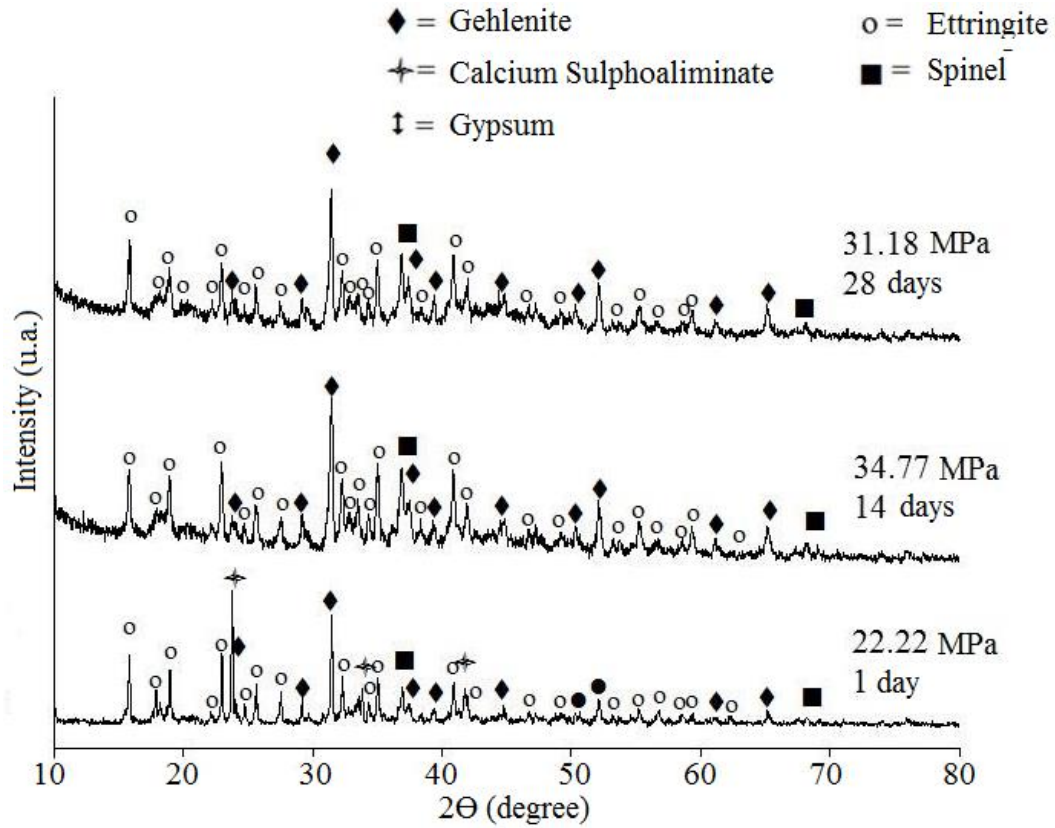
Figure 3. XRD patterns of system 515 at 1, 14, and 28 days of curing at 40 ℃.
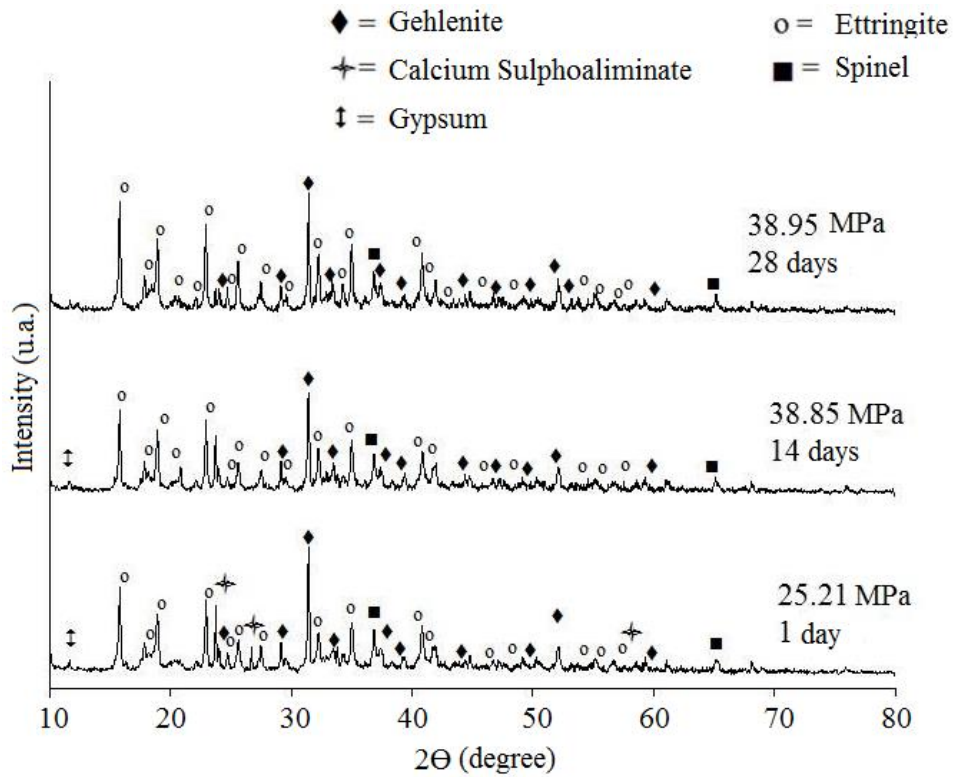
Figure 4. XRD patterns of system 525 at 1, 14, and 28 days of curing at 40 ℃

Figure 5 shows the micrographs of fracture surfaces of systems 515 and 525 at 1, 14, and 28 days of curing at 40 ℃. In system 515 during the first day, a dense microstructure is seen with the presence of some cracks distributed in the matrix. At 14 days, a microstructure is observed with a denser and more compact matrix where the cracks decreased in quantity explaining the increase in compressive strength that was presented in the curing time. At 28 days of curing, some weak zones were observed generated by the growth of hydrates giving rise to a decrease in the compressive strength of the material.
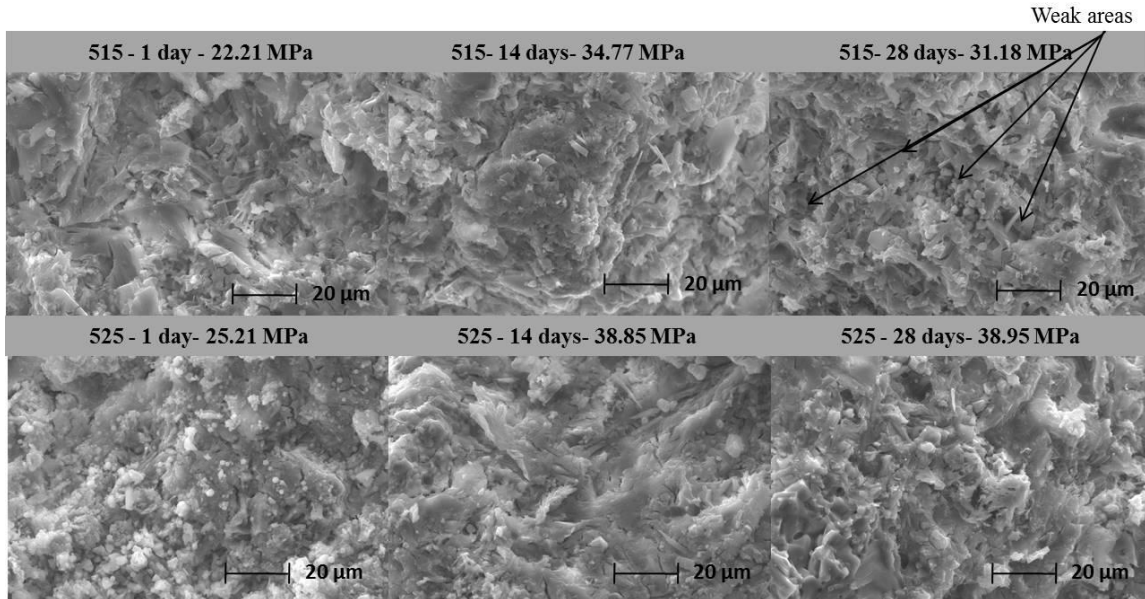
Figure 5. Micrographs of fracture surfaces of samples of systems 515 and 525 at 1, 14, and 28 days of curing at 40 ℃.

In the surface microstructures of system 525 on day one, white nodes were observed immersed in a dense ettringite matrix. These white nodes are associated with the formation of gypsum. At 14 days of curing, greater densification of the matrix was presented similar to the microstructure observed at 28 days, corroborating the similarity in mechanical properties at 14 and 28 days of curing. System 525 developed the best compressive strength, showing greater stability in function to time by not showing decreases in resistance. Due to the aforementioned, the stability of this system was evaluated immersed in aggressive solutions. Samples of this cement were cured for 7 days in potable water (38.95) and subsequently immersed in corrosive solutions.

Figure 6 shows the compressive strength results obtained from the samples after being immersed in corrosive mediums for 7, 14, 28, and 42 days at 40 ℃. The samples immersed in a solution of $NaSO_4$ 0.04 N developed the greatest compressive strength at 42 days of curing (34.63 MPa). The samples immersed in solutions of H_2SO_4 and $MgCl_2$ developed similar compressive strength at 42 days with values of 28.10 and 29.2 MPa, respectively. A decrease in compressive strength of 28.6 and 25.83% was observed in samples immersed in H_2SO_4 and $MgCl_2$ solutions, respectively. These variations could be attributed to the interaction of the samples with the Cl^-, Mg^{+2}, SO_4^{-2}, and Na^+ ions present in the corrosive solutions. The samples immersed in potable water did not show a decrease in compressive strength at any time during the curing (1-28 days).
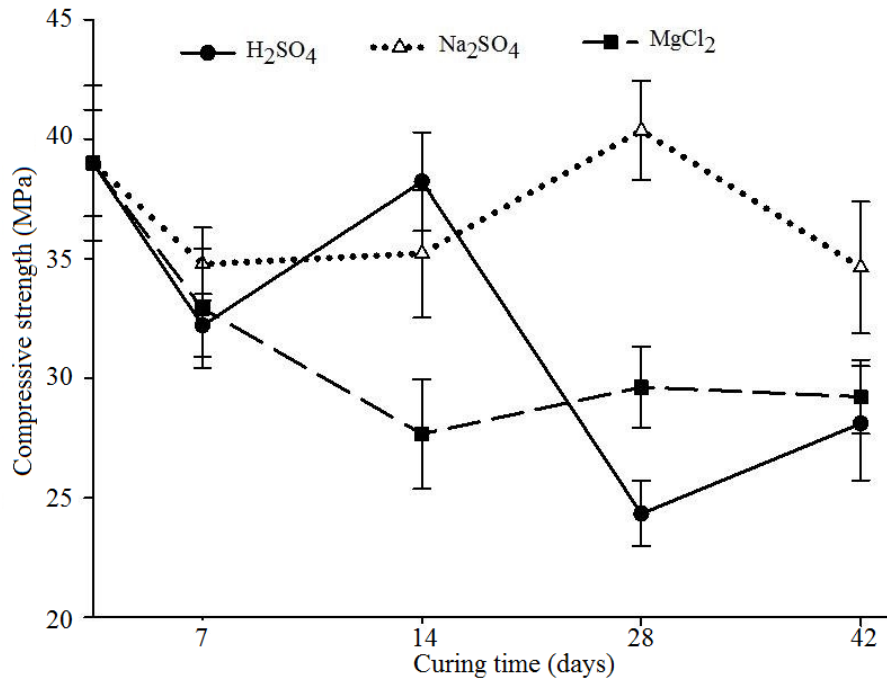
Figure 6. Compressive strength of system 525 cured in aggressive solutions at 40 °C.

The results obtained from the XRD characterization of the samples immersed in aggressive solutions at 42 days of curing are shown in Figure 7. High intensity reflections were observed corresponding to gypsum in samples immersed in a H_2SO_4 solution, indicating a degradation of the ettringite caused by the diffusion of SO_4^{-2} ions inside of the microstructure, causing a dissolution of the material. For samples immersed in $MgCl_2$ and Na_2SO_4, a pattern was observed similar to the one described above, except that the reflections corresponding to gypsum had low intensity indicating a moderate attack on the material.
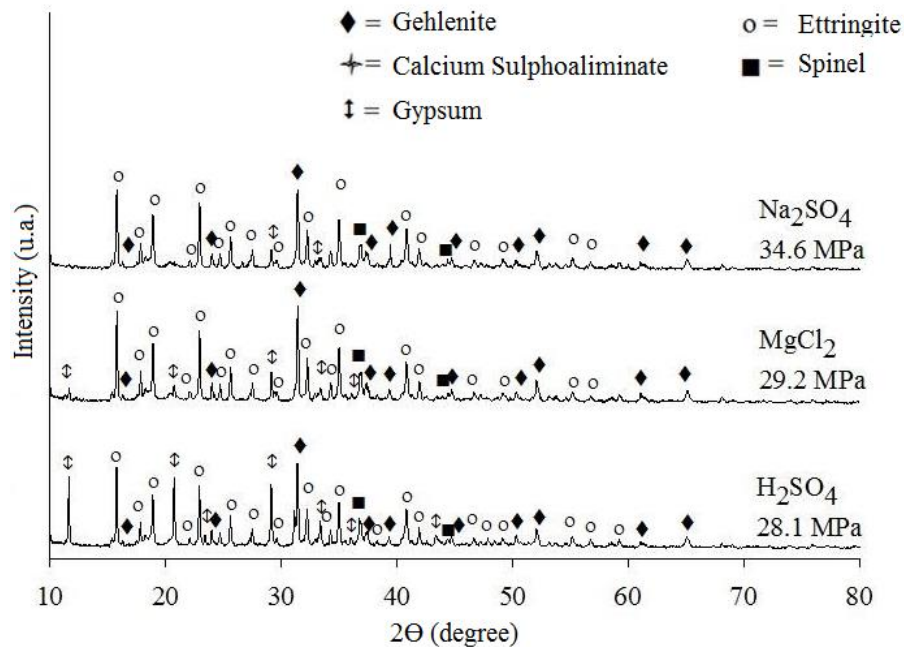
Figure 7. XRD patterns of system 525 immersed in aggressive solutions for 42 days at 40 °C.

Some damage could be seen during a visual analysis, where a softening of the surface was observed which was greater in the samples immersed in the acid solution, indicating a greater aggressiveness by this solution.

Figure 8 shows a micrograph of a sample immersed in a H2SO4 0.5 N solution at 40 ℃. The region of chemical attack was observed from the surface with a depth of approximately 129 µm, visually observing a grayer shade than the rest of the sample. The EDS analysis indicated a migration of Al^{+3} ions caused by the attack of the acid solution. A 22 µm thick crack formed due to a change in volume, caused by the migration of calcium ions and sulfates to the exterior, increasing the attack given that the new surfaces were exposed to the corrosive solution. Under the crack a dense and compact matrix was observed, suggesting that it is a zone where the corrosive medium did not penetrate.
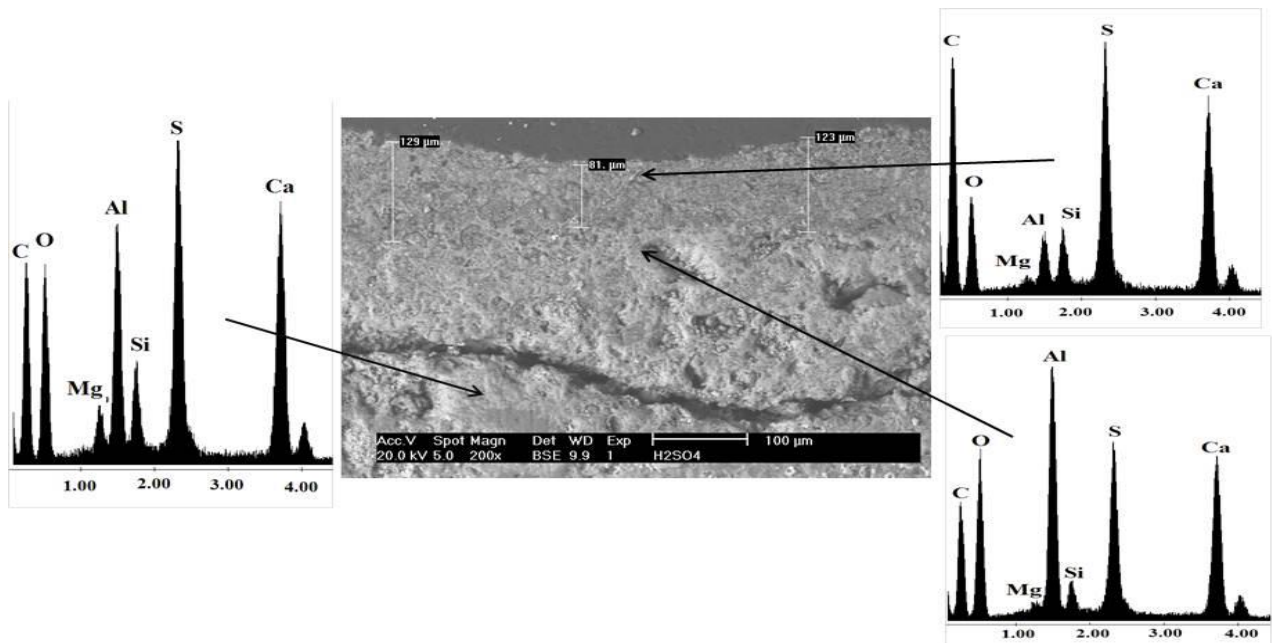
Figure 8. Micrograph of the cement after 42 days immersed in a H_2SO_4 0.5 N solution.

Figure 9 shows the microstructure of a sample immersed in a MgCl2 0.6 N solution for 42 days at 40 ℃. The depth of the chemical attack was approximately 380 µm, being greater than the one observed in the cement attack with a H2SO4 solution. In the area above the crack, an interface with a high Mg content was observed due to a slow diffusion of Mg^{+2} ions in the sample, indicating an ionic exchange with calcium ions. The non-corroded area showed a compact microstructure.
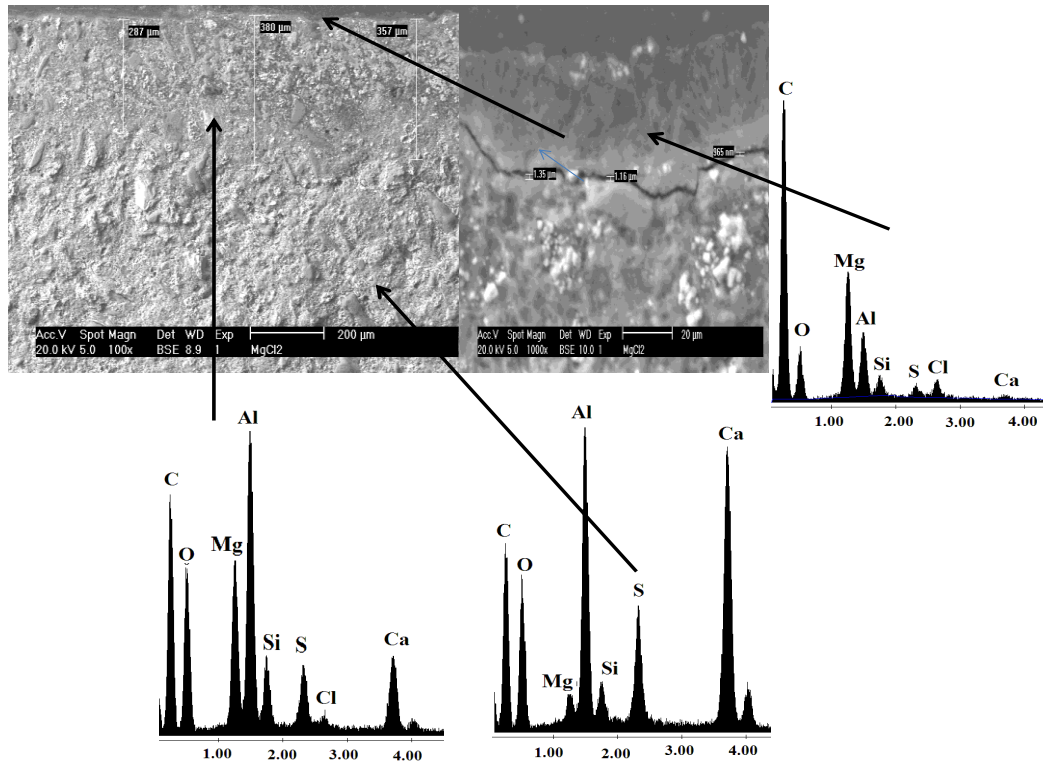
Figure 9. Micrograph of the cement after being immersed for 42 days in a MgCl2 0.6 N solution.

Figure 10 shows the microstructure of a sample immersed in a Na2SO4 0.04 N solution for 42 days at 40 ºC. An attack depth of 46.7 µm with a granular appearance was observed; these are possibly gypsum nodes, the product of a decalcification of the material. Alumina particles inside the matrix were observed, indicating a migration towards the exterior of calcium and sulfate ions. The cement immersed in this solution showed a greater resistance to the attack and its compressive strength was 34.63 MPa at 42 days of immersion; this is possibly due to the Na^+ ions having displaced the Ca^{+2} ions, forming part of the crystalline network.
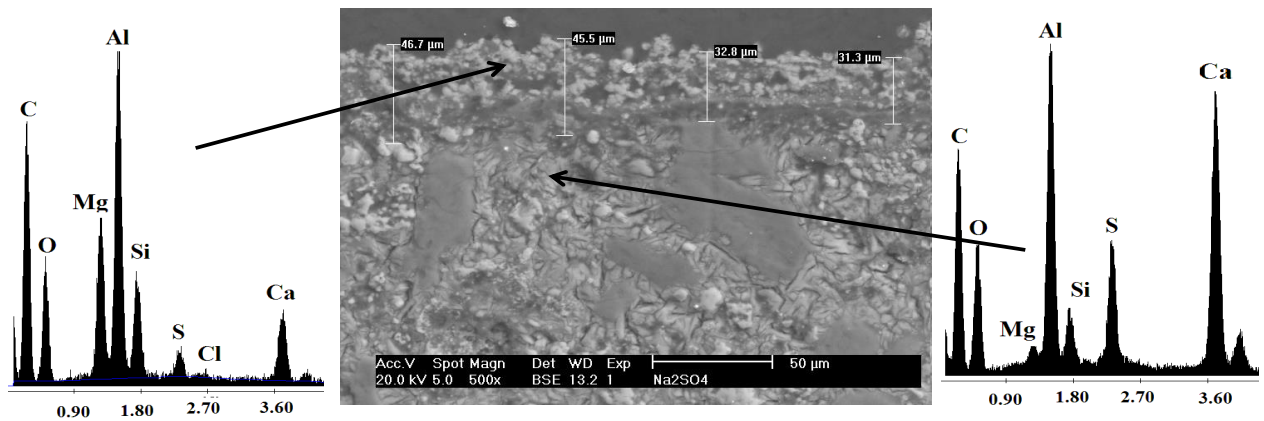
Figure 10. Micrograph of the cement after 42 days of immersion in a NaSO4 0.6 N solution.

4. CONCLUSIONS

A calcium sulfoaluminate clinker was obtained from the synthesis of a mixture of aluminum slag, fly ash, and fluorogypsum. The clinker showed in its composition stages such as calcium sulfoaluminate, gehlenite, calcium aluminate, mayenite, and belite.

The cements elaborated with calcium sulfoaluminate synthesized from industrial wastes developed compressive strengths of 38.95 MPa, similar to those developed by the Ordinary Portland pastes cured under the same conditions.

The pastes immersed in a (Na_2SO_4) solution showed a high resistance to attack by sulfates, developing a compressive strength of 34.63 MPa after 42 days of immersion.

The degradation of pastes by the attack of H_2SO_4 and $MgCl_2$ occurs by dealumination and decalcification processes. The samples immersed in H_2SO_4 and $MgCl_2$ developed a compressive strength of 28.10 and 29.2 MPa, respectively, after 42 days of curing.

5. REFERENCES

Arjunan, P., Silsbee, M. R., Roy, D. M. (1999) *"Sulfoaluminate-belite cement from low-calcium fly ash and sulfur-rich and other industrial by-products."* Cement and Concrete Research, Vol. 29: pp. 1305-1311.

ASTM C109/C109-M95, (1995), "*Standard test method for compressive strength of hydraulic cement mortars (using 2-in. or [50 mm] cube specimen*s)." Vol 04.01 Cement, Lime, gypsum.

ASTM C-204, (1995)," *Fineness of Hydraulic Cement by Air Permeability Apparatus, Annual* ", Book of ASTM Standars. Section 4. Construction. Volume 04.01. Cement, Lime, Gypsum.

Burciaga-Diaz, O., Escalate-García J.I. (2012) *"Strength and durability in acid media of alkali silicate activaded metakaolin geopolymers",* Journal of the American Ceramic Society, Vol 97, 7: pp.2307-2313

Gallardo M., Almanza J. M., Cortés D. A., Escobedo J. C., Escalante-García J. I. (2014) "*Synthesis and mechanical properties of a calcium sulphoaluminate cement made of industrial wastes",* Materiales de Construcción, Vol 64, 315, e023: pp. 1-8.

García-Maté M., De la Torre A., Leon-Reina L., Losilla E., Aranda M. A. G., Santacruz I. (2015), "*Effect of calcium sulfate source on the hydration of calcium sulfoaluminate eco-cement"*, Cement and Concrete Composites, Vol 55: pp.53-61.

Gartner, E. (2004), "*Industrially interesting approaches to "low-CO$_2$" cements".* Cement and Concrete Research, Vol. 34, 9: pp. 1489–1498.

Hargis C. W., Telesca A., Monteiro P. J. M., *"Calcium sulfoaluminate (Ye'elimite) hydration in the presence of gypsum, calcite, and vaterite",* Cement and Concrete Research, Vol 65: pp.15-20.

Katsioti, M., Tsakiridis P. E., Agatzini-Leonardou, S., Oustadakis, P. (2005), "*Examination of the jarosite–alunite precipitate addition in the raw meal for the production of Portland and sulfoaluminate-based cement s",* International Journal of Mineral Processing, Vol. 76: pp. 217 – 224.

Li, H., Agrawal, D. K., Cheng, J., Silsbee, M. R. (2001), "*Microwave sintering of sulphoaluminate cement with utility wastes",* Cement and Concrete Research, Vol. 31: pp 1257- 1261.

Li, J., Ma, H., Zhao, H. (2007), "*Preparation of sulphoaluminate-alite composite mineralogical phase cement from high alumina fly ash",* Key Engineering Materials, Vol. 334-335: pp. 421-424.

Martin, J. J., Márques G., Alejandre F. J., Hernandez M. E. (2008),"*Durability of API class cement pastes exposed to aqueous solutions containing choride, sulphate and magnesium ion",* Materiales de construcción, Vol 58,292: pp. 1701-1707.

Mehta, P. K. (1967) "*Expansion characteristics of calcium sulfoaluminate hydrates*". Journal of the American Ceramic Society, Vol. 50, 4: pp. 204–208.

Moore, A., Taylor, H. F. W. (1968), "*Crystal structure of ettringite"* Nature, Vol. 218: pp. 1048 – 1049.

NMX-C-061-ONNCCE-2001 (2001), *Industria de la construcción-cemento-determinación de la resistencia a la compresión de cementates hidráulicos*. Organismo Nacional de Normalización y Certificación para la Construcción y Edificación, México DF.

NMX-C-085-ONNCCE-2002 (2002), *Industria de la construcción-Cementos hidráulicos-Método estándar para el mezclado de pastas y morteros de cementantes hidráulicos*. Organismo Nacional de Normalización y Certificación para la Construcción y Edificación, México DF.

Older, I. (2005), "*Cements containing calcium sulfoaluminate*". Special Inorganic Cements, Modern Concrete Technology 8, Taylor and Francis Group: pp. 63-81.

Roy, D. M. (1999), "*Alkali-activated cements opportunities and challenges".* Cement and Concrete Research, Vol. 29, 2: pp 249–254.

Sersale, R., Frigiones, G., Bonavita, L. (1998), "*Acid depositions and concrete attack: main influences"*, Cement and Concrete Research, Vol. 28 pp. 19-24.

Sharp J. H., Lawrence C. D., Yang R., (1999) "*Calcium sulfoaluminate cements—low-energy cements, special cements or what?"*, Advances in Cement Research, Vol 11, 1: pp 3 –13

Singh, M., Kapur, P.C., Pradip. (2008),"*Preparation of calcium sulphoaluminate cement using fertiliser plant wastes",* Journal of Hazardous Materials, Vol. 157: pp. 106–113.

Singh, M., Upadhayay, S.N., Prasad, P.M. (1997), "*Preparation of iron rich cements using red mud, "*Cement and Concrete Research, Vol. 27, 7: pp. 1037–1046.

Taylor, H.F.W., Famy, C., Scrivener, K.L. (2001), "*Delayed ettringite formation",* Cement and Concrete Research, Vol. 31, 5: pp. 683–693.

Zhou, Q., Milestone, N. B., Hayes, M. (2006) "*An alternative to Portland Cement for waste encapsulation—The calcium sulfoaluminate cement system*", Journal of Hazardous Materials, Vol. 136, 1: pp. 120–129.

ALCONPAT Journal

Journal of the Latin-American Association of Quality Control, Pathology and Recovery of Construction

Material and casting methodology for SCC and HPC (70 MPa) concrete foundation blocks

C. Britez[1]; J. Gadea[1]; M. Carvalho[1]; P. Helene[2]

[1] PhD Engenharia.
[2] University of São Paulo, USP & PhD Engenharia.

ABSTRACT
The Brookfield Century Plaza Commercial Building, located in Alphaville District, in São Paulo, Brazil, was designed to be supported by two direct foundation concrete blocks. A high strength (70 MPa), self-compacting concrete SCC was developed for these two massive foundation blocks (each one measures 28.4m x 18.6m x 4.5m). A numerical model by employing a FEM software was developed to predict the thermal hydration gain of different casting procedures, to establish the most appropriate one to meet the construction and schedule requirements without cracks. Directions to control concrete production at mixing plant and placing at construction site were established as well as supervised. Finally, internal concrete temperatures were recorded to enable a better model calibration.
Keywords: high strength concrete, self-compacting concrete, concrete modelling, refrigerated concrete production.

RESUMEN
El Edificio Comercial Brookfield Century Plaza, localizado en Alphaville, São Paulo, Brasil, fue diseñado para ser sostenido por dos grandes bloques de hormigón. Un hormigón de alta resistencia (70 MPa) y autocompactante SCC fue desarrollado para estos dos bloques masivos de fundación (cada un mide 28.4mx 18.6mx 4.5m). Un modelo numérico utilizando un software FEM fue desarrollado para predecir la ganancia térmica de hidratación de diferentes capas de hormigonado con el fin de establecer el procedimiento más adecuado para cumplir con los requisitos de tiempo y de la construcción, sin que aparezcan fisuras. Fueron establecidos y supervisados procedimientos para controlar la producción de concreto en la empresa productora de concretos y aplicarlo en el sitio de construcción. Finalmente, la temperatura interna del concreto se registró para permitir una mejor calibración del modelo.
Palabras clave: concreto de alta resistencia, concreto autocompactante, concreto masivo, producción de concreto refrigerado.

RESUMO
O Edifício Comercial Brookfield Century Plaza, localizado em Alphaville, São Paulo, Brasil, foi projetado para ser apoiado em dois grandes blocos de concreto. Um concreto de alta resistência (70 MPa) e autoadensável SCC foi desenvolvido para estes dois blocos maciços de fundação (cada um medindo 28.4m x 18.6m por 4.5m de altura). Um modelo numérico empregando um software FEM foi desenvolvido para prever o ganho de hidratação térmica de diferentes camadas de concretagem, a fim de estabelecer o procedimento mais adequado para cumprir o cronograma e os requisitos de construção, sem fissurar. Diretrizes para controlar a produção do concreto na empresa de serviços de concretagem e procedimentos de como aplicá-lo no canteiro de obras foram estabelecidas e supervisionadas. Finalmente, as temperaturas internas do concreto foram registradas para permitir uma melhor calibração do modelo.
Palavras-chave: concreto de alta resistência, concreto autoadensável, modelagem de concreto massa, produção de concreto refrigerado.

_____

Contact author: Carlos Britez (carlos.britez@concretophd.com.br)

1. INTRODUCTION

The Brookfield Century Plaza Commercial Building (Figure 1), located in Alphaville District, in São Paulo, Brazil, was designed to be supported by two direct foundation concrete blocks. Each one measures 28.4m x 18.6m by 4.5m, high (which represents about 2,400m³ or 3,000yd³ of concrete) and has 200t of reinforcing steel. The concrete compressive strength (f_{ck}) at 28 days, was specified as $f_{ck} \geq 70$ MPa (10,000psi).

Figure 1. Illustrated perspective of the Brookfield Century Plaza Commercial Building (http://www.br.brookfield.com/).

The scope of this paper consisted in describing office and field procedures to achieve the best construction of these large high strength concrete blocks including: designing a concrete mix to meet the specifications, developing thermal calculations of the hydration heat, establishing concrete production and placing procedures and supervising the field execution at site.

2. CONCEPT OF MASS CONCRETE

If compared to "conventional" concrete, mass concrete is distinguished by the difficulty of dissipating the heat originated by the exothermic hydration reactions and the resultant volume variation, which requires special measures of control in order to minimize the cracking (ACI, 2005; Mehta and Monteiro, 2014; Isaia, 2011).

Portland cement hydration is an exothermic reaction, which releases thermal energy within the concrete mass after setting. The heat released to the exterior medium is influenced by the thermal

characteristics of the employed materials, by environmental conditions and by the structure dimensions.

Concrete, by its thermal expansion coefficient, undergoes expansive dimensional variations when exposed to temperatures resulting from this chemical exothermic reaction. In the beginning, during first ages, it expands quickly generating compression tensions, as main exothermic reactions occur in the first ages, about 50h-120h after casting.

When concrete cools back to ambient temperature, which occurs irregularly and from the exterior to the interior creating important thermal gradients, it will be submitted to a thermal contraction. This contraction, due to natural restrictions arisen by friction or geometry constraints, produces stresses that may be higher than the concrete tensile strength, resulting into cracks on the structural members (ACI, 2005; Furnas, 2007).

In this regard, it is understood that, for the conception of structural elements involving mass concrete, such as the foundation blocks focus of this article, special care need to be taken, regarding the proportions of concrete [for example, with the least cement (clinker) content, use or not ice and cold water, use or not supplementary materials as slag, fly ash and metakaolin], efficient thermal simulation (able to inform whether or not to cast in more than one layer, as well as providing input for the preparation of a detailed plan of casting), the appropriate executive procedure (able to provide guidelines to control the maximum temperature of the concrete and other important parameters) and also the specialized technical supervision of concrete events in order to minimize potential future pathological manifestations.

3. CONCRETE MIX DESIGN

The concrete mix design for this particular task was developed with extensive studies in laboratory and field. The mix proportions were based on the guidelines of IBRACON mix design method (Tutikian and Helene, 2011), on the available inputs, the site particularities and in accordance with the requirements of the ABNT NBR 12655:2006 (ABNT, 2006) and ACI 237R-07 (ACI, 2007), as well as the specifications of the structural design, oriented by two main goals to be achieved:

- As expected, a 70 MPa (10,000psi), 2,400m³ (3,000yd³) concrete block should produce quite high temperature during setting, so it was necessary to design a concrete capable of reducing hydration heat to a minimum,
- After analyzing the structural design drawings and discovering that reinforcing bars in some places were quite dense, it was necessary to choose a placing method capable of avoiding anomalies such as voids or honeycombs.

For these reasons, it was decided to replace all mixing water by ice and to use CP III 40 (50%-70% slag) and metakaolin HP in the concrete mixture (aiming to reduce hydration heat), as well as to employ self-compacting concrete, SCC, in order to speed up placing and avoid placing errors.

The concrete mix design was done at laboratory facility at São Paulo City. Different mixes were developed, with different proportions of mortar (Figure 2). For each mix, fresh concrete properties as entrapped air content, specific gravity and flow were measured, and three specimens were cast, to be tested at 3, 7 and 28 days, in order to verify their compressive strength, as shown in Figures 3 and 4, below.

Figure 2. Mixes with different mortar content.

Figure 3. Trapped air contents and specific apparent gravity measurement.

Figure 4. Flow test and specimens being cast for compressive strength tests.

The final mix that satisfied all needed characteristics was obtained with the concrete proportions shown in Table 1.

Table 1. SCC proportions for application in Brookfield Century Plaza foundation blocks.

$f_{ck} \geq$ 70 MPa (10,000psi) and water/binder ratio = 0.36	
Cement (CP III 40 Mizú)	447kg (313kg of slag + 134kg of clinker)
Metakaolin HP	38kg
Artificial sand (crushed)	481kg
Natural sand (river, quartz)	321kg
Crushed stone 9-19mm	194kg
Crushed stone 19-25mm	777kg
Total water (ice + aggregates humidity)	175L
Sikament 735 Plasticizer Additive(0.5% by cement mass)	2.2L
Sika 5700 Superplasticizer Additive (1% by cement mass)	4.6L

4. THERMAL STUDY

The thermal study was done with *b4cast 3.0 software*, which employs the maturity method (calculated by the equation of Arrhenius) as described in ASTM C 1074–04 (ASTM, 2004). This software is based on the Finite Elements Method FEM and it is able to simulate the temperature history of the structural element to be cast and the stresses arising from temperature differences inside the element. To estimate tensile strength, the equation (1) was employed, as prescribed by Brazilian concrete standard.

$$f_{ct,m} = 0,3\, f_{ck}^{2/3} \qquad\qquad (1)$$

Several simulations were done exploring different casting strategies. The Contractor wanted to investigate the possibility of casting the whole block in just one or two casts, which proved to be impossible, as internal tensile stresses would be higher than actual concrete tensile strength. As a result of simulations considering one or two casts, it was decided to investigate the behavior of temperatures and stresses by casting the block into 4 layers, 1,125m high each, with a gap of 3 days between casts. The temperature peak diminished from 64,6ºC to 54,0ºC, a 20% reduction. Tensile stresses also diminished and were very close to tensile strength evolution, which implies in a low possibility of cracks due to thermal stresses (Figure 5).
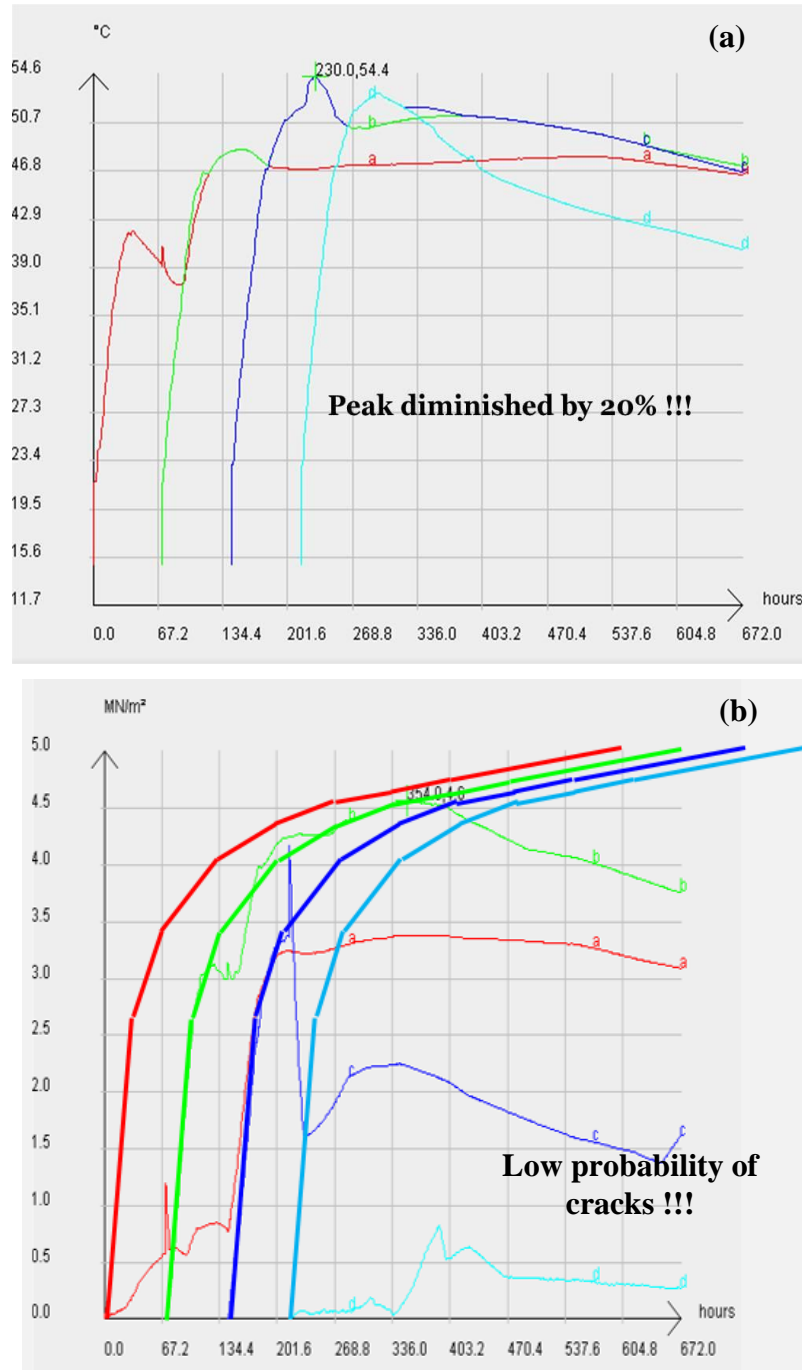
Figure 5. Block cast in four 1,125m high layers and three days gap between castings: (a) temperatures and (b) thermal stresses *vs.* tensile strength.

5. CONCRETE PRODUCTION AND CASTING PROCEDURES

The recommended procedures for casting of the foundation blocks were based on provisions of current national standardization (ABNT, 2004; ACI, 2010) and engineering good practices (Kosmatka and Wilson, 2011; Kennedy, 2005).
In order to ensure that concrete production at batching plant and casting at site would maintain the quality standards and specified characteristics, procedures (Table 2) were designed for site casting,

to be followed by the Concrete Ready-mix Company, by the Contractor team at site and by the Concrete Quality Control Laboratory.

Table 2. Concrete production and casting procedures.

Proposed control and intervener	Procedures which should be followed
Concrete production control at Batching Plant Responsible: Concrete Ready-mix Company and Concrete Quality Control Laboratory	• Coarse aggregate should be water-sprayed; • Aggregates and cement temperatures should be measured, aggregates should be below 25°C and concrete below 70°C; • All mixing water should be substituted by ice; • Ice bags should be weighted to determine their mean weight; • Sand humidity contents should be measured; • Each mixer truck should be loaded with only 6m^3, and additives should be already mixed at batch plant; • A constant flux of mixer trucks should be established.
Casting Control at site Responsible: Concrete Quality Control Laboratory	• Concrete temperature should be measured, and it should be ≤ 20°C; • Concrete flow should be measured; • Test specimens should be cast for compressive strength and diametrical tensile tests; • Temperature at defined points in each concrete layer of the foundation block should be recorded by thermocouples, at pre-established times.
Casting recommendations Responsible: Contractor	• Formwork and reinforcement in place, bottom layer cleaned, water table depression in operation, storm water drains/dikes already in place; • Concrete pumps in place for each block(three); • Preparing of concrete surface between layers to avoid "cold" joints; • Concrete curing and cleansing of joint surfaces.

It is very important to stress the fact that, in order that concrete arrives to the site at less than 20°C, a strict and periodical control of sand humidity and of the actual weight of ice that was being loaded in each mixer truck should be conducted. As in Brazil ice is normally sold in nominal 20kg bags, the mean weight of one bag should be averaged very frequently, to ensure that the stipulated water amount was effectively added to the mix.

6. TECHNICAL SUPERVISION

The concrete production and casting procedures were supervised at site, in order to ensure that the recommendations were followed and also to correct any deviation that could occur or to give technical support in specific occasions.

6.1. Supervision at the Batching Plant
At the batching plant of Concrete Ready-mix Company, situated at 20 min. drive from the site, the temperatures of cement and aggregates were checked at different hours during the day. Cement temperature never surpassed 50ºC. Water was sprayed over the aggregates (Figure 6), because in the afternoon the ambient temperature raised up to 30ºC. Water spraying kept aggregate temperature below 25ºC (Figure 7).

Figure 6. Coarse aggregate being water-sprayed at Ready-mix Company batching plant.

Figure 7. Register of coarse aggregate's temperature before and after the being water-sprayed at Ready-mix Company batching plant.

The number of ice bags was determined by measuring the sand humidity contents and then calculating the mean weight of ice bags. As temperature rose, ice could melt more quickly, forcing new measurements.
A movable platform was installed at the rear of the ice truck and the specified number of ice bags was loaded into the mixer truck. A technician from the Concrete Quality Control Laboratory verified the number of bags for each load.

6.2. Supervision at the site. Concrete temperature and flow
When concrete arrived at the site, its temperature was controlled. If greater than 20ºC, the concrete was rejected. Mean temperature was lesser than 18ºC (Figure 8).

Figure 8. Fresh concrete temperature was controlled for each mixer truck by means of an immersion digital thermometer (example: 13.2ºC).

If concrete temperature was within specification, then the concrete flow was measured. Concrete flow should be within the 600mm – 750mm range and should not be segregated, to be accepted. Flow measurements should be the mean of three different diametric measures, and were performed by the Concrete Quality Control Laboratory (Figure 9).

Figure 9. Measurement of concrete flow.

6.3. Supervision at the site – Temperature history of hardening concrete
To register the temperature history of hardening concrete, 12 thermocouples were installed by the Concrete Quality Control Laboratory at three points and at the middle height of each casting layer. The time intervals when temperature data should be collected were also given. The results were recorded for posterior analysis and thermal model calibration.

6.4. Supervision at the site – Concrete pump positioning and casting procedure
The concrete pumps positioning and the casting sequence were discussed together with the Contractor technical team. Three pumps were used (Figure 10). Concrete should be deposited in uniform sub-layers, with approximately 0,3m high beginning at the entrance side with pump Nº.1 and proceeding towards the rear with pumps Nº. 2 and 3.

Figure 10. General view – Concrete pumps positioned.

The described casting sequence was employed for all layers. The first two were cast without the superior reinforcement (Figure 11a). After finishing each cast, the surface was prepared to get the necessary roughness to promote a better adherence for the subsequent layer. Concrete curing begun immediately after, by creating a pond over the whole surface. Prior to concrete casting, the surface was drained and cleaned by water jets. Concrete was deposited on the saturated surface. After finishing the second layer, the reinforcement for columns and the superior reinforcement were placed and concrete was poured by tremies (Figures 11b and 12).
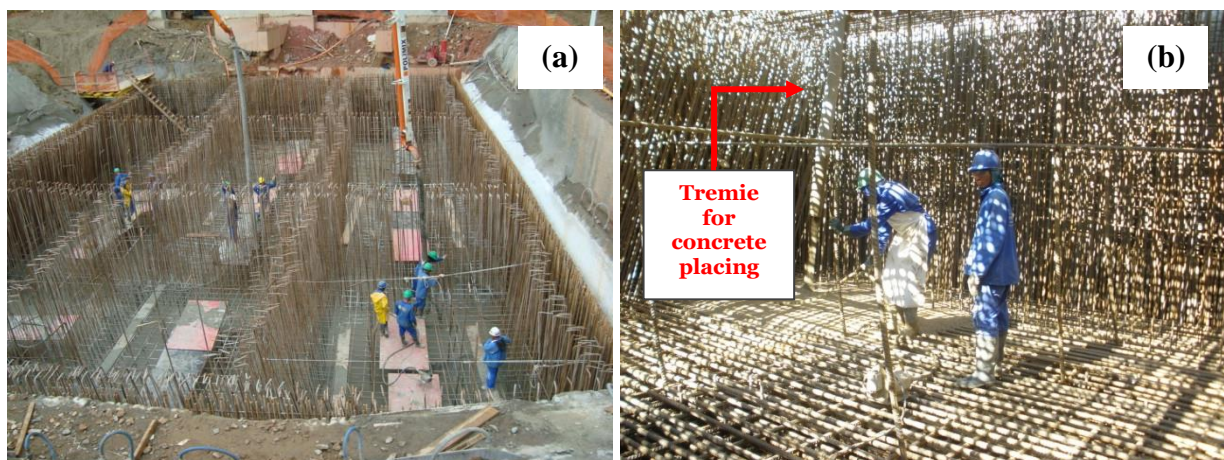
Figure 11. (a) Casting of the second layer without superior reinforcement and (b) placing of concrete after all reinforcement was put in place.

Figure 12. The superior reinforcement consisted in two double layers of 32mm rebars. SCC concrete mix was designed to pass through this reinforcement.

7. RESULTS

7.1 Technological control

With regard to the technological control of the concrete compressive strength tests were performed on the total sample (in 100% of mixer trucks) at 7, 28 and 63days age. Most of the results met the requirements of specified compressive strength ($f_{ck} \geq 70$ MPa) and specified in the structural design. The compressive strength results corresponding to one of the concrete layers at 28days age are shown graphically in Figure 13.
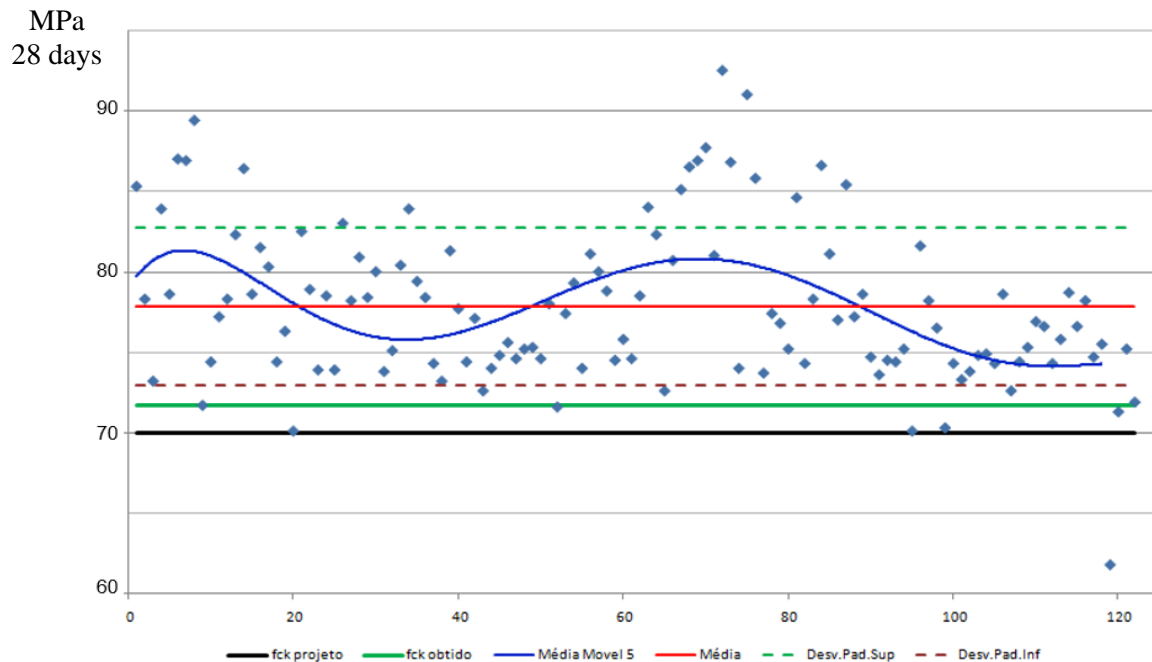
Figure 13. Example of the concrete compressive strength results from one of the concrete layers.

Besides, self-compacting concrete proved to work very well at site, speeding up concrete casting: the mean time needed to pump a 6m³ mixer truck averages 15 minutes (including acceptance tests), and there was almost no need of vibrating.

7.2 Measured temperatures inside the foundation blocks
Actual concrete temperatures were recorded. The temperature peak, 57ºC, was reached in the fourth layer after 582h. As it can be seen from the chart, time gap between castings were changed at site to better suit construction production. Instead of 3, 3, and 3 day gaps, 3, 10, and 2 were done, which lead to temperatures differing by no more than 10% (Figure 15).
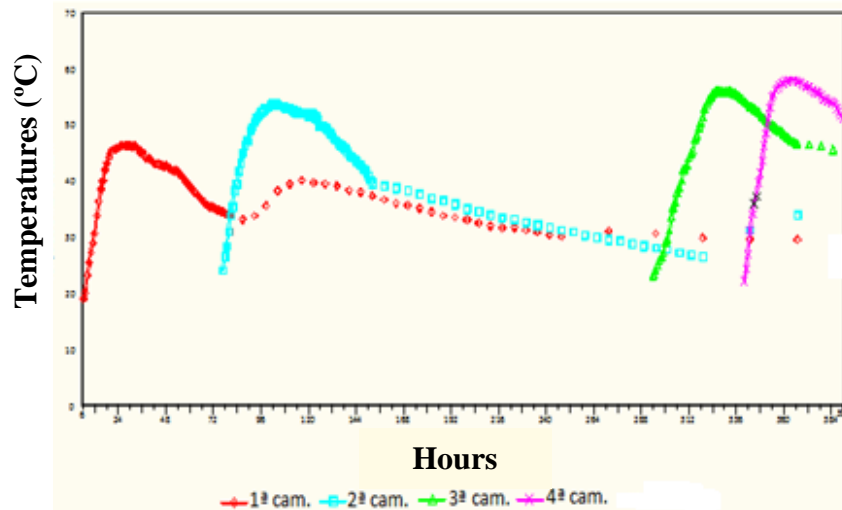
Figure 15. Concrete hydration temperatures, as recorded at site. Time gaps were 3, 10, and 2 days.

8. CONCLUSIONS

This article aimed to demonstrate that the previous development of mix design laboratory studies and thermal simulations, as well as the proposition of rigorous executive procedures and, especially, the control and technical supervision of concrete events, were determining factors for promoting a structural element with integrity and in accordance with design specifications.
So, as a final mention, it was observed that the assumptions noted in this article, both theoretical (prior to the concreting) and practical (during and after concreting), made possible a satisfactory result, revealing to be powerful tools for planning and executing challenging and technically complex concrete structures, such as those involving mass concrete.

9. ACKNOWLEDGEMENTS

10. REFERENCES

American Concrete Institute (2005), *"ACI 207.1R-05: Guide to Mass Concrete"*, (Farmington Hills, U.S.: ACI).
American Concrete Institute (2007), *"ACI 237R-07: Self-Consolidating Concrete"*, (Farmington Hills, U.S.: ACI).

American Concrete Institute (2010), *"ACI 301-10: Specifications for Structural Concrete"*, (Farmington Hills, U.S.: ACI).

American Society for Testing and Materials (2011), *"ASTM-C 1074: Standard Practice for Estimating Concrete Strength by the Maturity Method"*, (West Conshohocken, U.S.: ASTM International).

Associação Brasileira de Normas Técnicas (2006), *"NBR 12655: Concreto de cimento Portland – Preparo, controle e recebimento – Procedimento*", (Rio de Janeiro, Brazil: ABNT).

Associação Brasileira de Normas Técnicas (2004), *"NBR 14931: Execução de estruturas de concreto – Procedimento"*, (Rio de Janeiro, Brazil: ABNT).

Furnas. Laboratório de Concreto; Andrade, W. P. (Ed.). (1997), *"Concretos: massa, estrutural, projetado e compactado com rolo – ensaios e propriedades"*, (São Paulo, Brazil: PINI). 1v.

Isaia, G. C. (Ed.). (2011), *"Concreto: Ciência e tecnologia"*, (São Paulo, Brazil: IBRACON). 2v.

Kennedy, Lindsay K. (Ed). (2005), *"The Contractor's Guide to Quality Concrete Construction"*, (St. Louis, U.S.: American Society of Concrete Contractors – ASCC). 3ed.

Kosmatka, Steven H.; Wilson, Michelle L. (2011), "Design and control of concrete mixtures", (Illinois, U.S.: Portland Cement Association – PCA). 15ed.

Mehta, P. K., Monteiro, J. M. (2014), *"Concreto: Microestrutura, Propriedades e Materiais"*, (São Paulo, Brazil: IBRACON). 2ed.

Tutikian, B., Helene, P. (2011), "*Dosagem dos Concretos de Cimento Portland*". In: Geraldo C. Isaia. (Org.). "*Concreto: Ciência e Tecnologia",* 1 ed. São Paulo: Ibracon, v. 1, p. 415-451.

ALCONPAT Journal

Journal of the Latin-American Association of Quality Control, Pathology and Recovery of Construction

Durability of sustainable repair mortars exposed to industrial environments

J. M. Mendoza-Rangel[1], J. M. Flores-Jarquín[1], E. U. De Los Santos[1], P. Garcés Terradillos[2]

[1] Universidad Autónoma de Nuevo León, UANL, FIC, Av. Universidad S/N, Ciudad Universitaria, San Nicolás de los Garza, Nuevo León, C.P. 66451, Mexico.
[2] Civil Engineering Department, Universidad de Alicante, Carretera de San Vicente del Raspeig S/N, San Vicente del Raspeig, Spain

ABSTRACT

The repair and maintenance of concrete structures has increased in the activities of the construction industry. In this work, the durability of two mortars elaborated with fly ash substitutes (FA) is evaluated by weight with respect to the total cement; furthermore, its performance is compared to three commercial repair mortars, exposed to the CO_2 attack in an industrial environment. To evaluate its performance as repair material, tests were carried out to evaluate its resistance to compression, bending, and adherence. Durability tests are also presented as potential measurements, corrosion rate, permeability, and carbonation depth.
Keywords: Mortar; repair materials; corrosion; carbonation; durability.

RESUMEN

La reparación y mantenimiento de estructuras de concreto se ha incrementado en las actividades de la industria de la construcción. En el presente trabajo, se evalúa la durabilidad de dos morteros elaborados con sustituciones de ceniza volante (CV) en peso con respecto al cementante total, adicionalmente se compara su desempeño con tres morteros de reparación comerciales, expuestos al ataque de CO_2 en ambiente industrial. Para evaluar el desempeño como materiales de reparación se realizaron ensayos de resistencia a la compresión, flexión y adherencia. Se presentan también pruebas de durabilidad como mediciones de potencial, velocidad de corrosión, permeabilidad y profundidad de carbonatación
Palabras clave: Mortero; materiales de reparación; corrosión; carbonatación; durabilidad.

RESUMO

O reparo e manutenção de estruturas de concreto tem crescido dentre as atividades da indústria da construção. Foi avaliada a durabilidade de duas argamassas obtidas a partir de substituição de cinzas volantes (CV), em massa em relação à quantidade total de produto aglomerante. Foi comparado o desempenho dessa argamassa com o desempenho de três argamassas de reparo comerciais, frente a um ataque de CO_2 num ambiente industrial. Para avaliar o desempenho como materiais de reparo foram realizados ensaios de resistência à compressão, flexão e aderência. São apresentadas também provas de durabilidade com medidas de potencial de corrosão, velocidades de corrosão, permeabilidade e profundidade de carbonatação.
Palavras-chave: Argamassa; materiais de reparo; corrosão: carbonatação; durabilidade.

_____
Contact author: José Manuel Mendoza Rangel (jmmr.rangel@gmail.com)

1. INTRODUCTION

The main problem for which a concrete structure needs repair is the corrosion of steel, which negatively impacts the durability of the constructions, putting at risk their functionality and safety (Andrade C., Feliu S., 1989). In industrial and urban environments, the big concentrations of CO_2 represent a problem for the reinforced concrete due to the carbonation of the same, which causes a reduction in alkalinity and generates the depassivation and corrosion of steel. For the development of carbonation, the humidity and temperature are factors that modify its advance rate.

After having detected the corrosion in a structure, it is necessary to take actions to do repairs and prolong its useful life. The repair work can be divided into the following steps: elimination of the concrete, cleaning the exposed steel, and the application of a repair material (Fernández Cánovas, 1989).

The selection of the repair material is the most important criterion to consider in the repair work; normally, the resistance to compression is taken into consideration to select a repair mortar, this is completely insufficient if other parameters that are equally important, such as the compatibility of the mortar with the concrete substrate, are not taken into consideration. The topic of compatibility implies the study of the difference between the properties of the concrete substrate and the repair mortar, as said difference could cause negative effects on the repair, causing cracking and thus decreasing its durability (Decter, 1997).

Several studies have been conducted to evaluate the different types of repair materials that are available on the market. Unfortunately, the properties that should be considered for the evaluation and selection of the repair materials are not specified (Cabrera, 1997). Some authors (Emmons, 1994) present the considerations that affect the compatibility for a new selection of the repair materials. From these considerations, the most important is probably the capacity to support changes in volume, without loss of adherence or cracks; this is known as "Dimensional compatibility". In addition to the volume changes, a repair should also have a protector effect and to ensure this, the chemical, electro-chemical, and permeability of the repair material should be considered.

The problems related to the properties to be evaluated and the selection of the repair materials are attributed to the lack of regulation in relation to the repair activities, maintenance, and renovation (Kay, 1987; Treadaway, 1987), in addition to the lack of information that the manufacturers of the repair materials provide. For this reason, it is necessary to carry out researches on the repair materials that are adequate to the environment and the service conditions of each structure. In turn, the use of alternative cement materials such as fly ash, will allow the use of repair materials of low environmental impact, due to the decrease in the use of ordinary Portland cement (OPC), and that comply with the necessary characteristics for a lasting repair.

The objective of this work is to evaluate the durability and potential performance of three mortars prepared in the laboratory, two with substitution of FA (20 and 50%) for OPC and three mortars of commercial repair; in particular, their mechanical behavior, dimensional stability, adherence, and their capacity to protect steel from corrosion by carbonation in an industrial environment.

2. EXPERIMENTAL PROCEDURE

Table 1 shows the proportion of the mortars elaborated in the laboratory. The MR mortar is used as reference, mortars M1 and M2 were elaborated with the same water/cement and cement-sand ratio as the reference one, but with FA additions of 20 and 50% in substitution with regard to the weight of MR cement. The cement used is an OPC 40 and the FA is type F—it was obtained from the *Carboeléctrica* of the city of Nava Coahuila, Mexico. The chemical composition of the OPC and FA can be observed in Table 2, obtained by X-ray fluorescence (XRF).

Table 1. Proportions of the repair mortars manufactured in the laboratory.

Mortar	Component	Proportion
MR	OPC	1
	Sand	3
	Water	0,5
M1	OPC	0,8
	FA	0,2
	Sand	3
	Water	0,5
M2	OPC	0,5
	FA	0,5
	Sand	3
	Water	0,5

The commercial repair mortars are identified as C1, C2, and C3, these are pre-packaged mortars, cement based and of only one component; C1 is a reinforced mortar with fiber, C2 is fast-setting; C1 and C3 are modified with polymers and with additions of micro-silica in proportions that are known by the manufacturer. The mixture and the amounts of water used were the ones specified in the data sheet of each mortar.

Table 2. Chemical composition in oxides of the Portland Cement and Fly Ash

Oxides	OPC (%)	FA (%)
SiO_2	17,43	56,51
Al_2O_3	4,67	33,11
Fe_2O_3	2,25	1,49
CaO	63,27	0,70
MgO	1,23	1,67
SO_3	4,98	0,34
Na_2O	0,56	3,32
K_2O	0,75	0,52

Different types of specimens were manufactured in accordance with the test to be carried out; after their manufacture, the specimens were kept in a curing chamber at 100% Relative Humidity (RH) and at 21±2 ºC, for 14 days. After curing, the specimens were removed from the chamber until they reached 28 days of age.

For the corrosion potentials test, specimens with two steel bars of 6 mm in diameter were manufactured to leave a coating of 7 mm; additionally, a graphite column of the same diameter was placed to be used as a counter electrode.

To evaluate the capacity to resist the entry of aggressive agents, the specimens were exposed to carbonation in an industrial environment.

In the industry where the specimens were placed, industrial processes of sodium carbonate and bicarbonate are carried out, which creates an aggressive and damaging environment for concrete.

2.1 Resistance to compression and flexural strength

To determine the resistance to compression, mortar cubes with a side length of 50 mm were manufactured. The filling procedure of the cubes and the testing were done in accordance with the provisions in the standard (ASTM C 109). The flexural strength was done according to the procedure described in the standard, in 40x40x160 mm prismatic test tubes (ASTM C 348).

2.2 Adherence

The test used is known as inclined cutoff testing, which uses a 100x100x300 mm prism made from two identic halves joined at 30º and tested under axial compression (Momayez, 2005).

2.3 Permeability

The procedure to determine the air permeability of the repair mortars was done through the Torrent Permeability Tester (TPT) on 150 mm cubic test tubes (Torrent, 1992; Kucharczykova, 2010).

2.4 Carbonation Depth

For this test, 20x55x280 mm prismatic test tubes were used. The samples were placed in the industrial environment mentioned above, which does not present consistent values as it depends on the production in the plant; the data mentioned before -were reported in a previous article ((Durán-Herrera, 2015). The monitoring was done using phenolphthalein as depth indicator for carbonation on the samples that were freshly cut at different ages.

2.5 Corrosion potentials and rates

The corrosion potentials (E_{corr}) and rates (i_{corr}) are determined through the resistance to polarization test (ASTM G 59) with a sweep feed of 0.06 mV/s; only in the cathodic zone does it go from 0 to -10 mV. This methodology is applicable for the study of the protection that the repair mortars provide to reinforced steel.

The steel used was prepared and cleaned following the procedure established in the ASTM G1 (ASTM G 1) standard, which completely removes the corrosion products that it could have before starting the test. After the cleaning of the steel, it was weighted and carefully wrapped to define the area of study (50 mm).
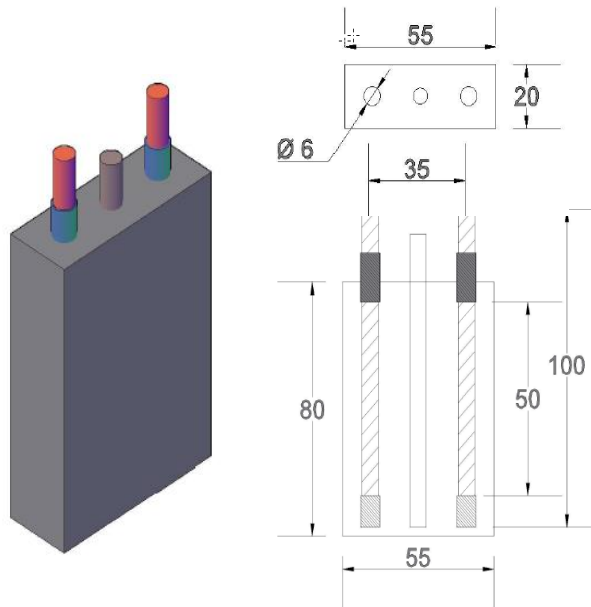
Figure 1. Specimen to evaluate the durability of the repair mortars (units in mm)

3. RESULTS AND DISCUSSION

Table 3 shows the mechanical behavior of each repair mortar and the results of the tests at 28 days. It can be observed that the C1 commercial repair mortar shows resistance at the highest compression, which is due to the content of fibers that decrease deformation in the face of a load and their role as reinforcement for the mortar.

The M1 mortar follows in the order of resistance, its value being higher than the MR mortar and the commercial C1 and C3 mortars. As per flexural strength, the C1 mortar shows the highest resistance due to the addition of fibers. The commercial C2 mortar is the lowest in regard to its mechanical behavior—its low resistance can be associated to the high porosity which, as is mentioned in figure 2, is not visible due to it being more permeable and it does not appear because it is outside the scale ranges. According to various investigations (Bjegovic 1990; Jiang, 2009), the lower resistance of the C2 and C3 mortars is probably the result of their additives.

Table 3. Mechanical behavior of the repair mortars.

Mortar	Resistance to Compression 28 days (MPa)	Flexural Strength 28 days (MPa)
MR	57,4	12,7
M1	65,8	11,7
M2	32,6	10,6
C1	75,4	16,4
C2	30,0	7,4
C3	49,2	14,3

C2 mortar, being a fast-setting mortar, could contain magnesium sulfate or higher amounts of calcium sulfate, thus increasing its setting speed but decreasing its final resistance; for its part, C3

mortar contains polymers and microsilica in addition to having a higher content of air in order to improve its resistance to freezing and melting, this is not evident on the permeability graph, due to the fact that the polymers allow creating a greater amount of pores, but in an isolated and well-distributed manner.

The adherence was evaluated by the type of failure that the prisms present; Table 4 shows the resistance to adherence of each mortar at 28 days as well as their type of failure. If there is good adherence, the sample malfunctions monolithically as one piece, presenting cracks that spread from the repaired concrete to the repair mortar, instead of faltering throughout the union in one plane at 45°.

The other type of failure presented is on the interface, where the adherence failure between the concrete and the mortar happens before either of the two materials fails. The results of the resistance to adherence show that the mortars with the best behavior are C1 and C3 due to the failure presenting itself along with the concrete (monolithic); even though the monolithic failure is desirable, it can be observed that the M1 mortar presented a failure in the interface and yet showed the highest resistance for adherence (Cabrera, 1997). This advantage is possibly due to the cement used for the manufacture of repair mortars being the same as the one used for the manufacture of the concrete samples on which the repair was done.

Table 4. Adherence of the repair mortars

Mortar	Resistance to Adherence 28 days (MPa)	Type of Failure
MR	22,2	Interface
M1	26,1	Interface
M2	13,4	Interface
C1	19,4	Monolithic
C2	0,0	Interface
C3	22,5	Monolithic

The C2 mortar, for its part, is the mortar with the least mechanical properties; in the adherence test, the failure immediately showed at the beginning of the test, not allowing the team to record anything. It is worth noting that the compatibility of the deformations is important to do a good repair, in materials with lower elasticity modulus (usually related to lower resistance) more deformations for the same level of load will manifest, originating the failure in the material with more deformations.

Figure 2 shows the relation of air permeability in time for the different mortars. It can be observed how permeability increases in almost all the mortars, with C3 mortar being the one that presents the lowest permeability values and without any increases in relation to time. The C2 mortar is not shown in the ranges on the scale because it is too permeable. While the commercial C1 mortar was not tested due to it having a rough surface and the presence of larger sized aggregates compared to the rest of the mortars, but as can be observed in carbonation, it is not possible to measure its advance as it does not present any reaction to phenolphthalein (Figure 3).

Therefore, it can be said that the M1 mortar shows a good resistance to the influx of CO_2, as this test has been shown to have a good correlation with other durability tests as good as the C3 commercial mortar. MR and M1 presented values classified as low permeability (0.01-0.1) while M2 presented moderate permeability coefficients (0.1-1.0), the rest of the classifications are shown in table 5. The results obtained through the quick permeability method have shown

a good correlation with the permeability tests to water, chlorides, and carbonation (Ebensperger, 2010).

Table 5. Permeability classification in terms of kT (Ebensperger, 2010).

Class	kT (10^{-16}m^2)	Permeability
1	<0,01	Very low
2	0,01-0,1	Low
3	0,1.1,0	Moderate
4	1,0-10	High
5	>10	Very high
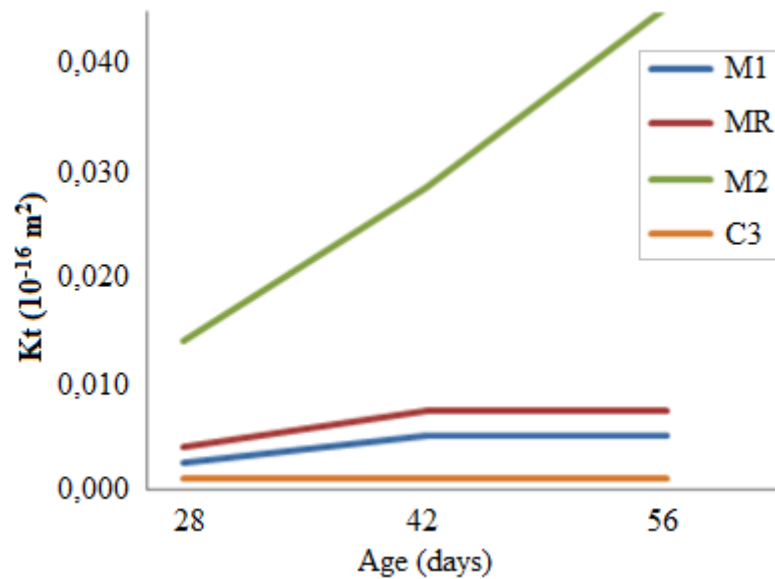
Figure 2. Evolution of the permeability of the mortar (Kt) over time.

The carbonation depth gives an indication of how the advance of CO_2 reaches the steel and causes a significant decrease in the pH of the mortar; with the decrease of pH, depassivation of the layer begins, which starts the corrosion of the steel. The coating for the steel is of 7 mm, the behavior of the repair mortars versus the advancement of carbonation can be seen in Figure 3. The mortars that showed more advancement in carbonation are M2 and C2, whereas M1, C1, and C3 mortars are the ones that show a lesser depth of carbonation; these results are related to the permeability of each mortar, their CaO content, and with the presence of some polymers which are frequently present in commercial products. The CaO content can be observed in Table 2, said content is lower for FA and its content in the mixtures in the mortars decreases with the increase of the substitution. It is important to mention that for the C1 mortar it was not possible to obtain the measurements as there was no reaction with the phenolphthalein indicator. The carbonation of M2 was higher due to the ingress being higher in relation to the short face of the specimens, thus influencing the final average.
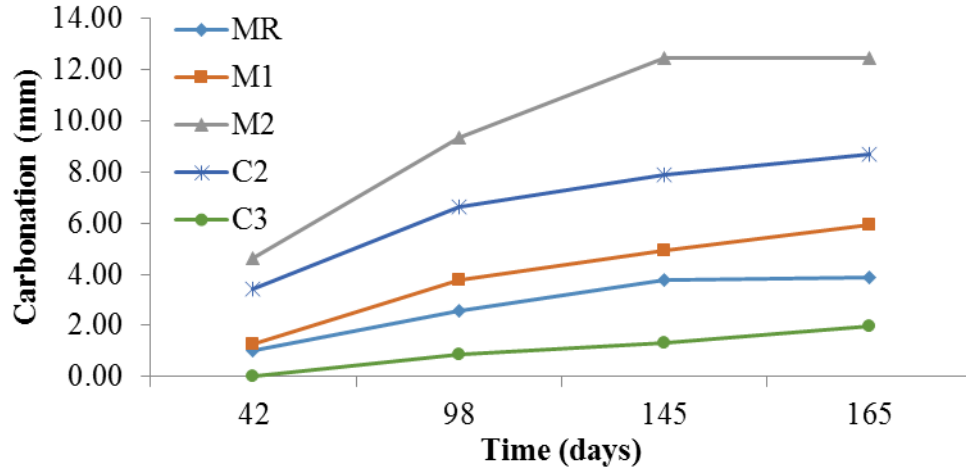
Figure 3. Carbonation Depth.
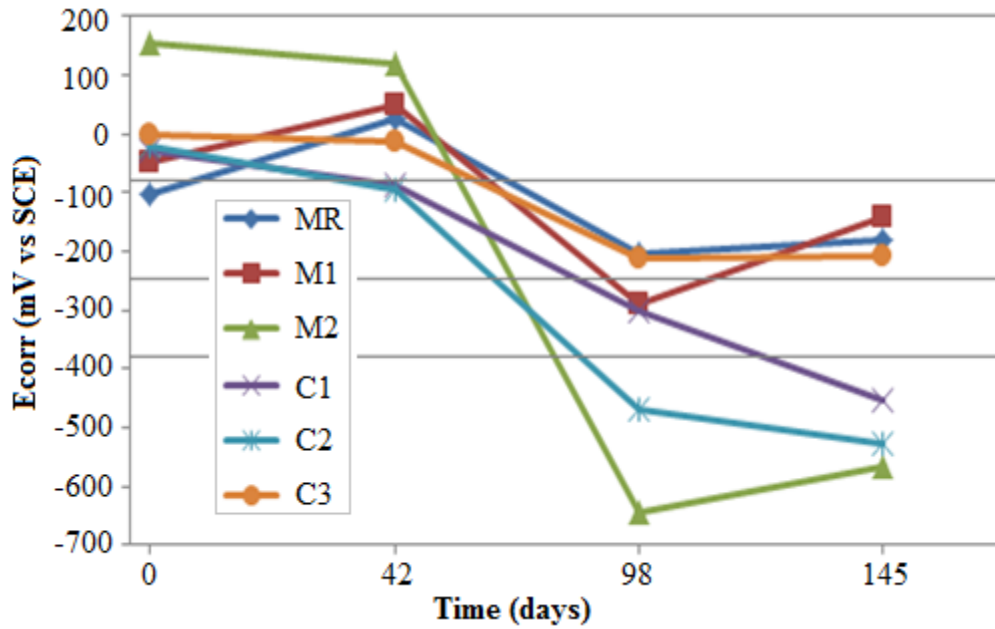
Figure 4. Ecorr evolution during the time of exposure.

Figure 4 shows the corrosion potentials (Ecorr) in regard to the Saturated Salomel Electrode (SCE). Mortars M2, C1, and C2 show a high probability that there could be corrosion on the steel starting from 98 days, as per what is presented in Table 6, and in accordance with the ASTM C 876 standard. The mortars that present a lower probability of corrosion are MR, M1, and C3 for which the behavior was very similar.

Table 6. Criteria used to evaluate the corrosion potentials in steel

Ecorr vs CuSO4 (mV)	Ecorr vs Calomel (mV)	Corrosion probability
> - 200	> - 80	10% chance that it occurs
- 200 to - 350	- 80 to - 230	Uncertain zone
< - 350	< - 230	90% chance that it occurs
< - 500	< - 380	Severe corrosion

The evolution of i_{corr} during the carbonation process is shown in Figure 5. From this, it is possible to say that, at the start, the values of i_{corr} at first age show passivity in the reinforced steel (lower than 0.1 $\mu A/cm^2$) in all mortars. However, as Ecorr indicates, for the steel within mortars M2, C1, and C2 depassivation occurs after 42 days.
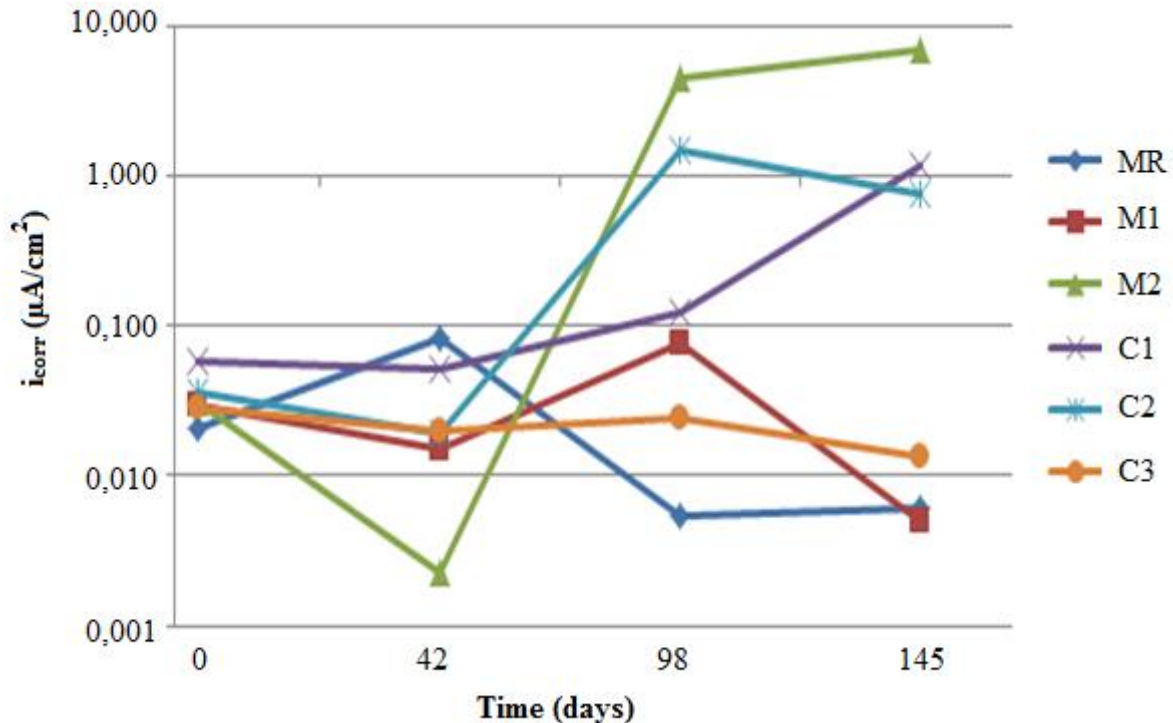
Figure 5. Corrosion rate (i_{corr}) in reinforcement Steel for each repair mortar.

The behavior of M2 and C2 mortars can be confirmed due to its low mechanical behavior with greater porosity and a greater carbonation depth. While for mortar C1, despite having excellent mechanical properties due to the use of fibers, it is very permeable and allows access of CO_2 to the steel, which creates high corrosion values.

As previously mentioned, mortar C1 did not present a reaction with the phenolphthalein indicator that allowed for a correct read of the carbonation.

4. CONCLUSIONS

In terms of performance and durability, the mortars that showed the best behavior are M1 and C3. The M1 mortar with a substitution of FA of 20%p/p surpasses the behavior of the reference mortar (MR) with regard to the attacks of CO_2, even showing a better behavior than the commercial mortars C1 and C2.

Regarding corrosion, only commercial mortar C3 shows good durability properties. If the use of traditional mortars with good durability properties is implemented, then it is not necessary to use a commercial mortar with a higher cost due to the additions and modifications that could be unnecessary for some repairs.

The durability tests carried out determine, with greater certainty, the protection given to a repair in terms of the corrosion on the reinforcement steel. These tests, in addition to the tests for resistance

to compression, flexure and adherence, leads us to think that a traditional mortar (cement-sand with mineral substitutions) could behave as an effective and durable repair.

5. ACKNOWLEDGEMENTS

6. REFERENCES

Andrade, C., Feliu, S. (1989). "*Manual de inspección de obras dañadas por corrosión de armaduras*", Publicado ICCT, Madrid, España.

ASTM C 109 (1999), *"Standard Test Method for Compressive Strength of Hydraulic Cement Mortars" (Using 50 mm Cube Specimens),* ASTM International.

ASTM C 348 (1997), *"Standard Test Method for Flexural Strength of Hydraulic Cement Mortars".*

ASTM C 876 (2009), *"Standard Test Method for Corrosion Potentials of Uncoated Reinforcing Steel in Concrete".*

ASTM G 1 (2003), *"Standard Practice for Preparing, Cleaning, and Evaluating Corrosion Test Specimens".* ASTM International.

ASTM G 59 (2014), *"Standard Test Method for Conducting Potientodynamic Polarization Resistance Measurements".* ASTM International.

Bjegovic, D., Ukraincik, V., Beus, Z. (1990). *"Evaluation and Repair of Concrete Structure in Urban Environment: Case Study"*, Special Publication 122: pp. 427-450.

Cabrera, J. G., Al-Hasan, A. S. (1997). "*Performance properties of concrete repair materials"*, Construction and Building Materials 11, 5: pp 283-290.

Decter, M. H. (1997). "*Durable concrete repair—Importance of compatibility and low shrinkage"*, Construction and building materials 11, 5: pp. 267-273.

Duran-Herrera, A., Mendoza-Rangel, J. M., De-Los-Santos, E. U., Vázquez, F., Valdez, P., Bentz, D. P. (2015). *"Accelerated and natural carbonation of concretes with internal curing and shrinkage/viscosity modifiers"*, Materials and Structures 48, 4: pp 1207-1214.

Ebensperger, L., Torrent, R. (2010). *"Medición" in situ" de la permeabilidad al aire del hormigón: status quo"*, Revista ingeniería de construcción 25,3: pp. 371-382.

Fernández Cánovas M. (1989). *" Hormigón",* Servicio de publicaciones del Colegio de Ingenieros de Caminos, Canales y Puertos, Madrid, 3ª edición.

Emmons, P. H., Vaysburd, A. M., McDonald, J. E. (1993). *"A rational approach to durable concrete repairs"*, Concrete international Detroit 15: pp. 40-40.

Jiang, C., Chen, D., Wu, Y., Zhang, W. (2009). *"Study on the Mechanisms and Properties of Repair Mortar for Hydraulic Concrete Surface"*, Advances in Water Resources and Hydraulic Engineering: pp. 1619-1624.

Kay, E. A., Regan, J. (1987). *"Acceptance and compliance testing of patch repair systems-- proceedings of the second international conference on deterioration and repair of reinforced concrete in the arabian gulf",* Bahrain, Publication of: Bahrain Society of Engineers. 1,2 :pp. 11-13,.

Kucharczyková, B., Misák, P., Vymazal, T. (2010). "*The Air-permeability measurement by torrent permeability tester*", In Proceedings of the 10th international conference on modern building materials, structures and techniques*, Vilnius*: pp. 162-166.

Momayez, A., Ehsani, M. R., Ramezanianpour, A. A., Rajaie, H. (2005*), "Comparison of methods for evaluating bond strength between concrete substrate and repair materials*". Cement and Concrete Research 35, 4: pp. 748-757.

Torrent, R. J. (1992)*. "A two-chamber vacuum cell for measuring the coefficient of permeability to air of the concrete cover on site*", Materials and Structures 25.6: pp. 358-365.

Treadaway K. W. J. (1987) *"Testing the properties of materials for concrete repair- A review".* Proceedings of the Second International Conference on Deterioration and Repair of Reinforced Concrete in the Arabian Gulf.

ALCONPAT Journal

Journal of the Latin-American Association of Quality Control, Pathology and Recovery of Construction

High performance cementitious compounds and their application as transition substrate for beams

V. J. Ferrari[1], A. P. Arquez[2], J. B. De Hanai[2]

[1] Department of Civil Engineering, Universidade Estadual de Maringá, Brazil.
[2] Escola de Engenharia de Sao Carlos, Universidade de Sao Paulo, Brazil.

© 2016 ALCONPAT International

ABSTRACT

This study presents the development and analysis of the behavior of high performance cementitious compounds reinforced with fibers. The material described was specifically developed for its application as a transition substrate, meaning, a repair layer that forms the tensed span of the flexion reinforced concrete beams with carbon fiber reinforced polymers (CFRP). Nineteen different compounds were produced by the hybridization process. The volume of the short fibers and of the steel microfibers varied. To analyze the behavior of the flexural material, tests were done in three points in tests tubes with their notches. The response of the material was analyzed considering the tenacity parameters (to flexion and fracture). The high performance of the compounds through the behavior of pseudo-hardening was confirmed.
Keywords: cementitious compounds; concrete beams; transition substrate.

RESUMEN

Este estudio muestra el desarrollo y análisis del comportamiento de los materiales compuestos de cemento reforzado con fibras de alto rendimiento. El material descrito se desarrolló específicamente para su aplicación como sustrato de transición, o capa de reparación de la formación de la brida tensada vigas de hormigón reforzado con polímeros de flexión reforzado con fibras de carbono (PRFC). Diecinueve compuestos diferentes fueron producidos por el proceso de hibridación. Se varió la cantidad de fibras cortas y microfibras de acero. Para analizar el comportamiento de los ensayos de flexión en tres puntos materiales prismas se realizaron Jagged. La respuesta del material se analizó teniendo en cuenta parámetros de tenacidad a la flexión y (fractura). Materiales compuestos de alto rendimiento evidencia a través de un comportamiento pseudo- endurecimiento.
Palabras clave: compuestos cementíceos; vigas de concreto; sustrato de transición.

RESUMO

Neste estudo apresenta-se o desenvolvimento e a análise do comportamiento de compuestos cementíceos de elevado desempeño reforzados com fibras. O material descrito foi especificamente desarrollado para aplicación como um sustrato de transición, ou seja, camada de reparo que forma o banzo traccionado de vigas de concreto reforçadas à flexão com polímeros reforçados com fibras de carbono (PRFC). Dezenove diferentes compuestos foram produzidos pelo processo de hibridização. Variou-se o volume de fibras curtas e de microfibras de aço. Para analisar o comportamento do material à flexão, ensaios em três pontos em prismas entalhados foram realizados. A resposta do material foi analisada considerando-se parâmetros de tenacidade (flexional e ao fraturamento). Ficou evidenciado o elevado desempeño dos compuestos através de comportamiento de pseudo-encruamento.
Palavras-chave: compuestos cementíceos; vigas de concreto; sustrato de transición.

_____
Contact author: Vladimir Ferrarí (vladimirjf@hotmail.com)

1. INTRODUCTION

According to Ferreira (2012), the resulting modifications of the addition of steel fiber to concrete, in relatively low proportions (a maximum of 2%), are restricted to the later stage at the historical load peak. In these conditions, the steel fibers are not enough to inhibit the cracking process of the matrix, which occurs before the application of the maximum load (sub-critical growth of the crack). The effect of the incorporation of steel microfibers, the short fibers studied here are an attempt to improve the behavior of the cementitious compounds in the historical load pre-peak.

Those materials were specifically developed to be applied as transition substrates (Figure 1). Nineteen different compounds were prepared in two phases: Phase I (compounds that were developed for their application as transition substrates for reinforced concrete beams for the external placement of CFRP covers- Figure 1.a) and Phase II (compounds developed for their application as transition substrates of reinforced beams through the insertion of CFRP sheets in the notches made in this substrate – Figure 1.b).

In engineering, it is common to find reinforced concrete beams with a tensioned underside damaged by mechanical action, corrosion effects on the reinforcement, or cracking. In such cases, the beam reinforcement process should be preceded by the recovery of the side. For this, Ferrari (2012) proposes a cement based, high performance compound cement intended to be part of the transition substrate such as the one indicated in Figure 1. The concept of the transition substrate is to create a new tensioned side formed by the cementitious compound with more appropriate characteristics to the adherence of the polymeric reinforcement.
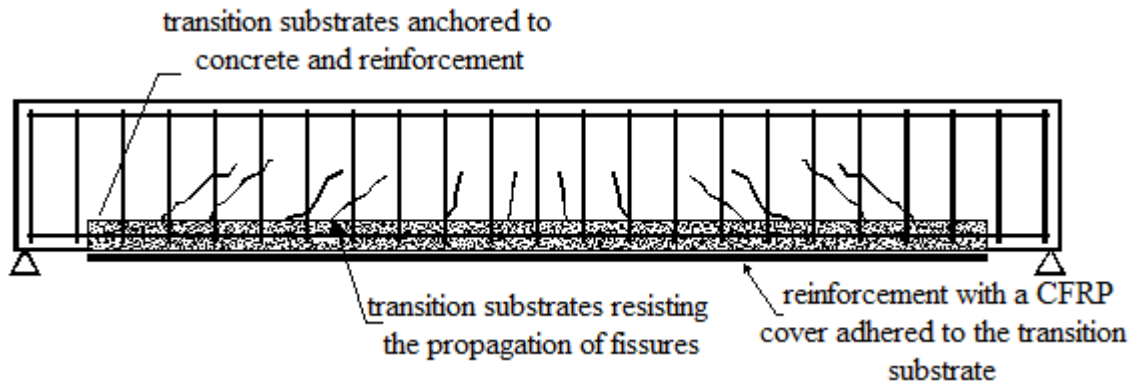
a) External reinforcement with a CFRP cover adhered to the transition substrate (Ferrari, 2012)
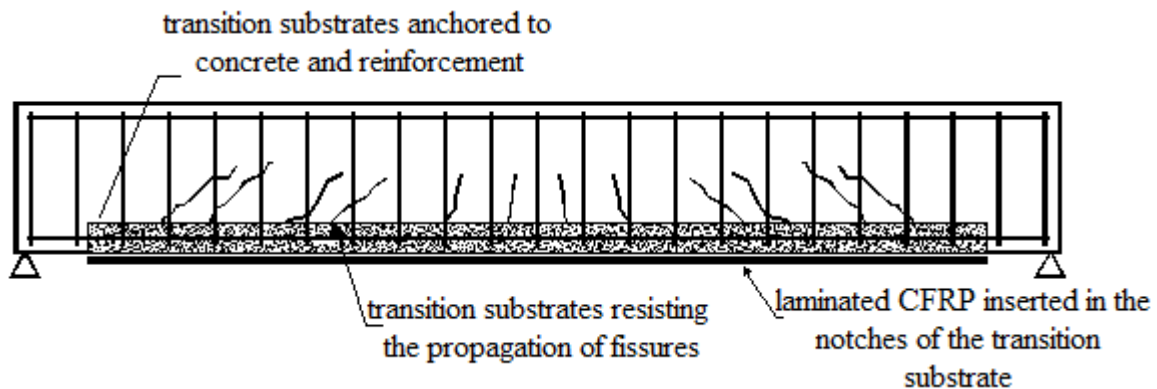
Laminated CFRP inserted in the notches of the transition substrate (Arquez, 2010)
Figure 1. Transition substrate with CFRP for reinforced concrete beam.

In this study, new results were added to the ones presented by Ferrari (2012). The new results were obtained through the development and analysis of cementitious compounds to form the transition substrate of reinforced beams through the insertion of CFRP sheets in the notch of the new substrate.

2. HIGH PERFORMANCE CEMENTITIOUS COMPOUNDS

To evaluate the resistance to traction in the flexion of the cementitious compounds, tests were carried out on three points of the prismatic test tubes (150mm x 150mm x 500mm) equipped with a central notch with a direct pass and following the Rilem (2002) recommendations. Figure 2 shows the general configuration of the test that was conducted by controlling the crack mouth opening displacement (CMOD).
In phase I, thirteen compounds were analyzed as shown in Table 1. The compounds were comprised of different volumes and types of steel fibers and by different types of cementitious matrices (mortar and micro-concrete). The compounds were divided into groups, each one comprised of three prismatic test tubes with the same characteristics. In phase II, an additional group comprised of six compounds (all made of micro-concrete) was studied.
The steel fiber specified by "A" is 25 mm long and has a diameter of 0.75 mm. The type "C", fiber, specifically produced for this investigation, is 13 mm long and has a diameter of 0.75 mm. This fiber has been designated as a steel microfiber (Figure 3).
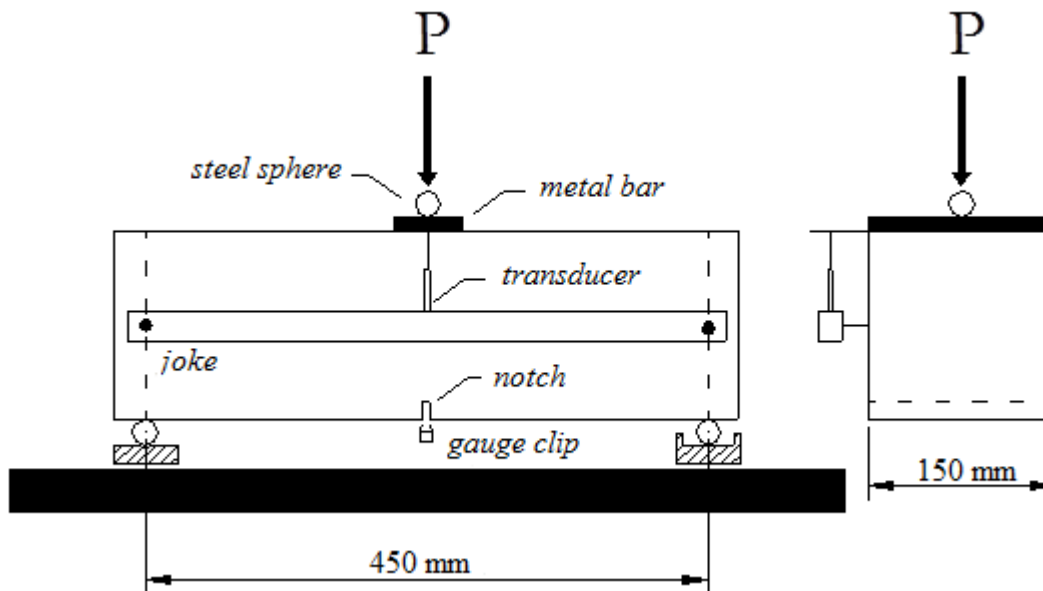
Figure 2. General configuration of the test

Table 1. Compounds analyzed

Matrix	Phase	Group	Compounds	Fiber volume	Type of fibers	Material	Age (days)
Mortar (A)	I	1	CPA	0%	-	Mortar	29
		2	CPA1A	1%	A	Mortar	29
		3	CPA1.5A	1.5%	A	Mortar	29
		4	CPA2A	2%	A	Mortar	29
		5	CPA1.5A0.5C	1.5%+0,5%	A+C	Mortar	28
		6	CPA1.5A1.5C	1.5%+1.5%	A+C	Mortar	28
		7	CPA1.5A2.5C	1,5%+2.5%	A+C	Mortar	28
		8	CPA1.5A3.5C	1.5%+3.5%	A+C	Mortar	28
Micro-concrete (M)	I	9	CPM	0%	-	microconcre	28
		10	CPM1A	1%	A	microconcre	28
		11	CPM1A1C	1%+1%	A+C	microconcre	28
		12	CPM1A2C	1%+2%	A+C	microconcre	28
		13	CPM1A2.5C	1%+2.5%	A+C	microconcre	28
Micro-concrete (M)	II	1	CPM1A1C	1%+1%	A+C	microconcre	50
		2	CPM1A1.5C	1%+1.5%	A+C	microconcre	50
		3	CPM1A2C	1%+2%	A+C	microconcre	50
		4	CPM1.5A1C	1,5%+1%	A+C	microconcre	50
		5	CPM1.5A1.5C	1.5%+1.5%	A+C	microconcre	50
		6	CPM1.5A2C	1.5%+2%	A+C	microconcre	50

CP X Y Y

corpo-de-prova — Type of fibers

Argamassa (A) ou

Microconcrete (M) — Fiber volume
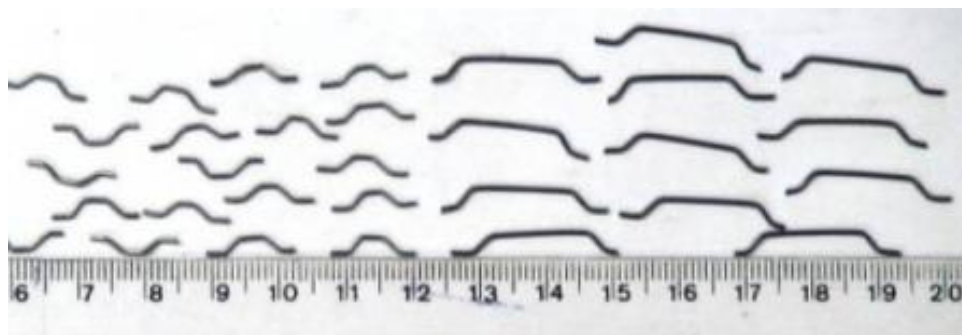
Figure 3. Steel microfibers (left) and conventional steel fibers (right)

3. RESULTS AND ANALYSIS

3.1. Compression tests in cylindrical test tubes

The values of the mechanical properties of the compounds are shown in Table 2: mean resistance to compression (f_{cm}), mean resistance to traction by diametrical compression ($f_{ctm,sp}$), and modulus of elasticity (E_{cs}).

Table 2. Average results of the characterization of the compounds on resistance to compression

Matrix	Phase	Group	Compounds	f_{cm} (MPa)	$f_{ctm, sp}$ (MPa)	E_{cs} (GPa)
Mortar (A)	I	1	CPA	52.5	3.1	23.8
		2	CPA1A	43.8	3.7	22.7
		3	CPA1.5A	42.2	3.7	23.1
		4	CPA2A	45.7	4.9	24.0
		5	CPA1.5A0.5C	49.2	4.4	28.2
		6	CPA1.5A1.5C	47.2	4.9	32.3
		7	CPA1.5A2.5C	43.6	4.8	31.0
		8	CPA1.5A3.5C	42.8	4.9	29.1
Micro-concrete (M)	I	9	CPM	62.3	3.8	35.2
		10	CPM1A	42.0	3.0	30.6
		11	CPM1A1C	40.6	3.7	26.3
		12	CPM1A2C	42.8	5.1	30.0
		13	CPM1A2.5C	20.8	2.8	19.9
	II	1	CPM1A1C	33.2	2.5	32.3
		2	CPM1A1.5C	30.6	2.2	31.0
		3	CPM1A2C	33.4	3.2	32.4
		4	CPM1.5A1C	28.3	2.6	29.8
		5	CPM1.5A1.5C	30.5	2.9	31.0
		6	CPM1.5A2C	29.2	2.4	30.2

3.2. Bending tests – loads and resistance

The tenacity of the compounds was determined following the recommendations of Rilem (2002), the results of which are those indicated in Table 3. The criterion for the evaluation of tenacity is based on the energy absorption capacity (P) *versus* the vertical displacement (δ).

According to Rilem, the contribution of the fibers on the tenacity of the compound is evaluated through the subtraction of the tenacity that comes from the response of the cementitious matrix. In Figure 4 we can observe the typical response of the behavior to flexion of compounds with fibers, along with the expressions used to calculate the equivalent resistances to traction in flexion ($f_{eq,2}$ e $f_{eq,3}$) and of the residual resistances during flexion ($f_{R,1}$ e $f_{R,4}$). The meanings of the parameters presented in that figure are:

- F_L – is the maximum *offset* strength within the δ=0,05 mm interval. This interval is obtained with the use of a parallel line to the initial tangent, going through the point that characterizes the displacement δ of the *offset*;
- δ_L – is the vertical displacement value that corresponds to F_L;
- $f_{fct,L}$ – is the tension that corresponds to the F_L force, given by the expression:

$$f_{fct,L} = \frac{3.F_L.L}{2.b.h_{sp}^2};$$

- L – is the free span of the test tube and b is its length;
- h_{sp} – distance from the top of the notch to the upper face of the test tube;
- D^b_{BZ}, $D^f_{BZ,2}$, and $D^f_{BZ,3}$ – energy absorption quota by the matrix and by the fibers, respectively. They are calculated through the area on the P-δ curve until specific displacements (see Figure 4);
- $F_{R,1}$ and $F_{R,4}$ – strength values corresponding to the δ_{R1}=0.46 mm and δ_{R4}=3.00 mm displacements. They are values used for the calculation of the residual resistances of the compounds.
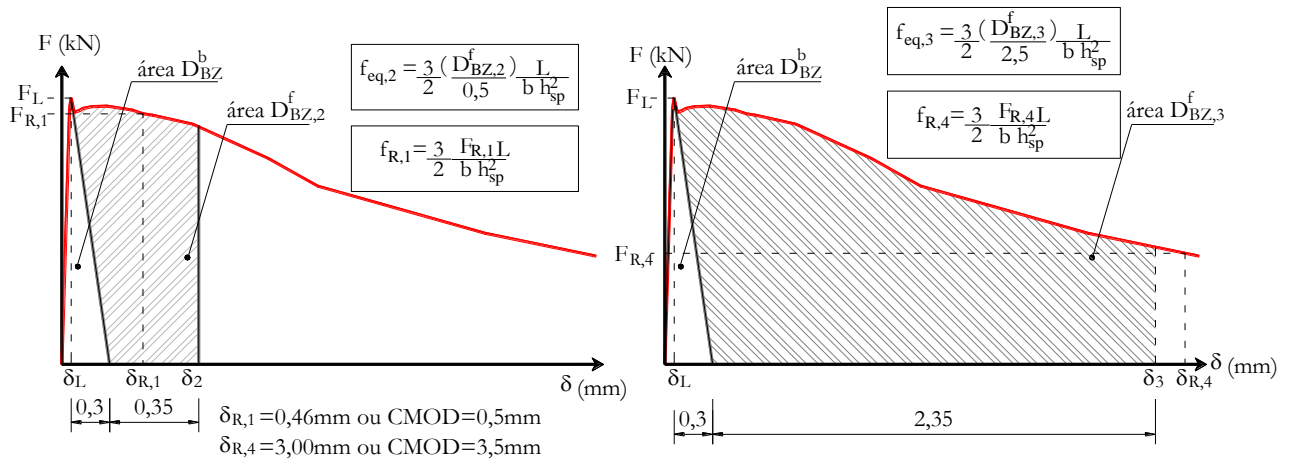
Figure 4 – Rilem (2002) criteria for the evaluation of the behavior of materials with fibers

Even according to the Rilem (2002), the quotas or tenacity parcels ($D^f_{BZ,2}$ and $D^f_{BZ,3}$) are transformed in equivalent flexural strengths ($f_{eq,2}$ and $f_{eq,3}$) for the different levels of displacement δ_2 and δ_3. The load capacity of the material in relation to a pre-defined arrow value is evaluated through the concept of residual flexural strength ($f_{R,1}$ and $f_{R,4}$).
Table 3 shows the value of the strength (F_M), which corresponds to the maximum strength reached by the compound throughout the load history.

Table 3. Loads and Resistance

Matrix	Phase	Compounds	Loads (kN)				Resistance (MPa)				
			F_L	F_M	$F_{R,1}$	$F_{R,4}$	$f_{fct,L}$	$f_{eq,2}$	$f_{eq,3}$	$f_{R,1}$	$f_{R,4}$
Mortar (M)	I	CPA	8.0	8.0	1.3	-	2.3	-	-	0.4	-
		CPA1A	13.4	13.4	12.5	5.2	3.9	3.3	2.6	3.6	1.5
		CPA1.5A	13.1	16.1	16.0	6.1	3.7	4.6	3.2	4.5	1.7
		CPA2A	14.5	17.6	17.4	7.6	4.6	5.5	4.2	5.5	2.4
		CPA1.5A0.5	16.4	17.8	17.2	9.3	4.6	4.9	4.0	4.8	2.6
		CPA1.5A1.5	16.0	21.0	20.9	9.4	4.8	6.5	4.8	6.3	2.8
		CPA1.5A2.5	22.1	23.7	23.5	12.8	6.1	6.5	5.0	6.5	3.6
		CPA1.5A3.5	20.0	21.4	20.8	6.1	5.5	5.7	3.8	5.7	1.7
Micro-concrete (M)	I	CPM	14.1	14.2	1.3	-	4.0	-	-	0.4	-
		CPM1A	12.0	12.1	7.5	3.7	3.3	2.0	1.6	2.1	1.0
		CPM1A1C	17.6	18.5	16.9	7.5	5.2	5.1	3.7	5.0	2.2
		CPM1A2C	19.4	21.9	19.7	8.0	5.5	5.7	4.1	5.7	2.3
		CPM1A2.5C	10.0	10.0	6.3	2.3	2.9	1.5	1.1	1.9	0.7
	II	CPM1A1C	12.2	14.3	11.4	1.0	3.6	3.5	2.4	3.4	0.3
		CPM1A1.5C	12.0	15.2	12.1	2.7	3.5	3.8	2.5	3.6	0.8
		CPM1A2C	14.4	18.9	15.9	1.8	4.1	4.9	3.0	4.5	0.5
		CPM1.5A1C	12.8	18.5	16.0	2.4	3.7	5.0	2.4	4.6	0.7
		CPM1.5A1.5	15.2	19.8	17.5	1.3	4.3	5.3	3.6	5.0	0.4
		CPM1.5A2C	11.0	15.6	13.4	3.2	3.2	4.4	2.9	4.0	1.0

It has been confirmed that the addition of steel fibers significantly contributes to the increase of the resistance defined by the parameter ($f_{fct,L}$), which represents the resistance quota of the compound that comes from the contribution of the cementitious matrix.

It is also possible to state that the addition of microfibers to the steel fibers resulted in even more significant improvements in this property for the mortar compounds in relation to the micro-concrete.

The performance of the mortar compounds from the contribution quota of the fibers ($f_{eq,2}$ and $f_{eq,3}$) was improved with the increase of the volume of fiber A and enhancing it with the addition of the steel microfibers.

For the micro-concrete compounds, the increase of the levels of equivalent flexural strength ($f_{eq,2}$ and $f_{eq,3}$) through the addition of steel micro fibers to fiber A is evident. In most those compounds, the strength ($f_{eq,2}$) exceeds the value of the strength ($f_{fct,L}$), showing significant strength gains after the cracking of the matrix.

3.3. P-CMOD Curves

The P-CMOD curves of the mortar compounds are shown in Figure 5. The presence of steel fibers and microfibers in the cementitious mortar matrix improved its behavior, translated in terms of an increase of the levels of strength, before and after the cracking of the matrix.

The increase in the volume of type "A" fibers provided a gradual improvement in the ductility of the mortar compounds. Similarly, the incorporation of the steel microfibers to the "A" fibers contributed even more in that sense.
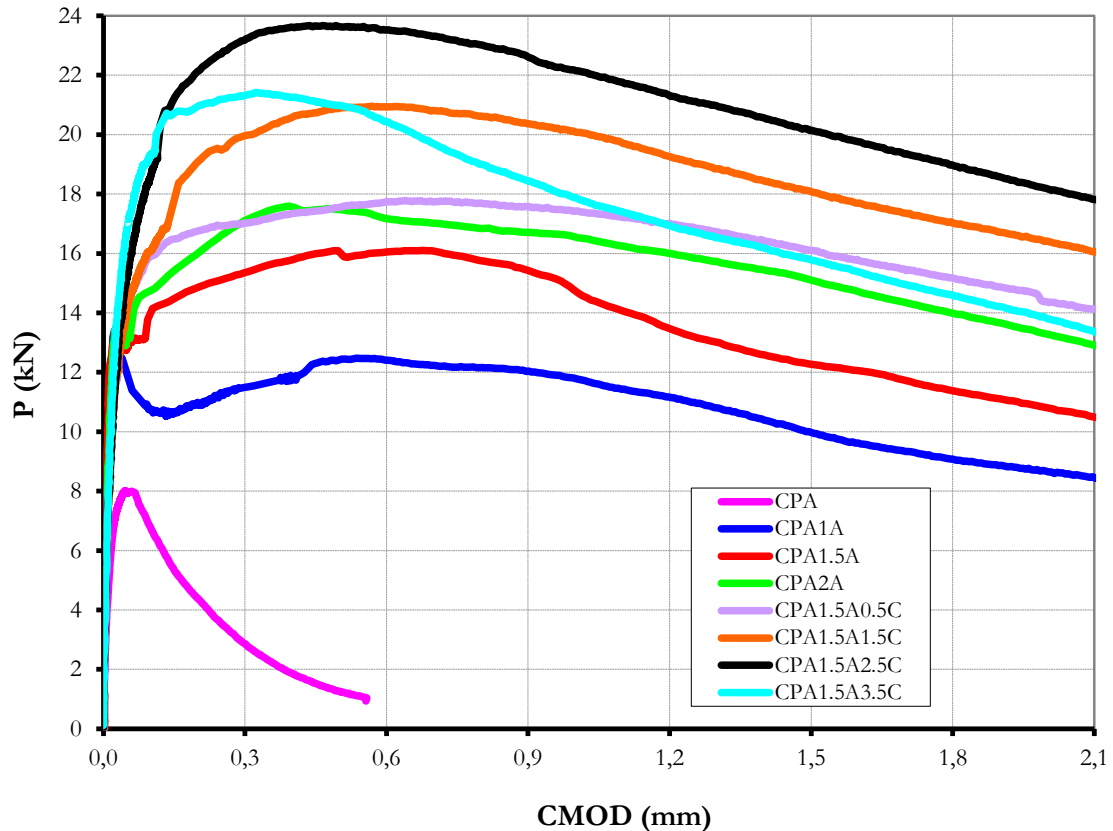
Figure 5. P-CMOD curves of the mortar compounds

The curves of the micro-concrete compounds are presented in Figure 6. The presence of fibers and microfibers primarily improved the energy absorption capacity of those compounds. The resistance capacity was decreased with the isolated presence of fiber A (CPM1A compound).
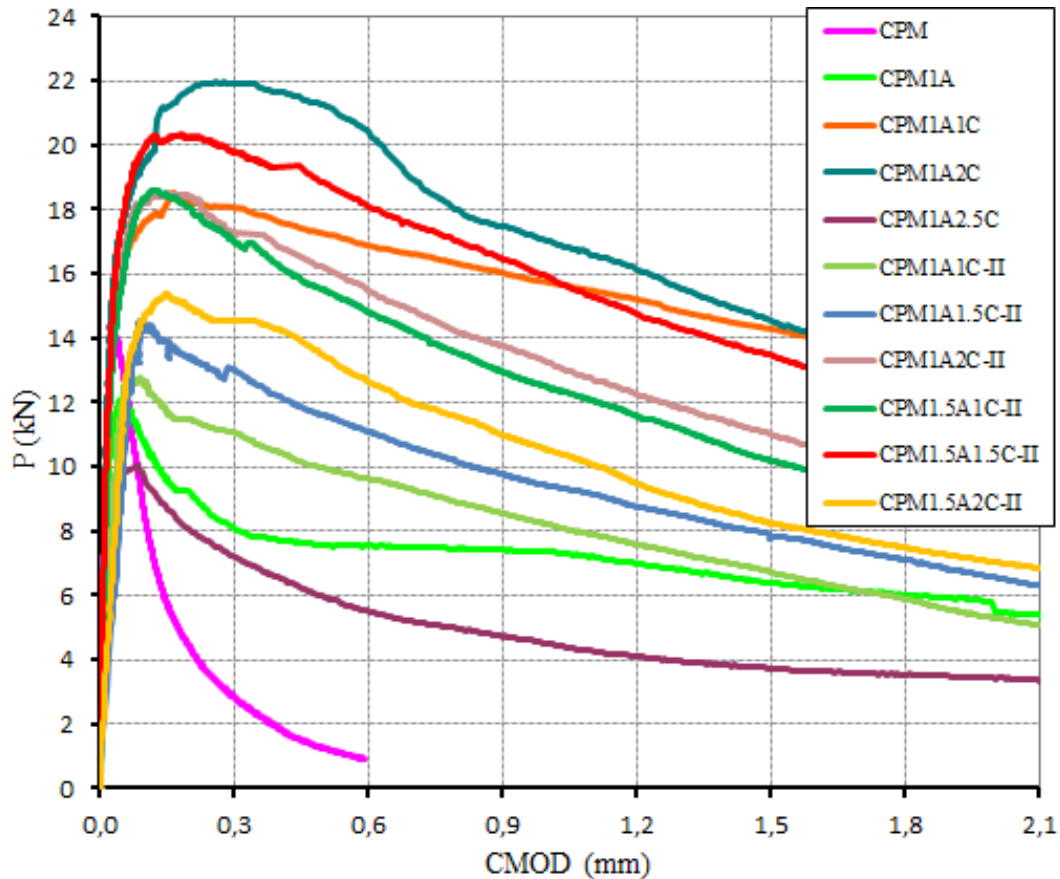
Figure 6. P-CMOD curves of the micro-concrete compounds

3.4. Fracture resistance curves

Figure 7 shows the fracture resistance curves of the mortar compounds. In Figures 8 and 9 the resistance curves of the compounds of the micro-concrete produced in phases I and II, respectively, are shown. Where "K_R" represents the resistance to the progress of the crack (resistance to the fracture of the compound) and "α" is the depth of the crack (a) relatively normalized to the height (W) of the test tube, i.e. $\alpha = a/W$.

The gain of resistance against cracking was mainly evidenced in the post-peak break regime (maximum strength), increasing between the different compounds with the increase of the range of metallic fibers incorporated to each one of them. With the exception of the CPA1.5A3.5C and CPM1A2.5C compounds, in which their resistances to fracture throughout the load history were inferior to those of the CPA1.5A2.5C and CPM1A2C compounds, respectively.

It is also possible to see that on the post-peak load phase, the final stretch of the resistance curve for the mortar compounds (CPA1.5A1.5C and CPA1.5A2.5C) and micro-concrete (CPM1A1C and CPM1A2C) are ascendant, which represents the high resistance gain to the propagation of the crack provided by the presence of the steel fibers and microfibers. This is associated to the energy dissipation of the pull-out process of the fibers and microfibers from the cementitious matrix.
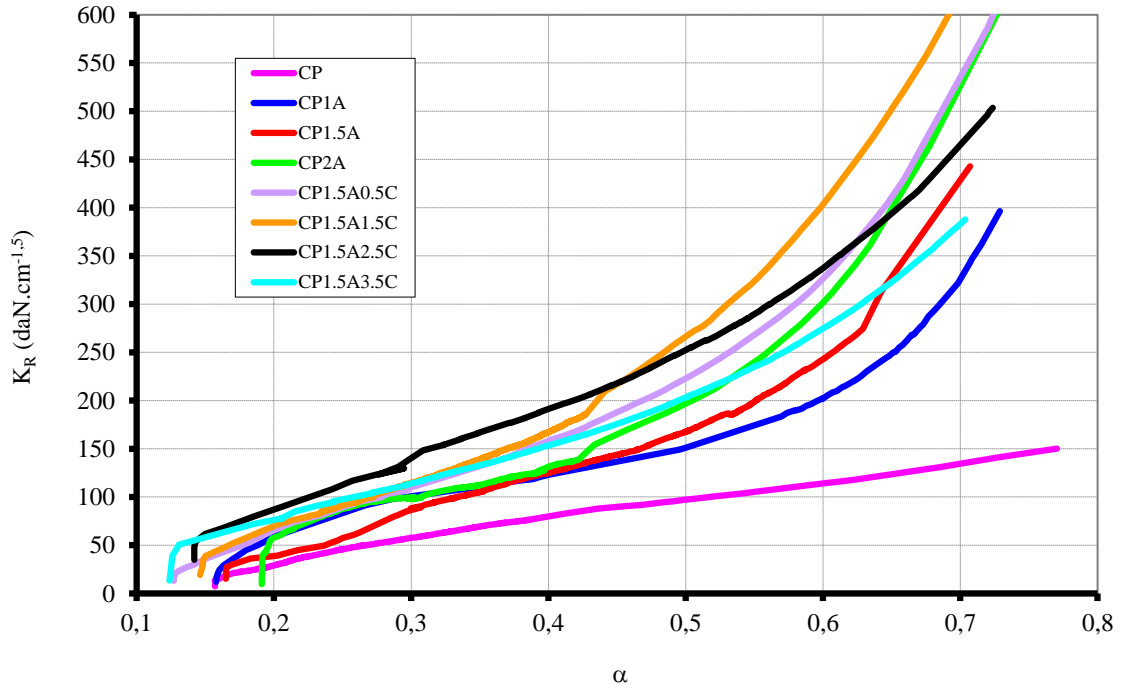
Figure 7. Fracture resistance curves of the mortar compounds
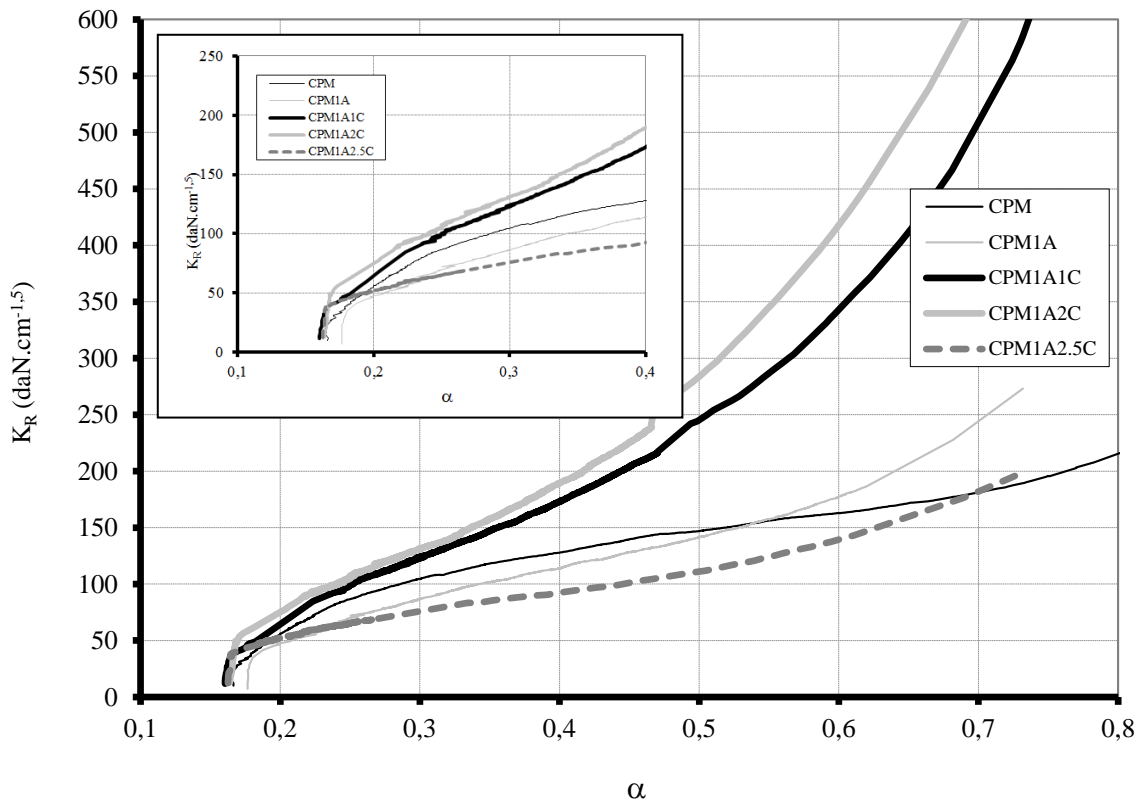
Figure 8. Fracture resistance curves of the micro-concrete compounds – Phase I
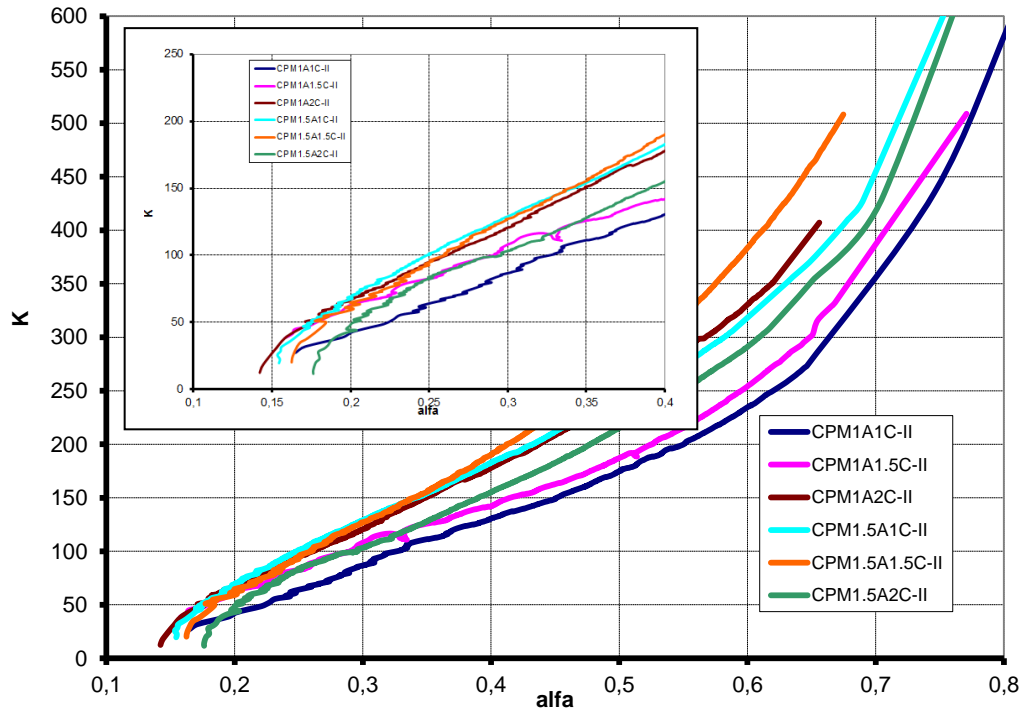
Figure 9. Fracture resistance curves of the micro-concrete compounds – Phase II

4. CONCLUSIONS

The following conclusions can be established based on the research done:
1. The hybridization process is an interesting alternative for the application in the recovery of the tensed concrete beam span, as the addition of steel microfibers to the short steel fibers increases the resistance to traction during flexion and increases the flexural tenacity of the mortar and micro-concrete compounds;
2. With the cracking of the matrix, the transfer of tensions was facilitated by the microfibers that, once dispersed in the matrix, conditioned the propagation of the crack to an increase of the load level of the compound;
3. Considering the pseudo-hardening characteristics and their specific application, the CPM1A2C compound was the one that presented the best properties among the ones produced in phase I;
4. Among the compounds produced in phase II, CPM1.5A1.5C-II stands out as it presented considerable increases in the maximum load through hybridization, as well as in the resistance to fractures and flexion.

5. REFERENCES

Ferreira, L. E. T., Bittencourt, T. N., Souza, J. L. A. O., Gettu, R. (2012), "*R-Curve behavior in notched beam tests of rocks*", Engineering Fracture Mechanics, N. 32, pp 27-40.

Ferrari, V. J., Hanai, J. B. (2012), "*Flexural strengthening of reinforced concrete beams with carbon fibers reinforced polymer (CFRP) sheet bonded to a transition layer of high performance cement-based composite*," Ibracon Structures and Materials Journal, Vol. 5, N. 5, pp 596-626.

Arquez, A. P. (2010), Dissertaçao mestrado, "*Aplicación de laminado de polímero reforçado com fibras de carbono (PRFC) inserido em substrato de microconcreto com fibras de acero para reforço à flexión de vigas de concreto armado*", Escola de Engenharia de Sao Carlos, Universidade de Sao Paulo.

Rilem TC 162-TDF (2002). *Test and design methods for steel fibre reinforced concrete. Bending test,* Materials and Structures, Vol. 35, pp 579-582.

ALCONPAT Journal

http://www.revistaalconpat.org

Journal of the Latin-American Association of Quality Control, Pathology and Recovery of Construction

Compressive strength of concretes with blast furnace slag. Re-visited state-of-the-art

J. A. Cabrera-Madrid[1], J. I. Escalante-García[2], P. Castro-Borges[3]

[1] Engineering department, Universidad Autónoma de Chiapas, Blvd. Belisario Domínguez Km 1081, s/n, Terán, 29050 Tuxtla Gutiérrez; Tel: (961) 6178000, 6150322, 6150527.

[2] Centro de Investigación y de Estudios Avanzados del IPN Unidad Saltillo, Carretera Saltillo - Monterrey km 13, PO box 663, Saltillo, Cohauila CP 25 000, México

[3] Centro de Investigación y de Estudios Avanzados del IPN Unidad Mérida, Antigua Carretera a Progreso Km. 6, 97310 Mérida, Yucatán, México; Tel.: (999) 942-94-00. Fax: (999) 981-29-23.

ABSTRACT

A state-of-the-art revision of the BFS-PC cementing system was done, emphasizing its effect on the mechanical compressive strength of the concrete. The use of the cementing characteristics of the BFS with high levels of replacements is viable, making it possible to improve the compressive strength, and in some cases, the resistance to the corrosion of the steel; said improvement will depend on the amount of BFS and on the exposure environment of the concrete. In this work, the replacements of BFS were confirmed as beneficial, up to 70% in humid microclimates or marine environments, and up to 50% in environments susceptible to carbonation. In these ranges, higher replacement efficiency with regard to resistance to compression can be achieved.
Keywords: slag; carbonation; industrial byproducts; corrosion.

RESUMEN

Se realizó una revisión del estado del arte del sistema cementante CP-EAH, enfatizando su efecto en la resistencia mecánica de compresión del concreto. El aprovechamiento de las características cementantes de la EAH con altos niveles de reemplazo resulta viable, pudiendo mejorar la resistencia a compresión y en algunos casos la resistencia a la corrosión del acero, dicho mejoramiento dependerá de la cantidad de EAH y del ambiente de exposición del concreto. En éste trabajo se confirmaron como benéficos los reemplazos de EAH hasta de un 70% en microclimas húmedos o ambientes marinos, y hasta 50% en ambientes propensos a carbonatación. En estos rangos se puede lograr una eficiencia del reemplazo mayor con respecto a la resistencia a la compresión.
Palabras clave: escoria; carbonatación; subproductos industriales; corrosión.

RESUMO

Foi realizada uma revisão do estado da arte do sistema aglomerante CP-EAH, enfatizando seu efeito na resistência mecânica de compressão do concreto. O aproveitamento das características aglomerantes da EAH com altos níveis de substituição resultou viável, podendo melhorar a resistência à compressão e em alguns casos a resistência contra a corrosão das armaduras. As melhoras observadas dependeram da quantidade de EAH e do ambiente de exposição do concreto. Foram confirmados como positivos as substituições de até um 70% de EAH, em microclimas húmidos ou ambientes marinhos, e até 50% em ambientes propensos a carbonatação. Nestes intervalos é possível obter uma eficiência maior da substituição com respeito à resistência à compressão.
Palavras-chave: escória; carbonatação; subprodutos industriais; corrosão.

_____
Contact author: Pedro Castro Borges (pcastro@cinvestav.mx)

1. INTRODUCTION

Since the earliest civilizations, the materials with a certain capacity of adherence (cementing material) have been crucial in the development and evolution of construction. Thus, throughout history, men have sought other cementing materials to obtain the best mechanical and durability properties. This evolution has led to Portland cement and reinforced concrete being the most used materials in the construction industry (Gamgbir, 2009).

On the other hand, the cement industry is one of the main sources of carbon dioxide (CO_2). It has been estimated that the CO_2 emissions into the atmosphere reach a value of 1.0 ton per Clinker ton (Cassgnabere, 2009), which is where Portland cement is obtained from after its grinding. In light of this inconvenience, man has searched for alternate materials with cementing capacities that are not damaging to the environment due to their origin and that could, when used carefully, provide advantages (Malhotra, 1996; Day, 2006). Although the quantity of residues/byproducts that are currently used is small compared to what is produced, research is being carried out worldwide to search for new applications for these as cementing materials and thus decrease the carbon footprint of the construction industry.

There are some industrial wastes that could be used as cementing materials, and would require little to no previous maintenance for their use in the mixture for concrete and/or mortar. On the other hand, there are other cementing materials of natural origin (for example, volcanic ash) that are available for their use in the mixture of concrete (Malhotra, 1996).

Some cementing materials that originate from industrial waste and that can be used as alternative materials are: fly ash, fumed silica, blast furnace slag, metakaolinite, and schist (Day, 2006), which could be used as mineral additions in the preparation of Portland cement manufactured in the plant (Modified Portland Cement, MPC); as addition in the grinding; or for the mixture of two or more types of fine materials that partially substitute Portland cement (Hydraulic Cement with Additions or Cement with cementing substitutes) used in the mixing of concrete or mortar (Kosmatka, 2004). The first property in the concrete that has been affected by the use of cementing materials of natural or industrial origin, is the resistance to compression, assigning for this work the real resistance (f_c) obtained from the compression tests, and therefore there is a big amount of works (Cassgnabere, 2009; Bagheri, 2013; Atis, 2003; Ashtiani, 2013) that under different mixtures, conditions, origin or atmosphere, allow the use of a certain amount of these materials without notably affecting the mechanical properties of the concrete. It is complicated to think about all the uses of these materials, but there is a need to know if the tendency to decrease the f_c is constant, or what its limit is regarding the parameters of research that have been used in different investigations. Similarly, even though there are already excellent combinations of cementing materials that give rise to binary, ternary, and quaternary cements (Nedi, 2001), the availability of the materials in one zone or region alone could constitute an economic obstacle for their generalized use, especially in developing countries. Therefore, the use of binary cement manufactured in the plant could be the most practical alternative, in economic and availability terms, for the time being. The objective of this work is to re-visit the state-of-the-art on the tendencies of the compression resistance of concretes and structures that use blast furnace slag (BFS) as cementing material, as well as review the levels of replacement of Portland cement that are considered in the standards of different countries for the classification of the cements with blast furnace slag, be it mixed during the grinding or by the separate mixture of each grinded material.

2. CHARACTERISTICS OF THE BLAST FURNACE SLAG

A cementing byproduct is the secondary or incidental material that is derived from the industrial manufacturing process through a chemical reaction, which possesses the conglomerating characteristic after a certain treatment (Malhotra, 1996). An industrial byproduct that is considered waste could possess a certain pozzolanic capacity, and could be useful and marketable when finding an application for it in another industrial sector, for example, as a partial substitute of Portland cement in the construction with concrete, or also as a stone aggregate as is the case of granulated slag.

Blast furnace slag is a (non-metallic) byproduct from the manufacture of melted steel in blast furnace, which consists mainly of silicates and calcium aluminosilicates and other phases (Siddique, 2008). Certain authors (Malhotra, 1996; Lea, 1971) describe blast furnace slag as a pozzolanic material, as it does not present cementing properties onto itself unless it is combined with other cementing materials for its chemical activation. Other authors, however, indicate that it should be classified as a latent hydraulic cement, as its components are comparable to the oxides of Portland cement (lime, silica, and alumina) in different proportions (Lea, 1971).

The slag generated in the steel industry can be divided into four types according to the method used for its cooling: the blast furnace slag air cooled; the expanded or foamed slag; the palletized slag, and the granulated blast furnace slag.

The air-cooled slag does not present the same hydraulic properties as the water-cooled slag, given that by slowly cooling with the fair, its compounds have the possibility of reaching a greater degree of crystallization, which would result in a material with low reactive activity. For its part, the expanded slag is used as a light weight coarse aggregate in the manufacture of concrete with a specific low weight (Malhotra, 1996). These materials are used in the construction of roads and buildings. The type of slag used as cementing material is the blast furnace granulated material; this byproduct is obtained through the accelerated cooling of melted slag, through the application of water on its surface to form a vitreous material which could have a certain degree of activation.

The fast cooling of the melted slag with water prevents the formation of bigger crystals, resulting in a granular material that comprises almost 95% of the compound of alumina-silicate of non-crystalline calcium. Granulated slag is processed through a previous drying and is subsequently grinded through a rotating ball mill, until a very fine powder is obtained known as Ground-granulated blast-furnace slag (GBS). The granulated slag has particle sizes between 4 to 15 mm, and less than 45 μm with a superficial area of 400 to 600 m^2/kg after grinding, which could be used as latent hydraulic cement (Lea, 1971). The grinded material is a powder with a lighter color than Portland cement; the coloration it gives the concrete is lighter and provides a smoother surface when compared to the concrete with Portland cement. The specific gravity that it presents is of 3.15.

In figure 1, we show an image of MEB (SEM) taken from the literature, with the morphology of a hydrated paste comprised of a cementing system of 30% blast furnace slag and 70% of ordinary Portland cement (Li, 2011). In this same Figure, we can observe angular particles that correspond to the slag and which have not been able to hydrate after 7 days. This behavior is normal in the cements with slag, as the slag presents a lower reaction activity when compared to ordinary Portland cement.
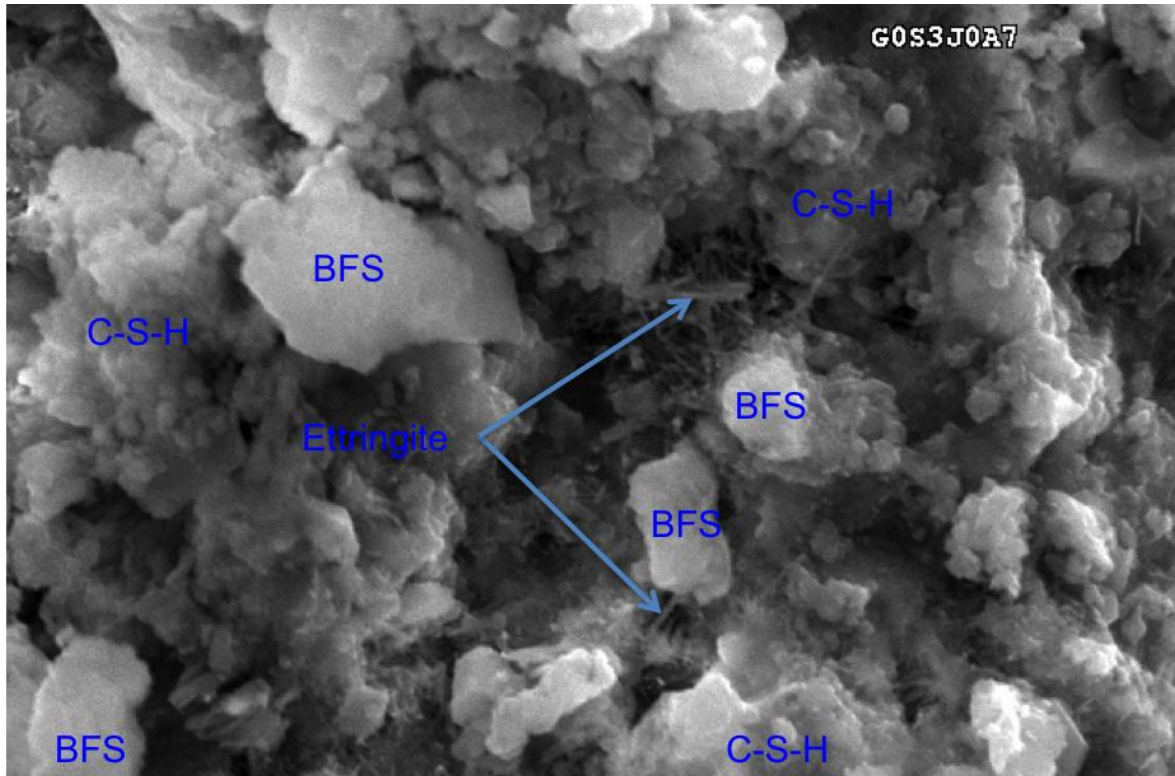
Figure 1. MEB microphotographs of hydrated pastes after 7 days, paste with 30% blast furnace slag and 70% ordinary Portland cement (BFS blast furnace slag, C-S-H hydrated calcium silicate) (Li, 2011).

The specifications for the granulated blast furnace slag as cementing material can be found in the ASTM C 989 (ASTM-C-989, 1999), where slag is classified in three degrees of resistance. These degrees are based on the activity index of the slag: grade 80 (with a low activity index), grade 100 (with a moderate activity index), and grade 120 (with a high activity index); other specifications for slag can also be found in AASHTO M 302 (ASSTHO-M302, 2000). The number of the quality designation corresponds to the compression resistance at 28 days, approximately, done in standard mortar cubes prepared with GBFS (mixture with an equal amount in mass of Portland cement). The degree of activity affects the reactive behavior in the fresh mix of concrete and the subsequent setting. On the other hand, the hydraulic activity of the slag will be determined by its chemical composition, the superficial area, and the size of the grinded slag particle (Puertas, 1993; Pal, 2003).

The chemical composition of the blast furnace slag could vary greatly depending on its origin, but to be considered a cementing material it is required that the chemical composition lies within the ranges of: CaO (30-45%), SiO_2 (30-48%), Al_2O_3 (15-25%), Fe_2O_3 (0.5-2%), and other oxides in lower quantities (Shetty, 2013). Among the chemical requirements provided by the ASTM 989 (ASTM-C-989), 2.5% and 4.0% are established as the maximum quantities of sulfides (S) and sulfates, respectively, with these quantities the presence of slag in the reinforced concrete does not represent a corrosion risk for the reinforced steel (Wang, 2010). The pulverized blast furnace slag is slightly alkaline and presents a solution pH that is within a range of 8 to 10, however, the slag leachate can exceed a value of 11, a level that could be corrosive for aluminum or galvanized steel pipes placed in direct contact with the slag (Wang, 2010).

The previously mentioned proportions of the oxide compounds will determine the basicity of the slag and its hydraulic capacity. However, for the slag to be able to truly develop its hydraulic potential, it is fundamental that its vitreous phase is largely superior to 70%. This vitreous characteristic will condition the ability of the slag to recreate the crystalline structure that will provide the concrete with its resistance and durability qualities.

As cementing material, the granulated slag has the following characteristics: it is a strong latent hydraulic cement when it is grinded, it has a high content of Na_2O and K_2O, light weight, a high permeability to water, it does not contain chlorides, and it does not produce alkali-aggregate reactions.

The replacement of cement for ground granulated slag (GBFS) will generally reduce the amount of water necessary to obtain the same shrinkage as the one obtained from a concrete with OPC. The reduction of the amount of water will be influenced by the increase in the level of replacement and by the fineness of the slag (Shetty, 2013). The typical water demand for the mixture of concrete with GBFS is approximately 3-5% less than for the concrete with Portland cement (Wang, 2004; Walker, 2011). This represents a reduction of 5 to 10 liters of water per cubic meter of concrete. For OPC replacements with GBFS within 70% and 80%, the reduction in the demand of water could be less, due to the much higher concentration of finer GBFS particles (Siddique, 2012; Oner, 2007). This behavior is due to the surface particles of GBFS being softer and having greater crystallinity than the ones of Portland cement, resulting is less water adsorption on the surface of the GBFS particles.

Among the advantages that the use of ground granulated slag has on fresh and hardened concrete are: reduction of hydration heat, refinement of the pore structure, reduction of the permeability of external agents, increase of the resistance to chemical attacks, resistance to attacks by sulfates, enhancement of the workability of the mixture, and in certain cases, it can improve the resistance to the corrosion of the reinforcement steel, as this will depend on the chemical composition of the slag. The concrete with the slag could reach a higher compression resistance for certain levels of replacement of the Portland cement. All of this, in addition to saving ordinary Portland cement in the concrete mixture (Shetty, 2013).

The incorporation of blast-furnace slag in the cementing mixture modifies the nature and characteristics of the hydrates formed, affecting the concrete capillary network, reducing the size and number of pores. This effect of the slag is shown on the concrete in its hardened state and in its durability. However, the beneficial effects of the slag on the mechanical properties and durability of the concrete will be in accordance with different factors, among which stand out the quality of the slag, the adequate design of the mixture, the placement and transportation of the fresh concrete, and the care in the time and type of curing.

Another considerable characteristic of the slags is the hydration process, which is slower than the Clinker one, as its dissolution is more difficult due to its vitreous nature as well as due to its need of a strong sulphatic (plaster, anhydrite) or alkaline (by the presence of alkali or portlandite) activation. The activation of the slag is caused by the presence of portlandite $Ca(OH)_2$ released by the hydration of the Clinker, due to the alkali in the slag and the actions of the setting regulator (plaster and/or anhydrite).

In this situation, other characteristics of the granulated blast-furnace slag, related to their hydration process, can be mentioned.

- There is no release of portlandite $Ca(OH)_2$ and we can consider the consumption of the amount released by the clinker.
- There is no formation of tricalcium aluminate (C_3A).
- The alkali (K_2O y Na_2O), that participate as catalysts in the hydration of the slags, are trapped in the crystalline net and are not in their free state.

On the other hand, as an environmental benefit, the ground granulated slag is also considered a sustainable material (Gjørv, 2000), as it is a byproduct of industrial waste and its use in concrete is acknowledged by the LEED certification (Leadership in Energy and Environmental Design) (Council U.S.G.B. 2014; Slag Cement Association). Considering this, slag may be used in concrete for superstructures, and with the right evaluation, it is also used in reinforced concrete exposed to environments with chlorides and sulfates; with the disadvantage of its slow setting, implying a greater time of execution for a certain project.

The fact that the slag added to the concrete mixture has a lower reactivity during the first couple of days, results in a considerable decrease in the compression resistance at early ages of the mixtures when compared to PC concrete mixtures. However, at subsequent ages the contrary occurs, meaning that in several cases, greater resistances than those in homologue concrete were reached (Oner, 2007; Berndt, 2009).

3. BLAST FURNACE SLAG AS CEMENTING MATERIAL IN THE REGULATIONS

The BFS can be used for the same purposes as Portland cement, as it sets and hardens due to its chemical reaction with water, therefore, it is considered a latent hydraulic cement due to having the same compounds as PC. However, in some cases, it is necessary for the slag to be mixed with hydrated lime to gain functionality (Gambhir, 2009; Lea, 1971).

The specification for the slag cement can be found in the ASTM C595 (ASTM-C595, 200) standards, where they are classified as IS and S type (Blast-furnace slag Portland cement and Slag or refractory cement), respectively.

The IS type cement is comprised of granulated blast-furnace slag (GBFS), which can be grounded along with the Clinker of the Portland cement or through separate grinding and then incorporated to the cementing mixture. The amount of GBFS in this type of cement is between 25% and 70% of the cementing mass. It is considered that the slag content of 70% of the cementing mass brings a certain benefit with regard to resistance and durability, but just up to a certain degree and in accordance with the environment where the concrete is exposed. On the other hand, if higher doses of this type are used, tests must be done on the concrete to verify the resistance, durability, and other specifications that are required for the project.

Table 1 shows the amounts of slag content considered in the standards of different countries. According to the standards presented in table 1, the European standard (UNE-EN-197, 2013) considers a level of slag of 95% in the cementing mixture, this being the highest level compared to those of the other countries shown in Table 1. As for American countries, Colombia considers up to 85% of slag in its standard, whereas Mexico considers up to 80%. On the other hand, it is important to mention that the use of high levels of slag should be subject to a certain level of verification control, due to the compatibility with other additions in the mixture, or due to the aggregates and the environmental conditions.

The use of other cementing materials, different to the traditional ones entails certain effects and changes in the fresh and hardened concrete. For the concrete mixture, a certain amount of water is needed for the hydration reaction to happen. Among its particularities, slag can diminish the

amount of water for the mixture by 1% to 10%, depending on the amount of substitution. It can also present a greater amount of tap without it having adverse effects on the concrete, but it also tends to diminish the heat of hydration when compared to Portland cement. Nevertheless, the combined use of ground blast-furnace slag and fly ash can decrease the setting time (Lee, 2013). For the hardened concrete, the use of slag could contribute to the enhancement of the resistance to compression. However, there is the risk that the resistance of the concrete will suffer a decrease with the addition when the proper curating method and care are not applied for the cementing system used. Therefore, the development of the resistance of concrete with GBFS can be comparable to normal concrete if it is cured at a temperature of approximately 23 °C.

Table 1. Slag content in cements according to the standards of different countries.

Country and Standard	Type of cement	Slag content
European Committee for Standardization UNE-EN 197-1, 2013.	Portland Cement with slag additions Portland cement with blast-furnace slag	6 to 35% 36 to 95%%
Argentina IRAM 50000, 2000; IRAM 50001, 2000.	Ordinary PC PC with slag Composite Portland cement Blast-furnace cement	Maximum 10% of BFS 11% – 35% of BFS 35% BFS 35-75%
Chile NCH148	Refractory Portland Cement Refractory Cement	Maximum 30% BFS 30% - 70%
Colombia NTC 30	Refractory cement BFS Portland Cement	>70 of BFS 15 – 85 GBFS
Mexico NMX-C414-ONNCCE	OPC Portland Cement with blast-furnace slag Composite Portland Cement Cement with blast-furnace slag	5 6 – 60 6 – 35 61 – 80
United States (ASTM C595, 2000; AASHTO M240)	Blast-furnace Portland Cement Refractory or blast-furnace slag Cement Portland Cement modified with slag	25 – 70 of GBFS Minimum 70% GBFS < 25%
Canada CSA A362, CSA A23.5 CAN/CSA-A3001-03	Portland Cement with Blast-furnace slag Portland Cement modified with slag	25 to 40% of slag 25 – 70%
Australia AS/NZS 2350.1; AS 3582.2; AS 3972,	Binary Cement mixed with slag Ternary cement with slag and other supplementary cementing material	30 – 70% 30% - 50%

4. RESULTS OF THE EFFECT OF THE GBFS SLAG ON THE COMPRESSIONRESISTANCE

For this section, we did a collection of data from researches reported in the literature used, paying attention to the replacement levels of Portland cement with blast-furnace slag and the effect caused on the resistance to the real compression (f_c) of the hardened concrete at ages of 28 and 29 days. It is important to mention that the mixtures of the cementing material that have been investigated are comprised of the system: Portland cement and slag.

Usually, the amount of water used to prepare the concrete mixture is implicitly indicated in the water/cement (*a/c*) relation. However, for cementing systems, the amount of water is indicated by the water/material relation expressed by *a/mc*. Nevertheless, there are some cases where water is not used exclusively for the preparation of the mixture, but where some activating solution of a byproduct is required; in this case the term *s/mc* is used, which represents the aqueous solution with the chemical agent (alkaline solution) and cementing material.

The curing techniques for concrete after 24 h of strain could be very varied, among these are: the humid curing or water immersion curing; room temperature curing; curing with temperature (*T*) and controlled relative humidity (*HR*). The curing period will depend on the cementing system used for the concrete mixture with a slag dosage as a cement replacement.

Table 2 shows some of the results reported in the literature about the resistance to real compression f_c of the concrete at ages of 28 and 90 days, with replacements of type I ordinary Portland cement with the byproduct of GBFS. The level of replacement, the *a/mc* relation, and the compression resistance at 28 and 90 days are indicated in the table.

As can be observed in Table 2, the amount of replacement by slag is a maximum of 80% for the research reported in 2007 (Atis, 2007), this amount being within the range reported in the standards of different countries such as Mexico and Colombia. Similarly, it is also worth mentioning that the concretes with different *a/mc* relations have been investigated, all within the range of 0.28 to 0.55, also indicating that in low relations of *a/mc* it is fundamental to use some water reducing additive or superplasticizer to confer the suitable properties to the fresh state of the concrete.

According to Table 2, there is a broad range of possibilities to use BFS as a partial substitution of the cement for the manufacture of concrete mixtures, but in some cases the result does not have a good effect with regard to the mechanical resistance. It is therefore important to provide certain details regarding the resistance to compression of the concrete in relation to the amount of slag used in the OPC-BFS cementing system.

Table 2. Compressive strength (f_c) of the concretes with cementing system type I OPC+ BFS with different levels of replacement according to different authors.

Authors	Replacement with byproduct (%)	a/mc	f_c (MPa) 28 days	f_c (MPa) 90 days	Authors	Replacement with byproduct (%)	a/mc	f_c (MPa) 28 days	f_c (MPa) 90 days
Kriker, 1992	0	0.50	30	35	Atis, 2007	60	0.40	53	
	15	0.50	26	39		80	0.40	43	
	30	0.50	30	33		0	0.50	52	
	40	0.50	28	36		20	0.50	51	
	45	0.50	26	38		40	0.50	46	
	50	0.50	21	29		60	0.50	40	
Kriker, 1992	0	0.60	29	31		80	0.50	27	
	15	0.60	34	37		0	0.30	73	
	30	0.60	32	39		20	0.30	70	
	45	0.60	25	33		40	0.30	66	
Amrane, 1994	0	0.55	24	27		60	0.30	68	
	15	0.55	26	31		80	0.30	54	
	30	0.55	27	33		0	0.40	66	
	50	0.55	21	29		20	0.40	63	
Ramezanianpour, 1995	0	0.50	41			40	0.40	62	
	25	0.50	40			60	0.40	59	
	50	0.50	35			80	0.40	47	
Polder, 1996	0	0.43	50			0	0.50	37	
	70	0.43	51			20	0.50	37	
Yeau, 2005	0	0.42	46	49		40	0.50	35	
	25	0.42	48	52		60	0.50	30	
	40	0.42	44	60		80	0.50	20	
	55	0.42	47	57		0	0.30	75	
Atis, 2007	0	0.40	68			20	0.30	73	
	20	0.40	69			40	0.30	76	
	40	0.40	62			60	0.30	58	
	60	0.40	54			80	0.30	56	
	80	0.40	43		Chidiac, 2008	0	0.31	61	
	0	0.50	42			25	0.31	64	
	20	0.50	36			40	0.31	70	
	40	0.50	35			50	0.31	64	
	60	0.50	28			60	0.31	64	
	80	0.50	18						

Tabla 2. Continuación.

Authors	Replacement with byproduct (%)	a/mc	f_c (MPa) 28 days	f_c (MPa) 90 days	Authors	Replacement with byproduct (%)	a/mc	f_c (MPa) 28 days	f_c (MPa) 90 days
Chidiac, 2008	0	0.38	76		Bilim, 2009	0	0.30	80	86
	20	0.38	86			20	0.30	82	90
	25	0.38	76			40	0.30	84	91
	33	0.38	70			60	0.30	81	92
	40	0.38	71			80	0.30	66	77
	50	0.38	79			0	0.40	64	71
	60	0.38	70			20	0.40	73	82
Bilim, 2009	0	0.30	81	85		40	0.40	66	81
	20	0.30	81	90		60	0.40	62	73
	40	0.30	82	88		80	0.40	47	55
	60	0.30	78	79		0	0.50	49	50
	80	0.30	68	76		20	0.50	50	56
	0	0.40	64	68		40	0.50	49	53
	20	0.40	66	72		60	0.50	39	49
	40	0.40	67	78		80	0.50	28	35
	60	0.40	61	75	Bouikni, 2009	0	0.43	55	
	80	0.40	53	57		50	0.43	57	
	0	0.50	51	57		65	0.43	55	
	20	0.50	53	61	Shariq, 2010	0	0.45	36	41
	40	0.50	52	58		20	0.45	31	37
	60	0.50	40	50		40	0.45	28	40
	80	0.50	25	34		60	0.45	24	29
	0	0.30	76	84		0	0.50	31	34
	20	0.30	81	87		20	0.50	27	31
	40	0.30	81	88		40	0.50	25	32
	60	0.30	73	81		60	0.50	22	26
	80	0.30	63	71		0	0.55	22	25
	0	0.40	64	71		20	0.55	20	23
	20	0.40	66	74		40	0.55	19	24
	40	0.40	67	76		60	0.55	15	19
	60	0.40	61	74	Topçu, 2010	0	0.50	34	36
	80	0.40	50	59		25	0.50	48	54
	0	0.50	54	61		50	0.50	44	45
	20	0.50	57	65	Abdelkader, 2010	0	0.50	30	34
	40	0.50	56	66		30	0.50	36	43
	60	0.50	45	58		50	0.50	30	39
	80	0.50	30	38					

Tabla 2. Continuación.

Authors	Replacement with byproduct (%)	a/mc	f_c (MPa) 28 days	f_c (MPa) 90 days	Authors	Replacement with byproduct (%)	a/mc	f_c (MPa) 28 days	f_c (MPa) 90 days
Johari, 2011	0	0.28	87	96	Hadjasadok, 2012.	0	0.65	36	42
	20	0.28	95	104		15	0.65	33	36
	40	0.28	88	99		30	0.65	28	40
	60	0.28	87	98		50	0.65	16	33
Lübeck, 2012	0	0.30	60	72		0	0.42	62	65
	50	0.30	59	68		15	0.42	61	63
	70	0.30	40	42		30	0.42	60	65
	0	0.42	48	59		50	0.42	53	62
	50	0.42	42	55	Li, 2012	0	0.41	48	
	70	0.42	30	38		10	0.41	48	
	0	0.55	39	48		30	0.41	47	
	50	0.55	30	40		50	0.41	46	
	70	0.55	20	31					

Figures 2 and 3 present the information shown in Table 2, corresponding to the resistance to real compression of the concrete at ages of 28 (figure 2) and 90 days (figure 3) in relation to the degree of cement replacement. Likewise, Figures 2 and 3 show the average correlation lines with the classification in three ranges of the *a/mc* relation; the values lower to 0.4, the range between 0.4 and 0.6, and the values higher to 0.6.

It is possible to observe in Figure 2, that there is a slight generalized tendency to the decrease of the resistance when the amount of slag in the cementing mixture is increased, even though it can be observed that there is a range where the resistance may be improved. The level of replacement that has been used in investigations reaches a value of 80%, but it can be observed that it is within the range of 20% to 60% that there are slightly higher values of f_c when compared with the reference concrete, that is, without slag. A similar behavior to the one of the resistance at 28 days can also be observed in the resistance at 90 days, shown in figure 3. Said graph also shows that for a longer period (concrete of older ages), the resistance f_c of the concretes with replacements of 20% to 60% tends to increase with age.

For both ages of the concretes (Figures 2 and 3), it can be observed that with cement replacement levels higher than 60% slag, the resistance of concrete is inferior to the concrete without replacement.

To determine the effect generated in the resistance f_c of the concretes for the ages of 28 to 90 days, a parameter called rate of change was determined. This parameter is a unidimensional value obtained from the fraction between the resistance f_c of the concrete with slag and the resistance f_c of the reference concrete. In the graphs of Figure 3, the rate of change (efficiency) of the concrete with slag is shown in comparison to the reference homologous concrete and in accordance with the different levels of replacement. The horizontal line indicates the rate of f_c for the reference concrete. An inferior value to said line indicates that the concrete with slag did not reach the resistance value of its counterpart without slag; whereas the values above the horizontal line mean that the concrete surpassed or improved the resistance of the concrete without slag.

Similarly to what was observed in Figures 2 and 3, Figure 4 shows that there is a known and expected tendency for the decrease of the resistance of the concrete f_c with the increase of the level of replacement of the cement with slag in the cementing system, making it consistent with what is reported in the literature (Abdelkader, 2010).

As before, the range in which a better effect on the resistance can be appreciated is between 20% to 60%, where similar or slightly superior values of f_c are reached with regard to the reference concrete; this effect is more distinct in the graph shown in Figure 5 for the 90 day-old concrete. Furthermore, it can be observed in Figure 4 that replacements higher than 60% have a decrease in the improvement of the f_c resistance. Similarly, this effect can also be seen at the age of 90 days, making it consistent with the observations in Figure 2 and 3.

According to the results reported by Ahmend Hadjasadok et al. (Hadjasadok, 2012), it can be observed that for the same a/mc relation, the resistance f_c is reduced when the level of replacement of the OPC is increased, but for an equal quantity of slag the f_c resistance is increased when reducing the a/mc relation.
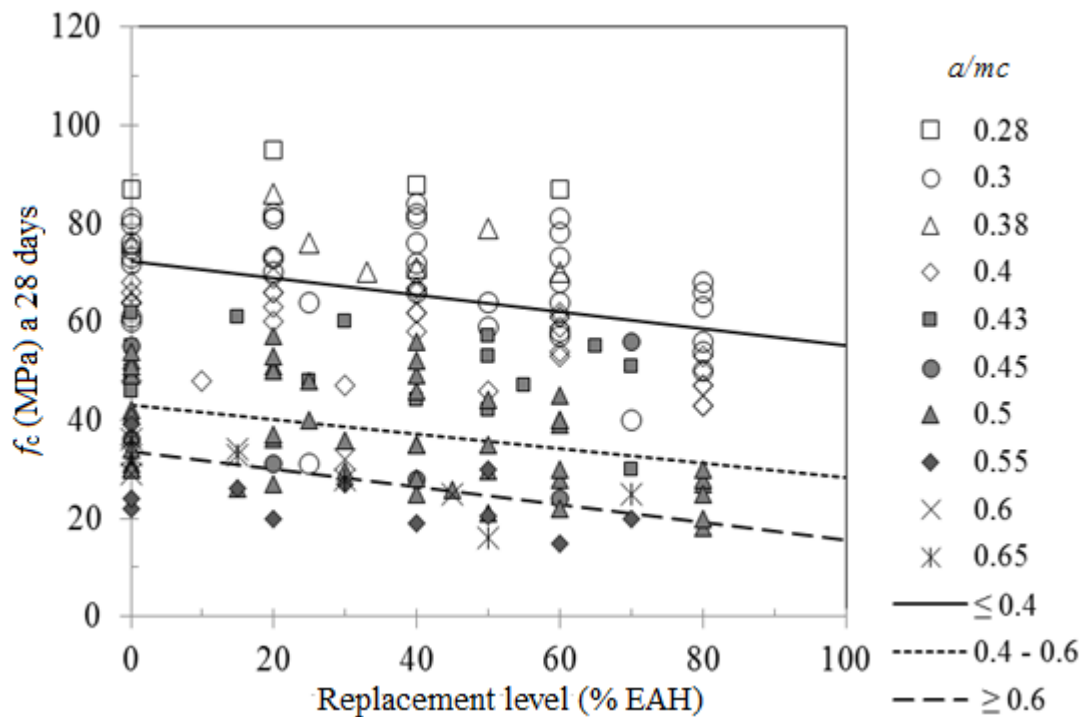

Figure 2. Data reported in the literature (Table 2) regarding the resistance to real compression (f_c) of the concretes with slag and tested at 28 days.
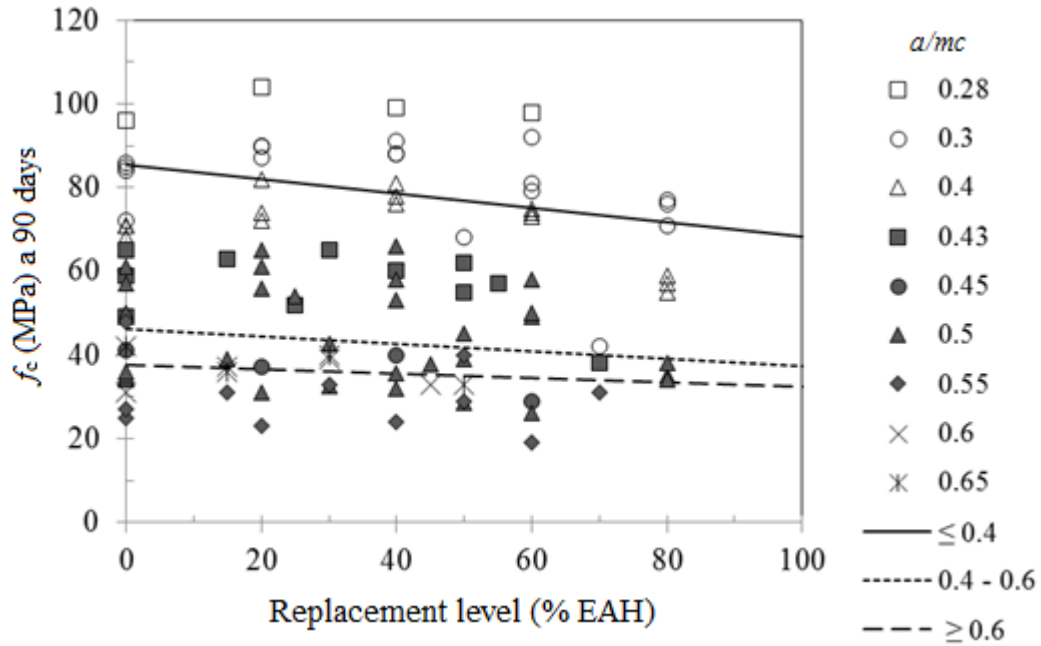
Figure 3. Data reported in the literature (table 2) regarding the resistance to real compression (f_c) of the concretes with slag and tested at 90 days.

On the other hand, Figure 5 shows that at an age of 90 days, the concrete acquires a higher resistance when compared to an age of 28 days (Figure 4). This observation was also presented in the works of Iker Bekir Topcu and Raif Boga (Topç, 2010), in which they also conclude that with replacements of 25% of GBFS to the cementing system there is a higher compression resistance for the concrete with underwater curing and during 28 days, as well as at 90 days. It is also worth mentioning that at 50% the resistance diminishes in similar curing times, this effect with a similar replacement level was observed by Bougara (Abdelkader, 2010). For their part, Chidiac and Panesar (Chidiac, 2008) concluded that the f_c resistance of concrete with slag is decreased with an increase in the replacement level of cement.

The behavior observed in the delay for the improvement of mechanical resistance in concretes with slag is thought to be due to the cementing steel byproduct taking more time to activate than conventional cement.

These characteristics have also been mentioned in other investigations carried out on pastes (Sanchez, 2011), on mortar (Hwang, 1991), and on concrete (Lee, 2013), having a similar result in the decrease of resistance at early ages, as consequence of the delay in the hydration time of the supplementary cementing material. This behavior causes a decrease in the precipitation rate of the most stable reactive products, which contribute to the mechanical resistance.

Due to the resistance being related to the phases formed in the pastes, we mention one of the results of the researches done by Chao-Lung Hwang y Der-Hsien Shen (Hwang, 1991) on pastes with OPC – GBFS systems, with replacements of 10% to 40% and three water-cementing material relations of 0.35, 0.47, and 0.59, bringing us to the conclusion that for a certain a/mc relation, a high GBFS content will require a longer setting time for the paste.

However, according to the investigation done by Martínez Aguilar et al. (Aguilar, 2010), they report that the f_c in pastes with GBFS could be improved with the activation of the slag through a type of alkaline sulfate (Na_2SO_4 or K_2SO_4 mixed with Al_2SO_4) or through a sulphatic source such as Fluorogypsum (Fy, $CaSO_4$), which is also another industrial byproduct, even though they also

mention that in some cases the f_c at 90 days was lower than at 28 days. The authors link said effect to the formation of unstable phases (ettringite and gypsum) in the internal structure of the cementing paste, which results in an imbalance (expansion) at subsequent ages.

In accordance with the foregoing, it can be said that for a constant content of slag, the setting time will change proportionally to the *a/mc* relation. This will lead to better results in the compression resistance at subsequent ages than those for a conventional concrete, which would lead to a higher hydration rate for the chemical compounds of the cementing material.

To appreciate the effect caused by the slag in hardened concrete throughout time, the frequency of change in the resistance of concrete was determined in accordance with three ranges of the rate of change: those concretes with BFS that presented a change <1 with regard to the reference concrete; those that did not present any change or change rate, which were considered equal to 1; and those that presented changes >1; this was done for both ages of the concretes. The foregoing is shown in Figure 6 through a graph of frequencies of a representative sample of the resistance data of concretes with slag analyzed in this work, which achieve rates of change that are lower, equal, and higher than 1 *fc*. In said Figure 6, it can be clearly observed that for the rate of change <1 there is a decrease in the frequency of the rate of change for the BFS concretes when going from 28 to 90 days of age, whereas for the rate of change >1 there is an increase in the frequency. This means that the incidence in the rate of change <1 for the concrete with BFS at 28 days is higher than for the reference concrete. Whereas the rate of change values >1, which are represented by the BFS concretes and which surpass the resistance of the reference concrete, have a greater incidence in the rate of change for those concretes that have more than 90 days of age. This is related to the above statements, as the slag has a slower hydration process than the OPC, therefore, it requires a longer time to reach the optimal hydration and thus develop compounds and more stable chemical phases that interfere in the improvement of the compression resistance of the concrete. Considering this, it is believed that in this situation the hydration characteristics are a conditioning factor for the development of the resistance and which interfere in the decrease of the resistance, in addition to the type of activity of the slag and the implementation of the curing of the concrete.

As mentioned in the above paragraphs, for the OPC + Slag system applied to hardened concrete, this could produce an effect on the resistance that surpasses that of the design at an age of 28 days of curing, according to the literature reports (Topç, 2010; Yeau, 2005). Prior to that age, the GBFS concretes presented lower f_c when compared to those of the reference concrete, but this can be overcome at later ages, with this behavior being present for all the levels of replacement. This result is due to the chemical secondary reactions and to the slow hydraulic reaction of the slag, which contributes to the densification of the micro-structure of concrete. The results presented by Chidiac and Panesar (Chidiac, 2008) confirm the above, plus the initial hydration rate is slower in concrete with GBFS than with OPC. Therefore, over the course of 7 to 28 days, the concrete with GBFS (60%) starts gaining resistance, making it similar or superior to the concrete with OPC.

With these results, it can be said that the possibilities of using a byproduct will be determined by the quality requirements of the concrete, understood as the mechanical resistance and durability properties. It is worth mentioning that the compression resistance is not an absolute parameter in selecting a certain concrete for any determined construction. Therefore, with the information presented above, it can be predicted that with the increase in the dosage of BFS in the cementing system, compressive strength comparable to a conventional PC concrete can be obtained, but with the notion that this will happen at later ages as with a normal concrete.
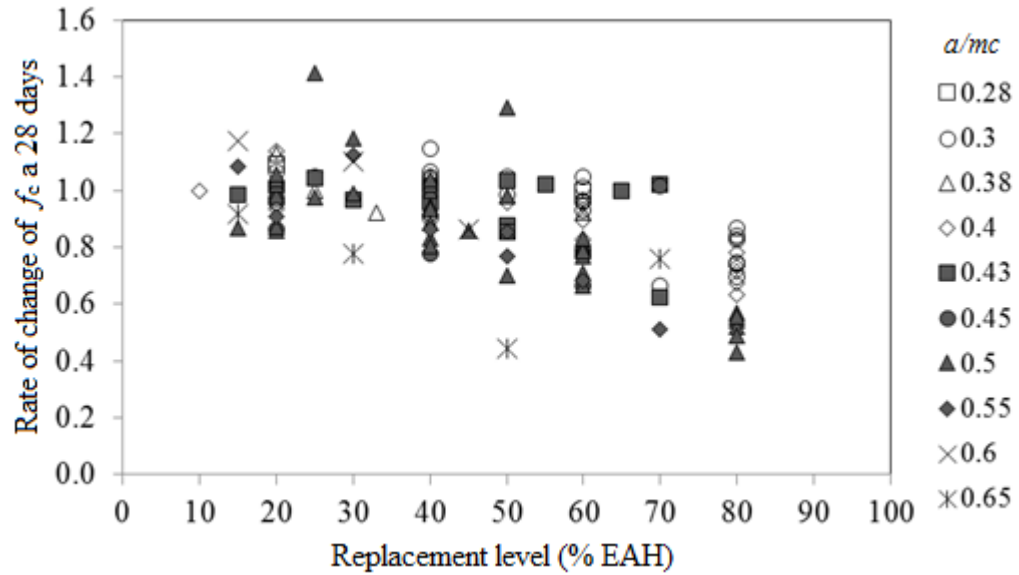
Figure 4. Rate of change (efficiency) of the resistance to real compressive strength f_c of the concretes with slag, at 28 days.
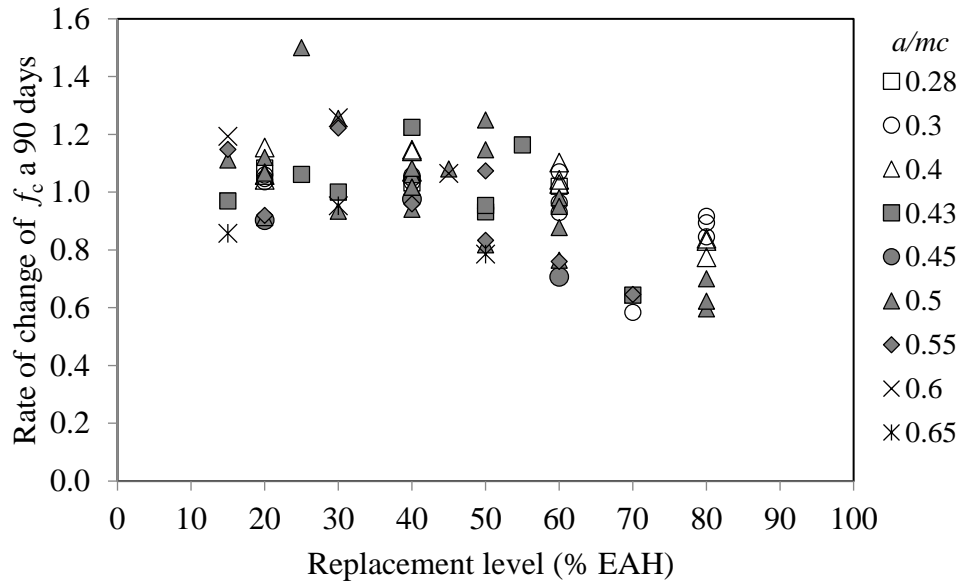

Figure 5. Rate of change (efficiency) of the resistance to real compressive strength f_c of the concretes with slag, at 90 days.
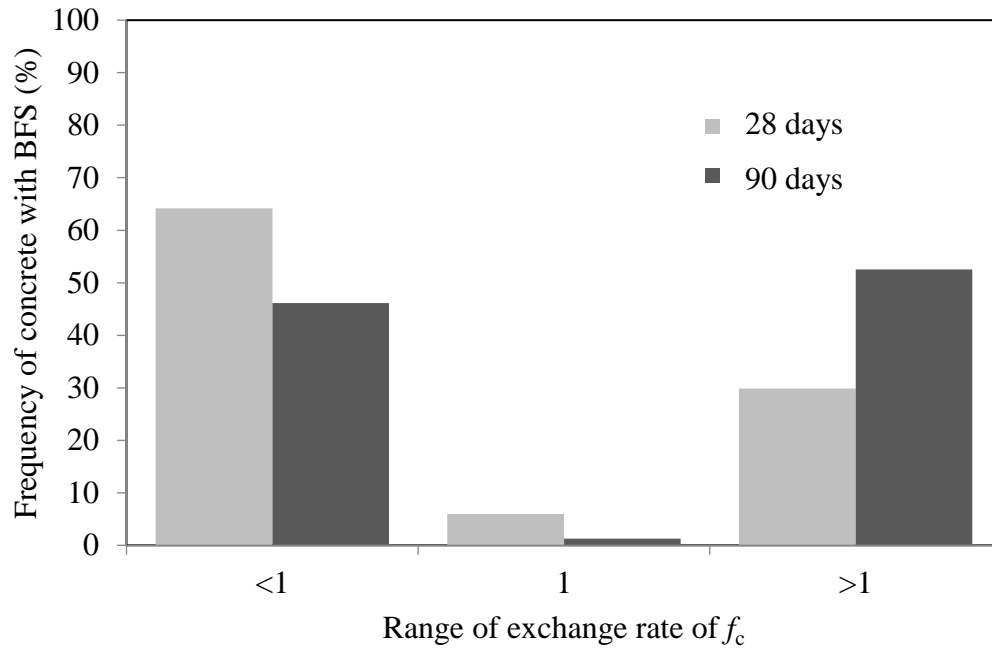
Figure 6. Frequency of the number of concrete samples with BFS related to the rate of change (efficiency) of f_c when compared to the reference concrete.

It has been previously observed that the incorporation and the increase in the level of slag in the mixture of concrete can have a beneficial effect on the mechanical properties of hardened concrete, but conditioned to a certain degree of replacement and to a certain age. As a counterpart, it can be said that the concrete elaborated with a high percentage of slag is very sensible to the conditions of curing, generating a premature drying on the surface of concrete, which would lead to the increase of permeability, in addition to the fact that the hydration of the cementing material is reduced, which would decrease the mechanical properties of resistance for the hardened concrete.

In a similar manner to the conventional concrete, the curing during the first hours following the hardening of concrete with a OPC+GBFS cementing system is highly essential, as this influences the development of the compression resistance, the decrease of porosity, and the high resistance to the penetration of chlorides. Under this premise, Ramezanianpour and Malhotra (Ramezanianpour, 1995) provide the results of their research with the replacement levels found in Table 2 and with a standard continuous humidity curing, corroborating that the concretes that were not cured showed poor performance with regard to the development of the mechanical resistance, as well as greater porosity and a weak resistance to penetration of chloride ions. It is worth pointing out that even when concretes were cured for 2 days, a significant improvement was seen with regard to their resistance in comparison with the concrete with no curing treatment. Therefore, the importance of curing the concrete with the OPC + BFS cementing system is reaffirmed, given that as it has already been mentioned, the hydration reaction of the slag is slower than that of the cement.

An important parameter in the prediction of the resistance of concrete with slag through the Feret model (Feret, 1982) is the efficiency coefficient of the slag. In the hydration time of the cementing system, the slag tends to improve its coefficient until reaching an optimal value when compared to Portland cement, but it has also been seen that it could decrease afterwards (Abdelkader, 2010). Therefore, efficiency will depend on the level of replacement, as it has been observed that with a 15% of slag, the activation is complete and there is 67% more efficiency than with regular cement.

Whereas for the high levels of replacement (50%), the efficiency of the slag decreases or manages, in the best of cases, to be comparable to cement (Abdelkader, 2010).

In Osborne's research, (Osborne, 1999), in studies conducted on structural elements with cementing mixtures with 30%, 50%, and 70% slag, good results have been achieved on the resistances to real compression f_c and when exposed to moderately aggressive environments; the results of which are shown in Table 2. On the other hand, the author states that the carbonation rate and the permeability of gas species are similar to concrete with a regular cement, however, he considers concrete with high levels of slag and exposed to open-air to be highly susceptible, making these factors highly aggressive in places with a dry environment. Nevertheless, he points out that by taking special care of the coating for the reinforcement steel, and limiting the amounts of slag for environmental situations with a high risk of carbonation, the effect could be lessened, thus limiting the level of slag replacement to a maximum 50%. For considerably humid environments and in the presence of chlorides, a level of up to 70% may be used (Osborne, 1999).

Considering the foregoing, it can be said that the proper curing of the concretes with blast-furnace slag should be considered as a fundamental factor for hydration, thus guaranteeing a good performance in the mechanical resistance and durability properties.

Consequently, it can be said that the use and the level of replacement of the blast-furnace slag in the cementing systems for concrete is defined in accordance with the design characteristics of the concrete mixture, both fresh and hardened, and on the environment to which the structural elements shall be exposed.

5. CONCLUSIONS

After re-visiting the state-of-the-art on the fc in concretes with blast-furnace slag, we were able to confirm that, through the experience of different authors who evaluated different conditions and types of slag, the level of replacement could be significantly high. However, when surpassing by 50% this level, a strict quality control plan would be necessary in the preparation and combination of other additives that contribute to the improvement of the mechanical resistance; otherwise, there may be adverse effects to the expected results.

The maximum replacement level recommended by several authors and in accordance with the results obtained by others, is of 70% slag in environments with little carbonation aggressiveness, otherwise it must be limited to a maximum of 50%.

The concrete where cement is partially replaced by BFS will require a longer hydration time to guarantee the desired f_c, with the curing of concrete being of major significance.

6. ACKNOWLEDGEMENTS

7. REFERENCES

AASHTO-M240-00. (2000), *Blended hydraulic cements.*
AASHTO-M302-00. (2000), *Ground granulated blast-furnace slag for use in concrete and mortars.*

Abdelkader, B., El-Hadj, K., and Karim, E. (2010), "*Efficiency of granulated blast furnace slag replacement of cement according to the equivalent binder concept*", Cement and Concrete Composites, 32: pp. 226-231.

Aguilar, O. A. M., Castro-Borges, P., and Escalante-García, J. I. (2010), "*Hydraulic binders of Fluorgypsum–Portland cement and blast furnace slag, stability and mechanical properties*", Construction and Building Materials, 24: pp. 631-639.

Amrane, A. and Kenai, S. (1994). "*Propriétés mécaniques et durabilité du béton au laitier en climat chaud*", in Proceedings of the international seminar on the quality of concrete in hot climate. (Ghardaia, Algeria).

Arezoumandi, M. and Volz, J. S. (2013), "*Effect of fly ash replacement level on the shear strength of high-volume fly ash concrete beams*", Journal of Cleaner Production, 59: pp. 120-130.

AS-3972. (2010), *General purpose and blended cements*, (Australia).

Ashtiani, M. S., Scott, A. N., and Dhakal, R. P. (2013), "*Mechanical and fresh properties of high-strength self-compacting concrete containing class C fly ash*", Construction and Building Materials, 47: pp. 1217–1224.

ASTM-C-989-99. (1999), *Standard specification for ground granulated blast-furnace slag for use in concrete and mortars*.

ASTM-C595-00. (2000), *Standard Specification for Blended Hydraulic Cements*. (USA)

Atis, C. D., Bilim, C. (2007), "*Wet and dry cured compressive strength of concrete containing ground granulated blast-furnace slag*", Building and Environment, 42: pp. 3060–3065.

Atis, C. D. (2003), "*Accelerated carbonation and testing of concrete made with fly ash*", Construction and Building Materials, 17: pp. 147–152.

Bagheri, A. (2013), "*Comparing the performance of fine fly ash and silica fume in enhancing the properties of concretes containing fly ash*", Construction and Building Materials, 47: pp. 1402–1408.

Berndt, M. L. (2009), "*Properties of sustainable concrete containing fly ash, slag and recycled concrete aggregate*", Construction and Building Materials, 23: pp. 2606-2613.

Bilim, C., et al. (2009), "*Predicting the compressive strength of ground granulated blast furnace slag concrete using artificial neural network*", Advances in Engineering Software. 40: pp. 334–340.

Bouikni, A., Swamy, R. N., Bali, A. (2009), "*Durability properties of concrete containing 50% and 65% slag*", Construction and Building Materials, 23: pp. 2836–2845.

Cassgnabere, F., Mouret, M., Escadeillas, G. (2009), "*Early hydration of clinker-slag-metakaolin combination in steam curing conditions, relation with mechanical properties*", Cement and Concrete Research, 39,1: pp. 1164-1173.

Chidiac, S. E., Panesar D. K. (2008), "*Evolution of mechanical properties of concrete containing ground granulated blast furnace slag and effects on the scaling resistance test at 28 days*", Cement and Concrete Composites, 30: pp. 63-71.

Council, U. S. G. B. (2014), *LEED For New Construction Fact Sheet*. http://www.usgbc.org].

Day, K. W. (2006), *Concrete Mix Design, Quality Control and Specification*. (NY, EE. UU). p. 7.

Feret, R. (1982), "*Sur la Compacité des mortiers hydrauliques*", Annales des ponts et Chaussées, 4,7: pp. 155-164.

Gambhir, M. L. (2009), *Concrete Technology, Theory and Practice*. (U.K): p. 3.

GjØrv, O. E., Sakai, K. (2000), "*Concrete technology for a sustainable development in the 21st century*", (London: E & FN Spon). P. 281.

Hadjasadok, A. et al. (2012), "*Durability of mortar and concretes containing slag with low hydraulic activity*", Cement and Concrete Composites, 34: pp. 671-677.

Hooton, R. D. (2000), "*Canadian use of ground granulated blast-furnace slag as a supplementary cementing material for enhanced performance of concrete*", Canadian Journal of Civil Engineering, 27: pp. 754 - 760.

Hwang, C. L. and Shen, D. H. (1991), "*The effects of blast furnace slag and fly ash on the hydration of Portland cement*", Cement and Concrete Research, 21: pp. 410-425.

IRAM-5000-0. (2000), *Cemento. Cemento para uso general. Composición, características, evaluación de la conformidad y condiciones de recepción*, (Argentina).

IRAM-5000-1. (2000), *Cemento. Cemento con propiedades especiales*, (Argentina).

Johari, M. A. M., et al. (2011), "*Influence of supplementary cementitious materials on engineering properties of high strength concrete*", Construction and Building Materials. 25: pp. 2639–2648.

Kosmatka, S. H. (2004), "*Diseño y control de mezclas de concreto*", Portland Cement Asociation (PCA), (México). P. 25.

Kriker, A. (1992), "*Durabilité du béton à base de laitier*", (Francia: ENP Alger): p.

Lea, F. M. (1971), "*The Chemistry of Cement and Concrete*". (N.Y. USA): p 414.

Lee, N. K. and Lee, H. K. (2013), "*Setting and mechanical properties of alkali-activated fly ash/slag concrete manufactured at room temperatura*", Construction and Building Materials, 47: pp. 1201-1209.

Li, Q., Li, Z., and Yuan, G. (2012), "*Effects of elevated temperatures on properties of concrete containing ground granulated blast furnace slag as cementitious material*", Construction and Building Materials, 35: pp. 687–692.

Li, Y. (2011), "*Microestructure and properties of high performance concrete with steel slag powder*", Materials Science Forum, 675-677: pp. 503-506.

Lübeck, A., et al. (2012), "*Compressive strength and electrical properties of concrete with white Portland cement and blast-furnace slag*", Cement and Concrete Composites, 34: pp. 392–399.

Malhotra, V. M. and Mehta, P. K. (1996), "*Pozzolanic and cementitious materials*". Advances in Concrete Technology. (UK): p. 102.

Mostafa, N. Y., et al. (2001), "*Characterization and evaluation of the hydraulic activity of water-cooled slag and air-cooled slag*", Cement and Concrete Research, 31: pp. 899 - 904.

NCh148.Of68. (1968), *Cemento - Terminología, clasificación y especificaciones generales*, (Chile).

Nedi, M. (2001), "*Ternary and quaternary cements for sustainable development*". American Concrete Institute, 23,4: pp. 34-42.

NMX-C414-ONNCCE. (1999), *Industria de la construcción. Cementos hidráulicos – Especificaciones y métodos de prueba*, (México).

NTC-30. (1996), *Cemento portland. Clasificación y nomenclatura*, (Colombia).

Oner, A. and Akyuz, S. (2007), "*An experimental study on optimum usage of GGBS for the compressive strength of concrete*", Cement and Concrete Composites, 29: pp. 505 - 514.

Osborne, G. J. (1999), "*Durability of Portland blast furnace slag cement concrete*", Cement and Concrete Composites, 21: pp. 11-21.

Pal, S. C., Mukherjee, A. and Pathakc, S. R. (2003), "*Investigation of hydraulic activity of ground granulated blast furnace slag in concrete*", Cement and Concrete Research, 33: pp. 1481 - 1486.

Polder, R. B. (1996), "*The influence of blast furnace slag, fly ash and silica fume on corrosión of reinforced concrete in marine environment*", Heron, 41,4: pp. 287-300.

Puertas, F. (1993), "*Escoria de alto horno: composición y comportamiento hidráulico*", Materiales de Construcción, 43,229: pp. 37 - 48.

Ramezanianpour, A. A. and Malhotra, V. M. (1995), "*Effect of curing on the compressive strength, resistance to chloride-ion penetration and porosity of concretes incorporating slag, fly ash or silica fume*", Cement and Concrete Composites, 17: pp. 125-133.

Sánchez, R., Palacios, M. and Puertas, F. (2011), "*Cementos petroleros con adición de escoria de horno alto, características y propiedades*", Materiales de Construcción, 61, 302: pp. 185-211.

Shariq, M., Prasad, J. and Masood, A. "*Effect of GGBFS on time dependent compressive strength of concrete*", Construction and Building Materials, 24: pp. 1469–1478.

Shetty, M. S. (2013), *Concrete technology - Theory and practice*. (India: S. Chand): p. 201.

Siddique, R. (1971), *Waste Materials and Byproducts in concrete*, (Berlin, Alemania): p 36.

Siddique, R. and Bennacer, R. (2012), "*Use of iron and steel industry by-product (GGBS) in cement paste and mortar*", Resources, Conservation and Recycling, 69: pp. 29– 34.

Slag Cement Association. LEED-NC 2.1, (2005). Guide: Using slag cement in sustainable construction. Available from: www.slagcement.org.

SP43. Australian Technical Infraestructure Committee. (2012), *Cementitious materials for concrete*, (Australia).

Topç, I. B. and Boga, A. R. (2010), "*Effect of ground granulate blast furnace slag on corrosion performance of steel embedded in concrete*", Materials and Desing, 31: pp. 3358-3365.

UNE-EN-197-1. (2013), Cemento. Parte I: *Composición, especificaciones y criterios de conformidad de los cementos comunes*. (España)

Walker, R. and Pavia, S. (2011), "*Physical properties and reactivity of pozzolans, and their influence on the properties of lime-pozzolan pastes*", Materiales and Structures, 4,6: pp. 1139-1150.

Wan, H., Shui, Z. and Lin, Z. (2004), "*Analysis of geometric characteristics of GGBS particles and their influences on cement properties*", Cement and Concrete Research, 34: p. 133-137.

Wang, L.K., Hung, Y.-T. and Shammas, N. K. (2010), *Handbook of Advanced Industrial and Hazardous Wastes Treatment*, (E. U.: CRC Press Taylor & Francis Group): p. 170.

Yeau, K. Y. and Kim, E. K. (2005), "*An experimental study on corrosion resistance of concrete with ground granulate blast furnace slag*", Cement and Concrete Research, 35: pp. 1391-1399.